SPIRE Beam Steering Mirror Design Description

v 4.1

Distribution List:

SPIRE-Project	Ken J. King	
	Bruce M. Swinyard	
	Matt Griffin	**x**
	Eric Sawyer	**x**
	Doug Griffin	**x**
UK ATC	Colin Cunningham	**x**
	Gillian Wright	**x**
	Ian Pain	**x**
	Tully Peacocke	**x**
	Brian Stobie	**x**
	Tom Paul	**x**
	Brenda Graham	**x**
	Ken Wilson/Tom Baillie	**x**
LAM	Didier Ferrand	
	Dominique Pouliquen	**x**
	Patrick Levacher	
MPIA	Ralph Hofferbert	**x**

Update:

Date	Index	Remarks
5 Jun 2000	1	Creation of the document
28 Aug 2000	2	Revision of the document, internal to ATC
	3.1, 3.2.	Revision of the document, internal to ATC
12 Oct 2000	3.3	Revision – adding significant mechanical, electronics & controls content. Produced summary description for verbatim release in SPIRE-ATC-PRJ-001 and -003
02 Feb 01	3.4	Updated update table to include unreleased versions. Amended images to latest mechanical design state. Included flex pivot call out.
20.Jul.01	4.0	Updated substantially for DDR
22.Feb.02	4.1	Revised and reformatted. Updated substantially

1. Table of Contents

1.1 Tables

1.2 Table of figures

2. Scope of the Document

This document describes the design of the Herschel-SPIRE Beam Steering Mirror mechanism subsystem. The intent of the document is to incorporate all design information available at a given release date, and it is expected that the document will be updated, on approximately a quarterly basis, as aspects of the design undergo changes under configuration control.

Section 5 of this document provides a summary design description that is referenced complete into AD1 and RD5.

3. Document List

3.1 Applicable Documents

	Title	Author	Reference	Date
AD1	SPIRE Beam Steering Mirror Mechanism Subsystem Specification	I. Pain	SPIRE-ATC-PRJ-000460 v 3.2	Jul.01
AD2	SPIRE Project Development plan	K.J.King	SPIRE-RAL-PRJ-000035	latest
AD3	Herschel-SPIRE BSM PA Plan	I.Pain	SPIRE-ATC-PRJ-000712 v1.1	12.Dec.01
AD4	Optical System Design Description	K.Dohlen, B.Swinyard	SPIRE-LAM-PRJ-000447 Draft 1	18.Dec.00
AD5	Spire Harness Definitions	D.K.Griffin	SPIRE-RAL-PRJ-000608 iss 0.3	30.May.01
AD6	ICD Structure - Mechanical I/F	B.Winters	MSSL/SPIRE/SP004.11 (formerly SPIRE-MSS-PRJ-00617)	29.Nov.01
AD7	SPIRE BSM FMECA	I. Pain	SPIRE-BSM-PRJ-0711	Jan 2002
AD8	SPIRE BSM Interface Control Documents	I. Pain	SPI-BSM-PRJ-0713	Jan 2002
AD9	SPIRE BSM Declared Process List	I. Pain	SPI-BSM-PRJ-0708	Oct 2001
AD10	SPIRE BSM Declared Parts List	I. Pain	SPI-BSM-PRJ-0709 v1.0	Jan.02
AD11	SPIRE BSM Declared Materials List	I. Pain	SPI-BSM-PRJ-0710 v1.0	Jan.02
AD12	SPIRE BSM Electronics Parts List	I.Pain /B.Stobie	SPI-BSM-PRJ-0714	Jan 2002

3.2 Reference Documents

	Title	Author	Reference	Date
RD1	Instrument Requirements Document	B.M.Swinyard	SPIRE-RAL-PRJ-000034 v1.1	02.Jan.02
RD2	Instrument Development Plan	K.King	SPIRE WE Review viewgraphs	6 Dec 1999
RD3	Proposal for Beam Steering Mirror	R.Sidey	ATC contract no. 017693	undated
RD4	Assessment of System Level Failure Effects for SPIRE	B.M.Swinyard	SPIRE-RAL-NOT-000319 v 4	4-APR-2001
RD5	BSM Development Plan	I.Pain	SPIRE-ATC-PRJ-000466	17.Jul.01
RD6	Space Engineering, Mechanical Part 3 - Mechanism Design	ESA	ECSS-E30(a)-part3	25 Apr 00
RD7	Optical design. Diffraction analysis & design.	M.Caldwell	SPIRE-RAL-DOC-000441 ISSUE: 1.0	14 Jun 00
RD8	Mirror Thermal Cycling Procedure	I.Pain	SPIRE-ATC-Internal-NOT-003 V 1.0	12.Jun.01
RD9	CM4 Hole Size Considerations and stray light control	T.Richards	SPIRE-RAL-NOT-000576 ISS 1.0	23 Jan 01
RD10	Spectrometer and photometer pupil imagery and CM4 SIZE CONSIDERATIONS	T.Richards	BSMSIZE_MEMO.DOC	21.Sep.00
RD11	SPIRE Optical Alignment Verification plan	A.Origne, K.Dohlen	SPIRE-LAM-PRJ-000445	10.Apr.01
RD12	SPIRE AIV plan	B.Swinyard	SPIRE-RAL-DOC-000410 issue 2.0	23.Feb.01
RD13	A cold Focal Plane Chopper for Herschel-PACS - Critical Components and Reliability	R.Hofferbert, D.Lemke et al	paper	undated
RD14	Thermal contraction sizing note.	T.Paul	SPI-BSM-NOT-0010	25.Jan.02
RD15	Report from FEA Study	Frazer Nash/ I.Pain	to be written	

4. Glossary

Abbr.	Meaning	Abbr.	Meaning
AD	Applicable Document	LAT	Lot Acceptance Tests
ADP	Acceptance Data Package	MAC	Multi Axis Controller
ATC	United Kingdom Astronomy Technology Centre	MAPTIS	Materials and Processes Technical Information Service
BSM	Beam Steering Mirror	MSFC	Marshall Space Flight Centre
BSM	Beam Steering Mirror dummy	MCU	Mechanism Control Unit
BSMe	Beam Steering Mirror electronics	MIP	Mandatory Inspection Point
BSMm	Beam Steering Mirror mechanism	MGSE	Mechanical Ground Support Equipment
BSMs	Beam Steering Mirror structure	MPIA	Max Planck Institute for Astronomy
CAE	Computer Aided Engineering	MSSL	Mullard Space Science Laboratory
CDR	Critical Design Review	NASA	National Aeronautical Space Agency
CoG	Centre of Gravity	NA	Not Applicable
CIL	Critical Items List	NCR	Non Conformance Report
CQM	Cryogenic Qualification Model	NCRP	Non Conformance Review Panel
CTD	Change to Drawing/Document	OGSE	Optical Ground Support Equipment
DCL	Declared Components List	PA	Product Assurance
DDR	Detailed Design Review	PAD	Part Approval Document
DM	Development Model	PFM	Proto Flight Model
DML	Declared Materials List	PPARC	Particle Physics and Astronomy Research Council
DPA	Destructive Physical Analysis	PI	Principal Investigator
DSP	Digital Signal Processor	PID	Proportional – Integral - Derivative
ECSS	European Co-operation for Space Standardisation	QA	Quality Assurance
EGSE	Electrical Ground Support Equipment	RAL	Rutherford Appleton Laboratory
ESA	European Space Agency	RAL SSD	RAL Space Science Department
FMEA	Failure Modes and Effects Analysis	RD	Reference Document
FMECA	Failure Modes, Effects and Criticality Analysis	rms	Root mean square
FPGA	Field Programmable Gate Array	SDOF	Single Degree of Freedom
FPU	Focal Plane Unit	SMEC	Spectrometer Mechanism
FS	Flight Spare	SPIRE	Spectral and Photometric Imaging Receiver
FSM	Flight Spare model	TBC	To Be Confirmed
GSFC	Goddard Space Flight Center	TBD	To Be Defined
GSE	Ground Support Equipment	TBW	To Be Written
HoS	Head of Specialism	UK ATC	United Kingdom Astronomy Technology Centre
Herschel	ESA Mission name (formerly FIRST)	UK SPO	UK SPIRE Project Office
ICD	Interface Control Document	WE	Warm Electronics
IBDR	Instrument Baseline Design Review		
KIP	Key Inspection Point		
LAM	Laboratoire d'Astrophysique de Marseilles		

5. Outline Description of the Beam Steering Mirror mechanism subsystem.

5.1 Overview

The Beam Steering Mirror mechanism subsystem (BSM) is a critical part of the SPIRE Instrument. It is used to steer the beam of the telescope on the photometer and spectrometer arrays in 2 orthogonal directions, for purposes of fully sampling the image, fine pointing and signal modulation.

The BSM comprises 4 main deliverables:

1. **The cryogenic mechanism** (BSMm).
2. **The structural interface** (BSMs).
3. **The warm electronics** (BSMe)
4. **Mass and optical alignment dummies, and Ground Support Equipment (GSE) as required for SPIRE system level integration,** (BSMd)

The position of the BSMm & BSMs are indicated in Figure: 1

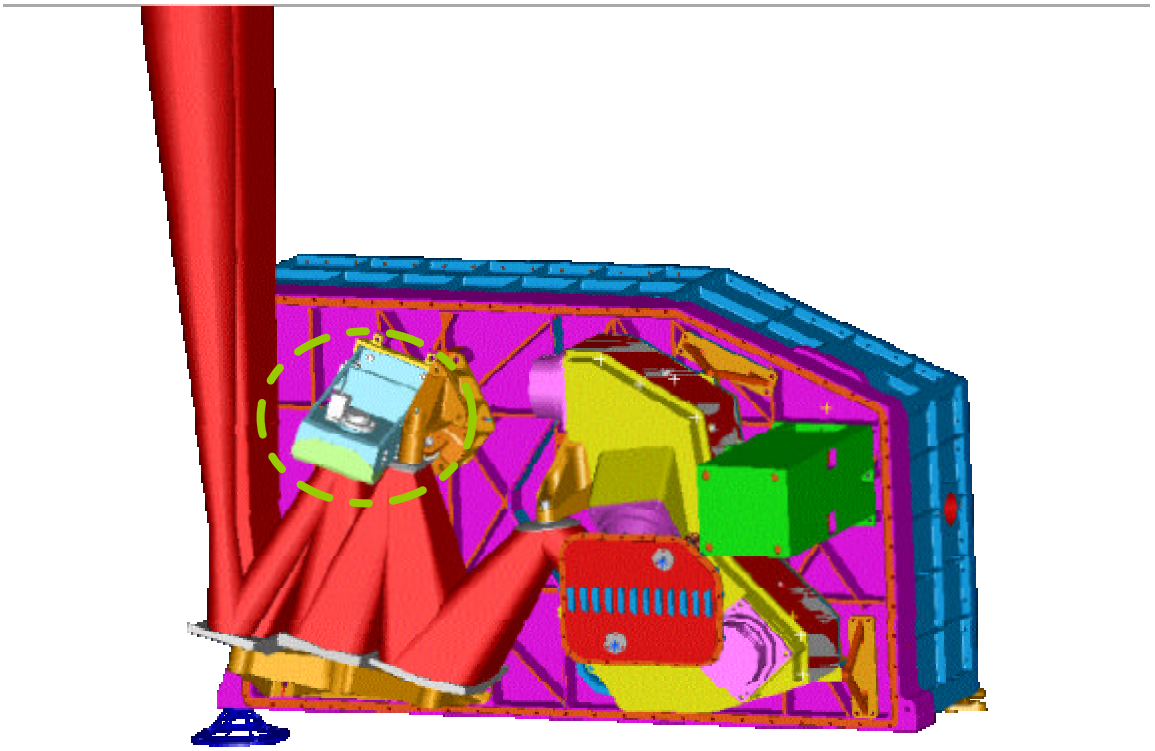

Figure: 1 Photometer Layout, BSM in green, highlighted with green dashed oval

The BSMm consists of an aluminium alloy mirror, nominal diameter 32mm, machined as part of the chop axis. This is mounted orthogonally within a gimbal-type frame which provides for jiggle axis motion. The axes are suspended by flex-pivot mounts. The BSMm is a cryogenic device with nominal temperature 4-6K. Nominally, the chop axis provides 2.53° of mirror motion at 2 Hz and the jiggle axis provides 0.57° of motion at 1 Hz. The mirror also provides an aperture through which the Photometer Calibration Source is directed towards the detector arrays

The BSMs provides location of the BSMm on the SPIRE optical bench, and will also provide for a light tight enclosure and structural support for harnessing and thermometry. The BSMs integrates to the SPIRE Photometer Calibration Source (PCAL), supplied by the University of Cardiff, a baffle (supplied by ATC) and the SPIRE optical bench (MSSL). The BSMs is a cryogenic structure with nominal temperature 4-6K.

The BSMe provides electrical actuators which are used to provide motion of the mirror. Electrical transducers are used to measure the mirror position to allow control of the mirror position. The BSMe baseline design makes use of cryogenic motors used in PACS and magneto-resistive sensors used in ISOPhot. Each axis houses a rare-earth (NdFeB) permanent magnet moving pole piece and is driven by a motor coil fixed to the mechanism housing/structure.

The cryogenic electronics are connected to the analogue power and amplifier electronics on the Warm Electronics (WE) by a cryogenic harness which will also feed out signal cables from thermocouples on the BSMs. The BSM operates under control of the Detector Readout and Control (HSDRC) sub-system's Mechanism Control Unit (MCU) supplied by LAM. The BSMe will be specified and designed by the UK ATC, then manufactured by LAM in conjunction with the SMEC electronics. Integration and test will be at LAM, with support from ATC.

The BSMd may comprise several actual dummies, with at least (1) an optical dummy for initial alignment work and (2) a mass-representative model for structural vibration tests. Designs for mass and optical alignment dummies will not be specified in detail until the BSMs/BSMm design is complete.

5.2 Mission profile

The BSM is developed as a sub-system and then integrated to the SPIRE FPU. The SPIRE instrument is subsequently integrated to Herschel. The instrument is to be cryogenically cooled, and will be cold during launch. Launch is scheduled for 2007 to an L2 orbit. The mission duration is a minimum of 4.25 years.

Per RD1, in normal operations the satellite is expected to have a 24-hour operational cycle with data being collected autonomously for 21 hours and a 3 hour ground contact period – the Data Transfer and Commanding Period (DTCP). During the DTCP the data will be telemetered to the ground and the commands for the next 24-hour period will be uplinked.

6. BSM Block Diagram

The block diagram below is adopted from RD1 Fig 3.1-1 and shows the relationships between the sub-systems of the SPIRE instrument.

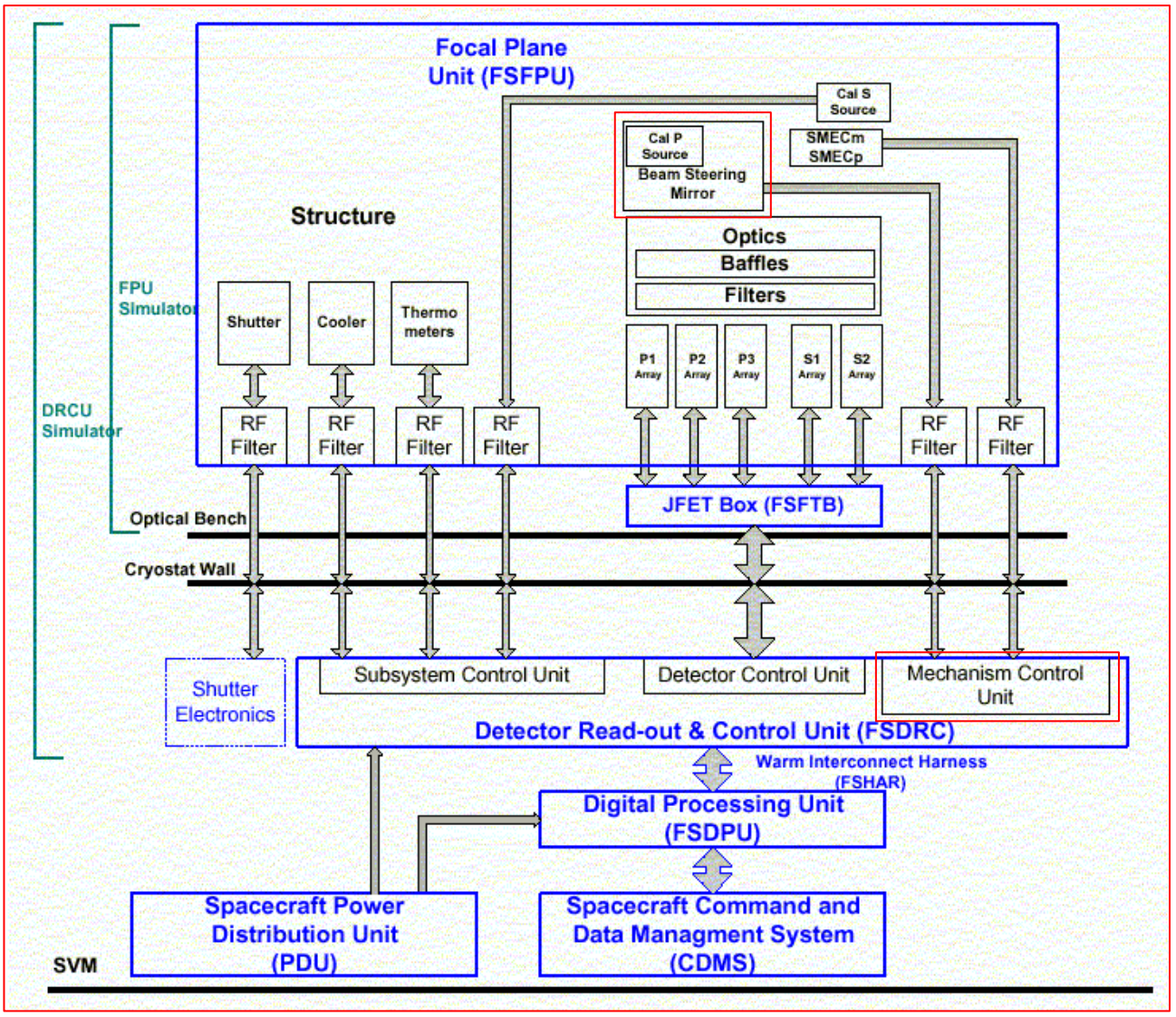

Figure: 2 SPIRE Block Diagram[1] showing BSM, Mechanism Control Unit (MCU).

[1] *Note that the terminology in this figure is in need up an update, as the spacecraft has been re-named Herschel, formerly FIRST. Hence FIRST-SPIRE Focal Plane Unit, or FSDPU should now read HSDPU.*

7. Detailed Description - Mechanical

7.1 Load environment

The BSM is a cryogenic mechanism, attached to the SPIRE Level 1 thermal straps to give a temperature in orbit at 3.5-6K. It is cooled down prior to launch and experiences a vibration load from the spacecraft, potentially amplified by the SPIRE optical bench structure. On orbit, the mechanism operates in a micro-gravity environment where the principle loads are self-induced fatigue loads during chop and jiggle motion.

During manufacture, qualification and integration the design must survive warm vibration tests (room temperature), bake-out to 80°C, thermal cooldown at a rate of at least 20K/hr (space-craft), life tests of many million cycles at 20K and cold vibrations (at 4K). Not all of the BSM models to be built will experience all of these tests, but the same design must be useable across all environments (i.e. no use of parts only clamped when cold, as they would fail during warm vibration).

The load environment is specified in AD1, as derived from AD6. In summary the maximum quasi-static loads are 25g, sine vibration 40g and random vibration 11g $_{rms}$.

The random vibration environment is summarised graphically as:

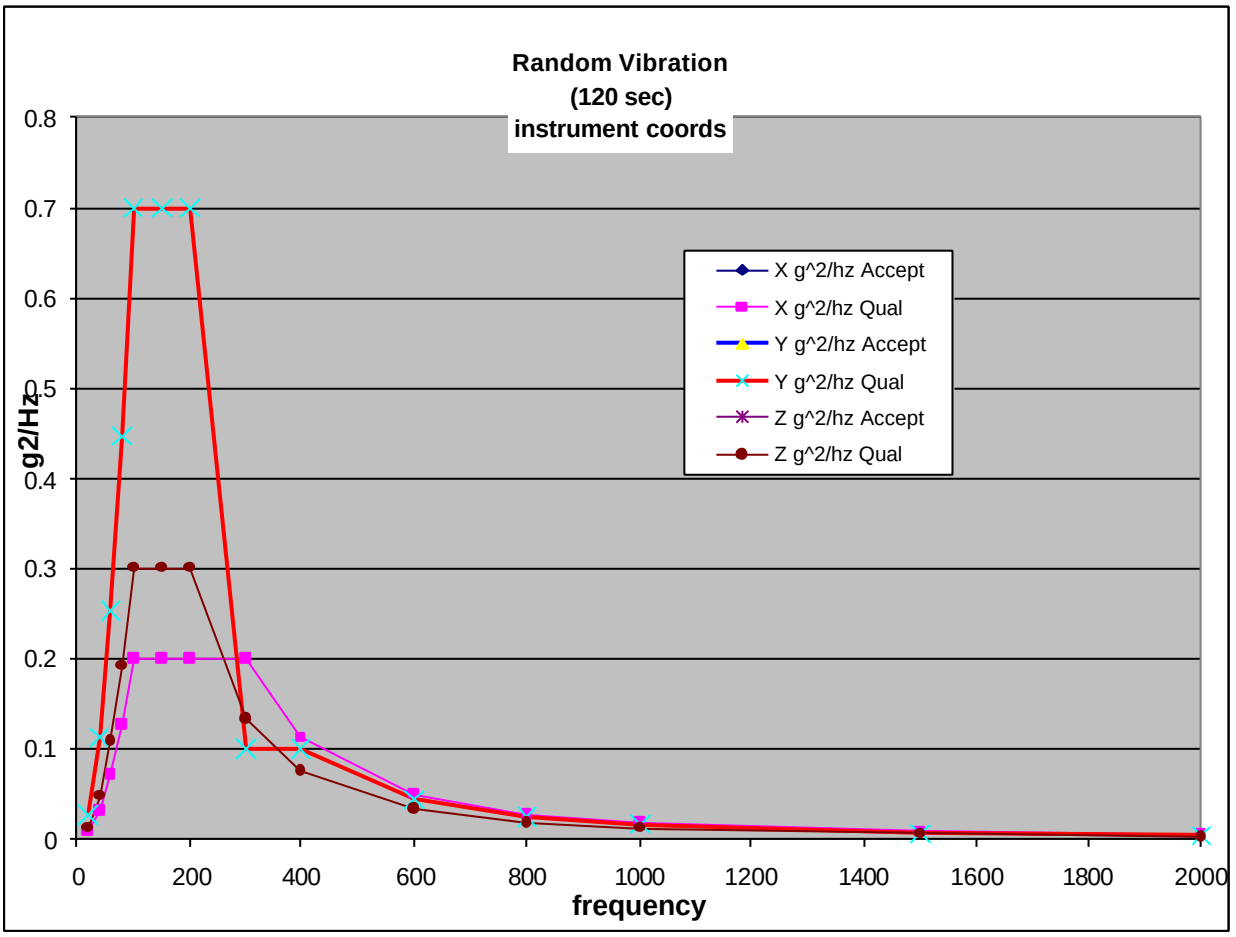

Figure 3 BSM launch load random vibration requirements

7.2 The Cryogenic Mechanism BSMm

7.2.1 General

The BSMm comprises a mirror of diameter 32.5mm, mounted so as to pivot on two axes to provide chop and jiggle motion.

The jiggle axis lies directly coincident with the mirror surface. The chop axis is recessed by 2.25mm from the mirror surface.

Each axis houses a rare-earth magnet moving pole piece and is driven by a motor coil fixed to the mechanism housing/structure. Lucas TRW or C-Flex flex-pivots provide low friction motion and a small restoring torque.

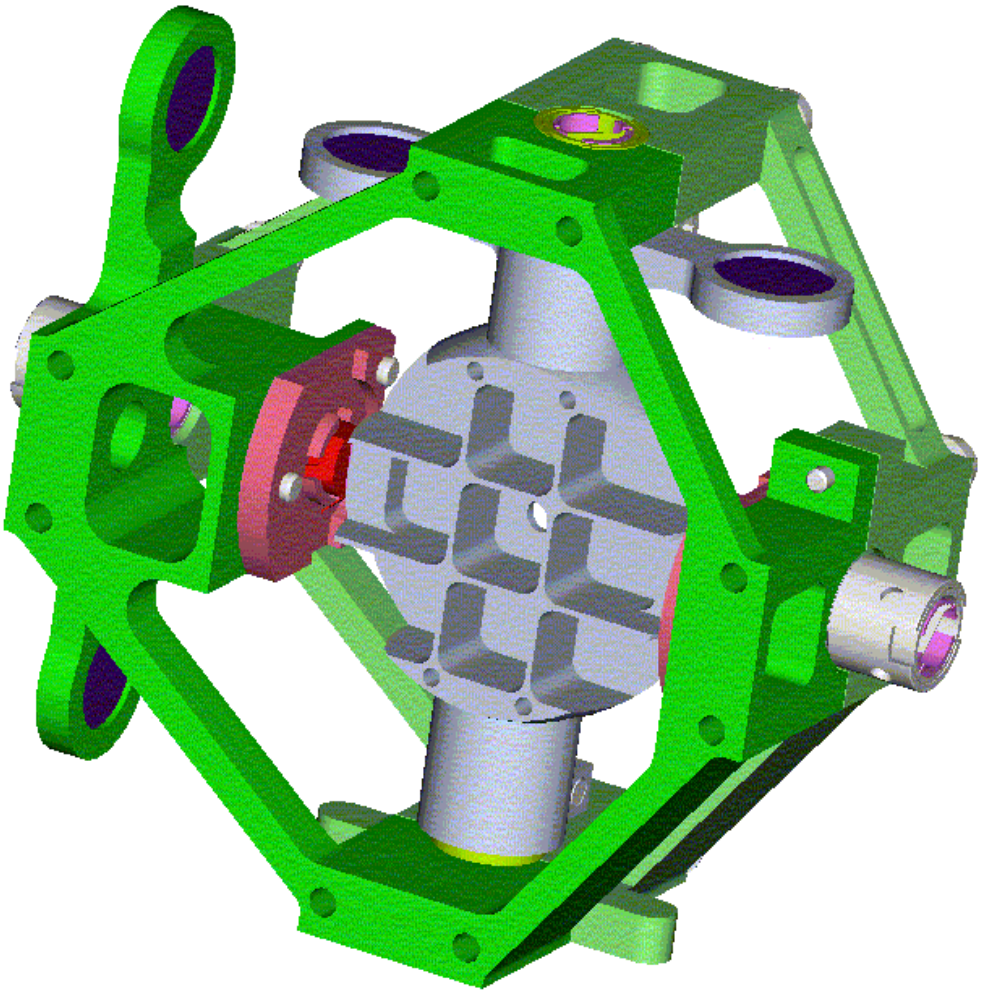

Figure 4: View on underside of mirror - Chop stage grey, jiggle stage green, motor magnets purple and sensor mounts (shown without

The chop and jiggle stages are shown above. The chop stage is monolithic with the mirror machined integrally. The underside of the mirror is light-weighted and has pockets for the iron plates for the magneto-resistive position sensors. The chop direction is along the long axis of the array (the spacecraft y-axis). A 2.8mm diameter (TBC) hole in the centre provides an optical path for the calibrator mounted behind the BSMm

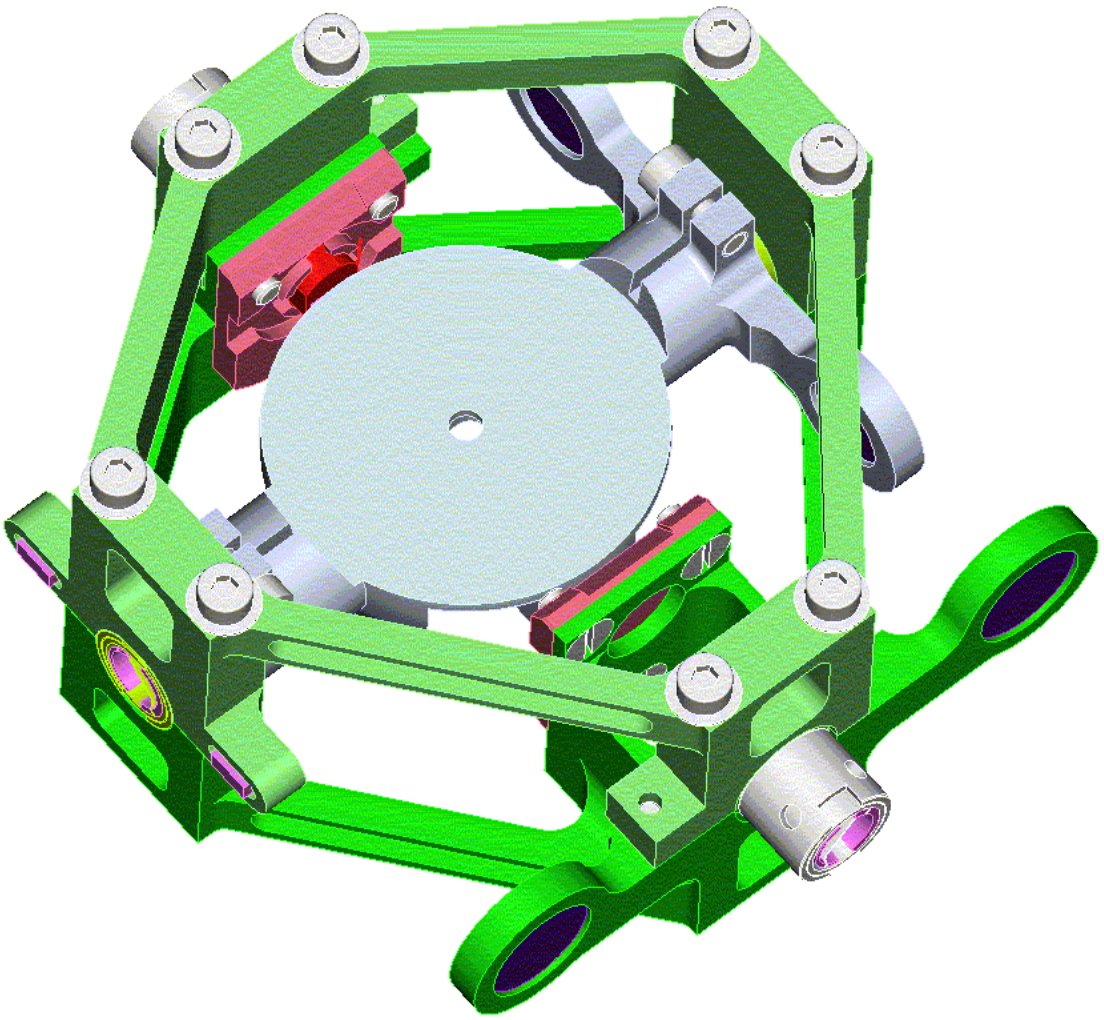

Figure 5: top side of jiggle frame and mirror. All fasteners are M2.5.

The moment of inertia of the chop stage has been minimised to reduce power consumption during chop transitions. At 2.68 kg.mm^2, it is little more than the ISOPhot rotor which was 1.57 Kg.mm^2. Rotating mass, at 21 gm is also minimised to keep loads on the flex pivots down during qualification and launch.

The jiggle stage is in the form of a split frame split and clamps together around the flex pivots. Stainless steel fasteners (M2.5) are used in self locking inserts, with a stainless steel disc-spring to retain clamping forces during cooldown. [RD14 refers]

To balance the jiggle stage the framework in the opposite corner to the coils has been made solid. This also increases the stiffness of the structure. This structure carries the chop stage, and is inevitably heavier. The moment of inertia is estimated at 47.9 kg.mm^2 and mass at 96gm. Fortunately, the requirements call for lower amplitude and frequency in this axis, so we can use stiffer flexures.

Both stages are designed to be stiff, so that the first resonant frequencies are high enough (> 700 Hz (TBC) that the system modelling can regard them as rigid bodies. [RD15 refers]

Figure 6 BSMm and BSMs with baffle ommitted. Jiggle frame in green, motor coil assemblies in orange, sensors are red/pink.

The coils and sensors are shown in Figure 6. There will be a 'primary' and 'cold redundant' motor for each axis. The baseline is that motor for a single axis will have the two prime coils on the outer side of the rocker beam, and the two redundant coils on the inner side of the rocker beam.

The coils are adopted directly from the PACS chopper design, RD 13, as it has been determined to be more cost effective to buy into a well tested coil meeting the SPIRE requirements than to design our own.

All the motor coils mount directly to the BSMs, i.e. the chop stage air gaps must be slightly over-size to accommodate chopping whilst in various jiggle modes. The current magnetic circuit has not been modelled.

Position sensors for the chop axis are mounted on the jiggle stage, which means flexible cable connections are required, unlike the jiggle stage position sensors, which mount directly on the non-moving housing.

7.2.2 Finite Element Analysis

Initial FEA work of the structure and mirror was been performed to calculate approximate strength and resonant frequencies. The original report is found in ATC document, spire-bsm-001-tdn-001.doc, see Appendix 3A.

This analysis has been be repeated to reflect design changes since this early concept work. [RD15 refers]

This early analysis assumed a slightly lighter structure than implemented in the later stages of design, where manufacturing costs and feasibility were folded in to a greater degree. The results are thus conservative in the sense that stiffness and hence resonant modes will have been increased, but non-conservative where gravity induced loads will have been increased by extra mass (about 96gm compared to 55 gm).

A full update of the analysis reflecting all design changes up to Jan.02 is in progress, under sub-contract.

7.2.2.1 Modelling

Modelling was performed using the COSMOS-M FEA package, and was based on the Pro/Engineer design models at the time of the analysis. The jiggle stage structure was been represented by thin shell elements. The chop stage was represented by a tube of solid elements together with lumped masses (shown red in the illustration below) to give the same mass and moments of inertia as the solid model. The flex pivots were modelled using a combination of solid and shell elements.

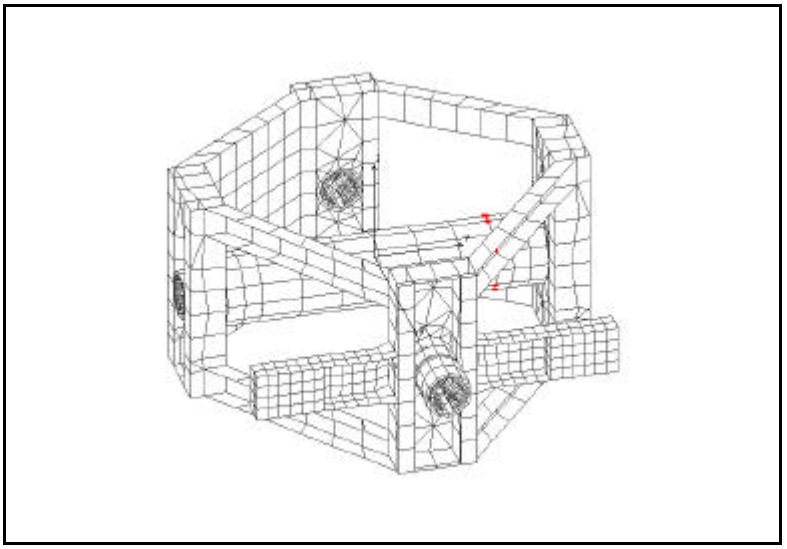

Figure 7 FEA mesh for initial stiffness modelling

The jiggle stage framework between the flex-pivot housings was modelled as 5mm x 5mm x 0.5mm channel section. (the subsequent manufacturability enhancements make this 5mm x 5mm x 1mm channel on the upper arms and 3mm square on the lower arms of the cage). The pivots have been moved as far as reasonably practical towards the mirror to minimise the inertia and maximise the stiffness. To clear the coils this leads to an asymmetric arrangement. To balance the jiggle stage the framework in the opposite corner to the coils has been made solid. This also increases the stiffness of the structure. Due to the use of lumped masses which do not give the correct products of inertia and also because the jiggle stage has not been dynamically balanced there will be some inaccuracy in modelling coupling of the stages.

7.2.2.2 Load cases

The following analyses have been made:

- 50 g static load in X,Y and Z directions
- Frequency response analysis for excitation of the chop and jiggle stages by couples of 1 Newton forces at the centre of the drive magnets (equivalent forces for the chop stage.)

7.2.2.3 Dynamics

The full report is found in Appendix 3A

7.2.2.4 Static stress analysis results

The three load cases (50g in X, Y and Z) lead to stresses in the flexures of similar magnitude, The predicted highest stress, 265 MPa, occurs in the jiggle axis flex-pivots. The 0.2% proof and ultimate tensile stresses of 420S29 equivalent to the stainless steel used for these items are 555 MPa and 755 MPa respectively so the design appears relatively safe. It should be noted however that the model is a simplified representation for dynamic analysis and would need refinement for accurate stress calculation. A more accurate appreciation of load capacity is provided by the manufacturer's rated loads, and peak loads discussed in the following section.

7.2.3 Flex Pivots

Two flex pivot types are envisaged, a light pivot for the Chop axis, and a heavier one for the Jiggle.

The baseline units are supplied by Lucas Aerospace TRW (formerly Bendix). The jiggle axis uses type 5010-600 and the chop axis the lighter 5010-800 units. These units are standard commercial off-the-shelf and use AISI grade 420 and 429 stainless steel components, assembled by brazing. The off-the-shelf grade material can suffer from cryogenic embrittlement and this high risk approach

is being taken due to budgetary constraints (inconel pivots were investigated up to DDR, but with costs for a minimum quantity >$100,000 were not obtainable within the BSM budget).

An alternative, CuBe type pivot (sizes E-10 and E-20) is being investigated, supplied by C-Flex. These pivots are dimensionally equivalent will be used if initial samples prove satisfactory.

To reduce material and tooling charges it could be desirable to use a common type of pivot in both axes. Note that if the jiggle axis were to employ a lighter type (5010-800 or E-10) pivot to obtain commonality with the chop axis the survival loading would be 90g (bucking failure): this would be inadequate to meet the 3 sigma peak launch loads from random vibration. Commonality would only be obtainable by stiffening the chop axis pivot (and increasing power budget). It is therefore NOT base-lined.

7.2.4 Flex Pivot Protection

The flex pivots are the most critical element of the BSM design, and the most vulnerable. Much design effort is thus directed towards their protection. In general flex pivots are observed to fail under shear load, by buckling of the pivot flexures or 'blades'. This failure mode is more likely if the pivots are prevented from rotating - hence any form of launch locking is undesirable.

7.2.4.1 Load control & Margin

As a first approach, the loads on the pivots are controlled as far as possible.

- Mass of the structures carried by the flex pivots (the chop axis and jiggle frame) is kept as low as practical, as this minimises loading during launch. Additional margin could be obtained by further light-weighting of the jiggle frame components, but is currently not required on technical grounds.
- The BSM mounting structure, jiggle frame and chop stage are kept stiff so that that the risk of amplification of the loads transmitted during launch are minimised.

Initial FEA work of the flex pivots has been performed to calculate stresses in flex pivots upon launch.

In addition, a static analysis is presented in Appendix 3C. The safety factor for 3-sigma peak response during vibration testing is:

BSM margin - flex pivots & structural bolt

Temp	Component	mass (incl contingency)	load limit of component (N)	required FoS	survival load (in g) for 2 pivots	margin on rms response	margin on 50% peak response	margin on 3-sigma peak response
WARM 290K	C-Flex Chop axis flex pivot	21.0	25.4	1.0	246.6	8.70	1.84	1.45
	C-Flex Jiggle axis flex pivot	96.0	248.3	1.0	527.3	18.60	3.93	3.09
	LUCAS chop axis flex pivot	21.0	25.4	1.0	246.6	8.70	1.84	1.45
	LUCAS jiggle axis flex pivot	96.0	245.0	1.0	520.3	18.35	3.87	3.05

COLD 4K	C-Flex Chop axis flex pivot	21.0	28.1	1.0	273.1	9.63	2.03	1.60
	C-Flex Jiggle axis flex pivot	96.0	275.0	1.0	584.0	20.60	4.35	3.42
	LUCAS chop axis flex pivot	21.0	26.9	1.0	260.9	9.20	1.94	1.53
	LUCAS jiggle axis flex pivot	96.0	259.2	1.0	550.4	19.42	4.10	3.23

Table 1: Rated static loads and margins.

The 'required 'FoS' is set to 1.0 as the Qualification load factor incorporates the ESA mechanism FoS.

The C-Flex CuBe grade pivots are manufactured in a higher grade material and have additional margin. The manufacturer's quoted rated load should be treated with caution, but is nominally as shown.

The rated life for these flexures, is in the 'infinite life' range of the spectrum, assuming 1g loadings. The flight hardware will receive the bulk cycling in zero-g.

7.2.4.2 Protection Sleeves

To prevent damage by shear of the mechanism on launch a flex pivot capture sleeve, similar to this used by Goddard on COBE, will be utilised, as sketched below.

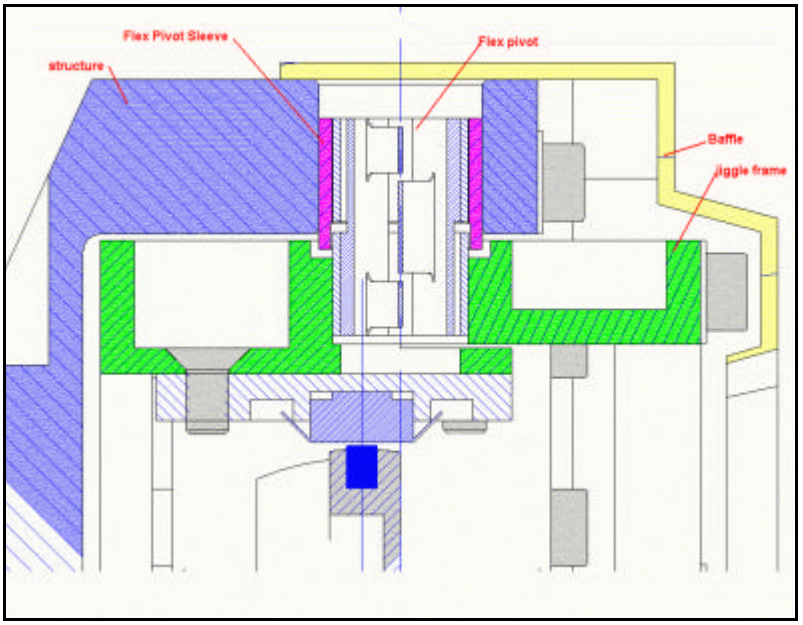

Figure 9 : Flex pivot protection sleeves, á la Goddard

Based on holding the +/-0.18° requirement on the nominal (0,0) position, in the BSM specification a ~ 125 micron diametral clearance would be required on the pivot sleeves given the ~80mm distance between pivots. This would prevent slop in the jiggle pivots producing an apparent chop motion, or vice versa. Without constraint, the standard flex-pivots would produce about +/-200um of slop (though they would fail before this was reached).

A working flex pivot produces some de-centring motion as it twists anyway: about +/-20um of linear motion in our case. We would arrange for this to be in the plane of the mirror (careful of course to install flex pivots in handed pairs, to prevent twist).

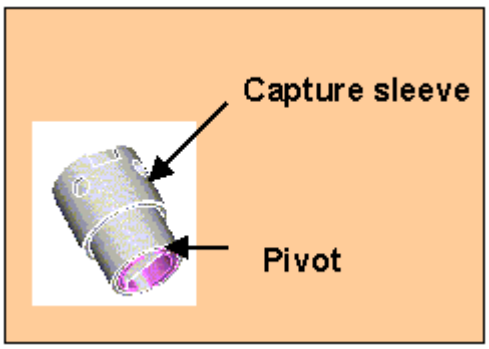

Figure 10 : Flex pivot and sleeve

The ATC pivot sleeve design provides for 50-75um of clearance, which is sufficient to

- allow normal rotation (and associated de-centre),

- prevent buckling failure of the pivot by shear loading (TBC by load tests)
- provide for capture of any broken pivot with 0.111 degrees of slop, sufficient to meet the fail-safe regime

Assembly of the sleeve to the pivot is by a light push fit, which becomes a close fit on cooldown. As this would be inadequate to survive warm vibration, an adhesive (will be used to ensure the flex pivot is secured. The adhesive is supplied via radial holes drilled in the sleeve. The sleeve also contains an alignment slot to aid assembly.

7.2.4.3 Flex-pivot failure modes:

Launch loads are a much larger concern than long term fatigue life, which is well characterised and easily tested. Tests performed by LAM suggest that the primary failure mode on launch would be where the flex pivots suffer shear in the radial direction, and the flex pivots fail in a buckling mode.

a) In the event of flex pivot failure, we could control position by motors alone and the random slop of the pivots would remain within spec. Long term chop or jiggle would not be advocated as we presume the capture sleeves would make poor journal bearings and would wear relatively quickly. However, the aim would be to move the mirror to a rest position and then hold it against spacecraft micro vibration.
b) In the event of motor failure (or launch damper failure to disengage), the flex pivots would provide self-centring (note that alignment of the centred position on integration will thus be critical, unless this is adjustable elsewhere in the optical path).
c) If both motors and pivots fail the position would be completely indeterminate, probably an end-stop out of the spectrometer field of view.
d) One other failure mode could occur - the linear de-centre of the flex pivot is produced by a combination of opposing de-centre of each flex spring. If only one of them fails we assume that the de-centre will include an out-of plane component. e.g. if one chop pivot 'half failed' then a chop demand to the end-stop would also produce a 20um lift of that end of the chop axis (a small jiggle and a mirror translation of 10um upwards). This failure mode would probably only exist for a short while until the second flexure also failed, and would be correctable in software if identified.

7.2.4.4 Launch Latch

The failure mode (c) above advocates for a launch latch. The argument against a launch latch is that

- the added protection against mission loss from this dual failure is set against the risk of de-scoping to scan-mode only from a launch latch failure,
- over constraint of the pivots would increase the risk of failure.

Only a full program of launch latch and mechanism qualifications sufficient to quantify this trade off statistically would generate a logical decision one way or the other and funds for such a programme do not exist.

The baseline that has been agreed is to provide a compromise ‘deployable end stop’. In this scheme, a launch lock pin is used, but instead of deploying firmly into a detent, it would deploy into a hole with sufficient clearance to allow for +1.5°/-2.4°[2] of chop axis motion and unrestricted (0.6°) jiggle motion. In the event of combined motor and flex pivot failure it would limit the wander of the chop stage to within the spectrometer field of view. This baseline design would be included in the early qualification tests, and would be deleted later if proven that it was demonstrated not to be required.

A candidate launch latch has been identified by LAM for the SMEC mechanism and is illustrated below. LAM are undertaking a flight qualification programme for this device. With

[2] TBC whether this is +1.5/-2.4 or -1.5/+2.4

small modifications (e.g. front mounting, increased length of pin) the LAM device will meet the BSM requirement.

An ATC space envelope drawing has been prepared for exchange of information with LAM, drawing number SPIRE-BSM-020-001-007.

The LAM supplied solenoid lock pin may be exchanged for a slightly longer pin on receipt by ATC (TBC). Use of a compliant pin (e.g. Vespel SP1) would be desirable to reduce impact (chattering) between the pin and be mirror on launch and will be considered.

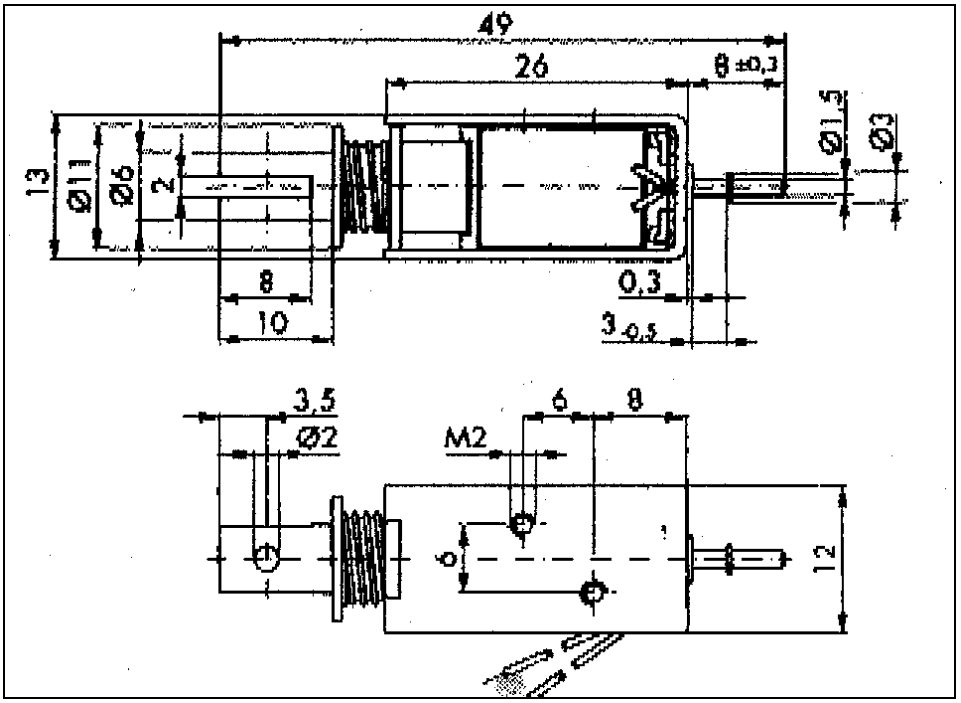

Figure 11 Candidate Launch latch (courtesy LAM)

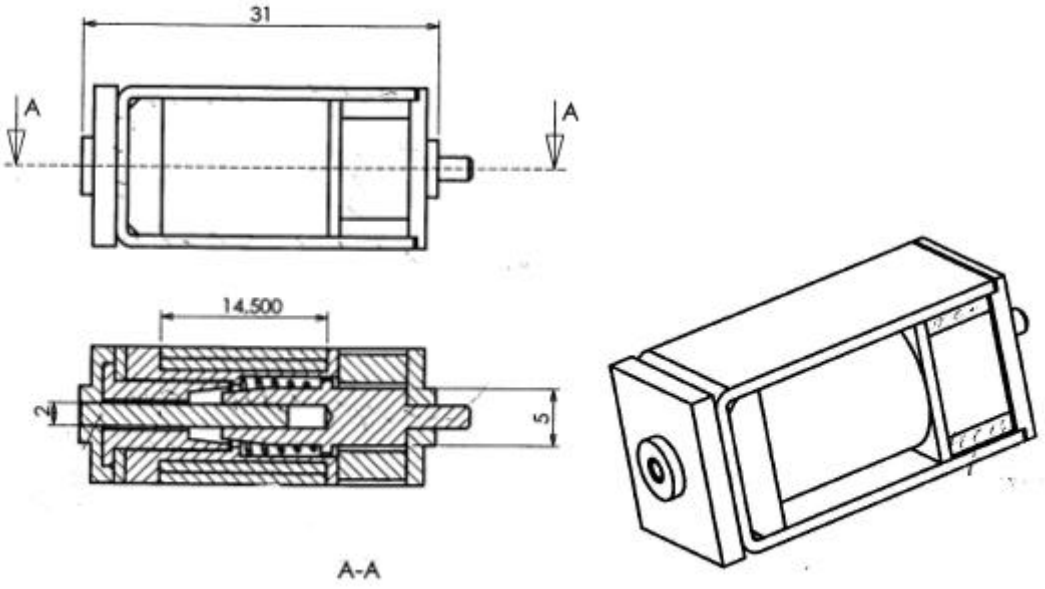

Figure 12 : LAM redesign of launch latch for space approval

Another alternative could be to request a reduction of the maximum chop axis throw, such that when its at its end stop half the FTS field of view is available. This would be based on a trade off decision that user demand for the full chop throw might be limited. G. Wright advises that mostly observers will do pixel-pixel chopping on small sources and scan map with (small) chop on the big ones, and there just aren't that many medium sources in the sky. However, this option is not the baseline.

7.3 Structural Interface

7.3.1 The Support Structure BSMs Design

The BSM Structure – or BSMs is a machined stiff aluminium alloy mount with a mass of ~ 310 gm, and an associated baseplate (or 'mounting shoe') of mass ~ 85gm.

The mounting and alignment functions of the baseplate are described in section 9 (optics)

The BSMs provides for mounting of the:

- jiggle stage flex-pivots,
- jiggle stage sensors
- the jiggle and chop stage motors
- thermometry
- Photometer calibration source (PCAL)
- harness and connector mounts
- baffle

Figure 6 Above (page 16) shows the BSM with baffle omitted.

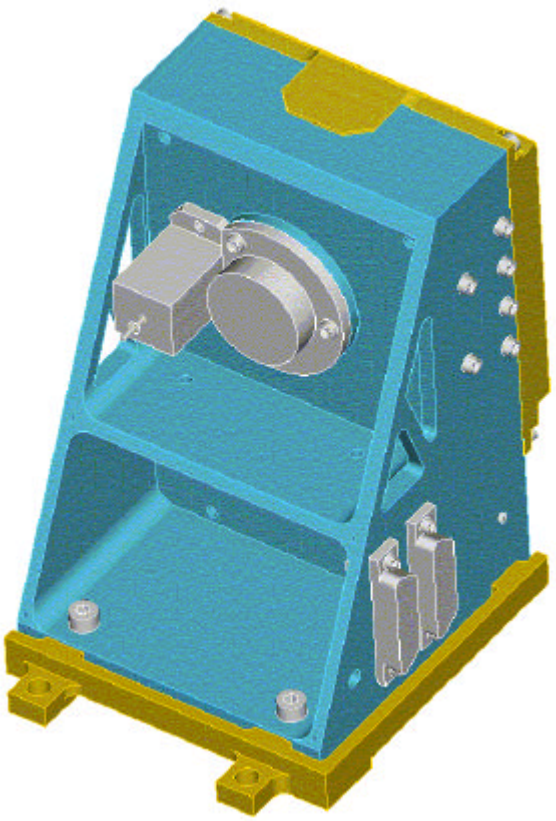

Figure 13: BSMm and BSMs, with baffle. 3D view from Pro/E model looking from the rear.

The PCAL unit is shown mounted to the flat surface to the rear of the jiggle frame and motors. The launch latch is shown on axis, but in practice will be behind one of other chop motor arm, once sign conventions have been determined

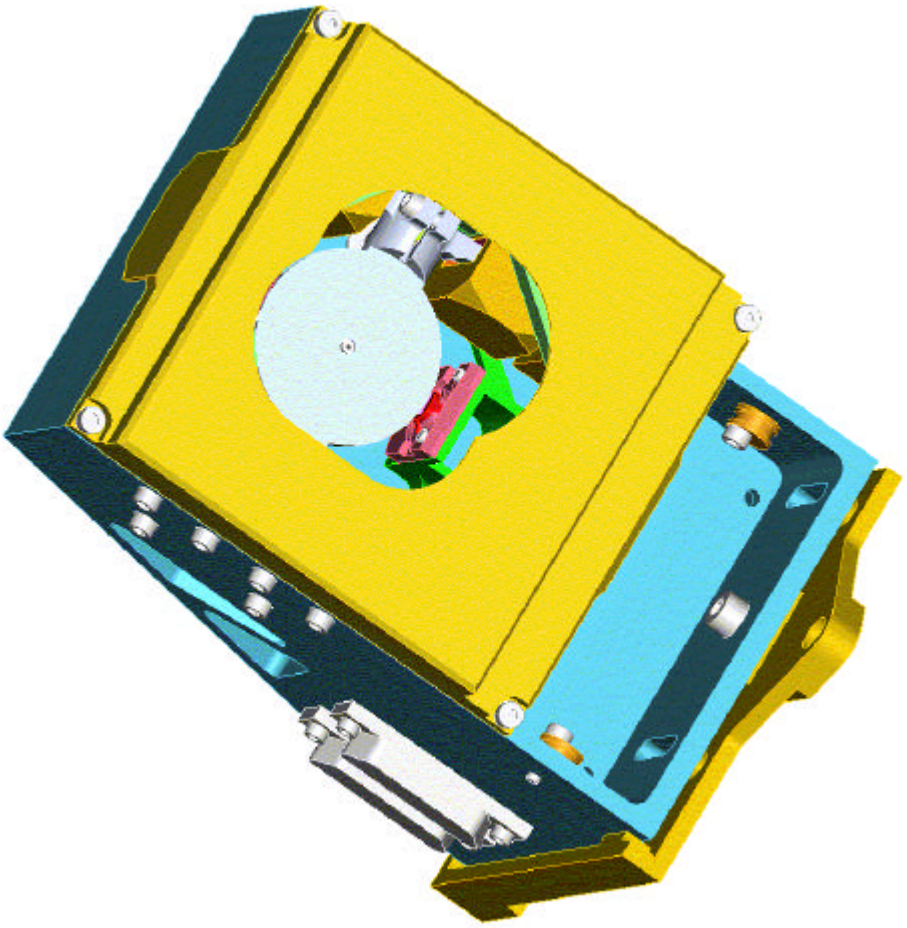

Figure 14 BSM showing the baseline baffle.This view from a marginal ray point (apparent as the full circle of the mirror is projected on the baffle edge from the line of sight), shows much of the mechanism is visible (non-conformal baffle)

7.3.2 BSMs FEA

An FEA of the structure has been performed to establish the likely induced stresses on launch, and the vibration modes. The results are detailed in Appendix 3B.

The model was analysed in Pro/Mechanica, based on the Pro/Engineer solid model with some small simplifications. Three runs were performed:

1. A three-axis static gravity load of 50G in each axis was applied to the structure. These were applied to give maximum tensile loads at the rear harness connection points.
2. A second run was performed as (1) but with point loads also applied at the relevant positions to simulate loads from the motors, jiggle and chop stage and attached components.
3. A basic vibration mode search for the first 12 resonant modes was performed.

Reported peak von-Mises and principle stresses were stresses peak at 36 MPa, situated around the connector mounting points. Using conservative values of permissible load (per BS8118), allowable stresses would be:

For fatigue

- 67 MPa friction grip bolted zones (not strictly applicable here as loads are not construction level friction grip)
- 96MPa for re-entrant features
- 76MPa small holes (dia < 3t)

For parent plate

- 240 MPa with suggested load factor of 2.5, i.e. a target of 96 MPa in this case

The permissible stresses for space rated components per RD6 are

- Margin of Safety = allowable stress limit / (actual stress x factor of safety)
- Where factor of safety = 1.25 on yield, 1.5 on ultimate, factor of 4 x (cycles) on fatigue.

7.3.3 Vibration Response

The principal resonant modes of the structure and the two suspended masses are presented below. The following discussion is repeated definitively in Annex B, as part of the BSM structural ICD.

The BSM structural interface forms a stiff body. The first twelve structural modes were determined by finite element analysis

Response of structural interface (SPIRE-BSM-020-001-001 Rev1)		Approximate assembly response
Mode	Frequency (Hz)	Frequency (Hz)
1	688	419
2	864	526
3	1781	1085
4	2715	1654
5	3058	1863
6	3284	2000
7	3345	2037
8	3614	2202
9	3957	2410
10	4097	2495
11	4677	2849
12	5185	3158
	mass of structure	305
	mass of assembly	822
	scaling for resonance	0.609

Table 4: Structural Interface Principal Modes

7.3.4 Scale factor

Pending a full resonant modes analysis, we may note that since the stiffness of the structural interface design remains unchanged, the assembly natural frequency scales as:

$$f_n = \frac{v\,(k/m)}{2\,?}$$

hence, $f_{n(assy)} / f_{n(struct)} = v(m_{struct} / m_{assy})$

This yields a scaling factor of ~ 0.61, used in Table 4. More up to date analysis is underway at the time of writing (se RD15).

7.3.5 Assumptions

As the structural response remains above 250 Hz it may be assumed to be stiff for subsequent analysis of the SPIRE structure. The actual combined system modes will differ from those presented, due to contributory effects from:

- the effect of bolted joints,
- the contribution of point masses mounted to the structure as distinct from the distributed structural mass
- the resonances of components mounted to it (particularly the baffle, launch lock and motor mounts)

7.3.6 Suspended Masses

The BSM suspended masses have first natural frequencies approximately as follow (Lucas TRW stainless steel pivots):

Axis	Mode	Spring Stiffness (N-m/rad or N/m) - WARM	Spring Stiffness (N-m/rad or N/m) - COLD	Inertia (kgm^2)	Mass of suspended part (grammes)	1st Resonant frequency (Hz) - warm	1st Resonant frequency (Hz) - cold
Chop	**Torsional**	0.05875	0.062275	2.68E-06		23.6	24.3
	Radial Orthogonal	1225888	1299441		20.59	1228.1	1264.4
	Radial 45 degrees	875634	928172		20.59	1037.9	1068.6
	Axial	1751268	1856344		20.59	1467.8	1511.2
Jiggle	**Torsional**	0.4625	0.49025	4.79E-05		15.6	16.1
	Radial Orthogonal	2101522	2227613		96	744.6	766.7
	Radial 45 degrees	1576141	1670710		96	644.9	663.9
	Axial	3152282	3341419		96	912.0	939.0

Table 5 : Suspended Mass Principal Modes

The radial orthogonal rate is where the load is z-x plane or in the plane formed by the optical bench y axis and the BSM gut ray.

The 45 degree radial rate is where the load is applied in line with the plane of a flexure (oriented at 45 degrees to the orthogonal planes).

These values assume the baseline Lucas TRW stainless steel brazed flex pivots. If a change is made to C-Flex CuBe brazed pivots the spring stiffnesses would change slightly: chop axis to 0.90x the values above, jiggle axis to 1.08x the values above (TBC):

7.3.7 Outputs

The BSM will output a vibration to the Optical Bench during chopping and jiggling. The primary output will be at the chop and jiggle frequencies : 2 Hz and 0.5 Hz respectively, with harmonics TBD. Local TBD resonances of the BSM (eg of the baffle) may modify the harmonics.

Neglecting harmonics and any structural amplification (which should be small anyway, as the structure is stiff) the output forces take the form of a torque reaction in the structure in response to the acceleration of the mirror and jiggle frame in chop and jiggle.

An approximation to this torque reaction may be made by taking the inertia of the moving masses, and an average acceleration over the specified rise time.

BSM reaction loads summary table	Chop (*)	Jiggle (**)	Units
Torque reaction about chop axis (average)	11.25E-06	0	Nm
Torque reaction about jiggle axis (average)	0	10.03E-06	Nm
reaction force at hole at (242.57, 117.2, 526.863)	10.65-05	1.47E-04	N
reaction force at hole at (351.861, 117.2, 521.426)	-5.32E-05	3.81E-05	N
reaction force at hole at (334.299,117.2, 467.198)	-5.32E-05	3.81E-05	N
** Chop reaction forces in optical bench y-axis* *** Jiggle reaction forces in optical bench z-x plane (normal to BSM jiggle axis)*			

Table 6: BSM Reaction Loads

Strictly, these reaction forces are in matched pairs with no net thrust effect. Thus an equivalent 'micro-g' output cannot be attributed to the BSM, i.e., a 'micro-g' input is only resolved at the interface between the optical bench and another supported system.

As a working figure, at a BSM mass of 0.82kg, the 'g' loading required to provide this type of force input combining the chop and jiggle loads gives a nominal acceleration at the front hole of 3.09E-04 m/s², i.e. an 'equivalent g loading' of 31.5 micro-g. In reality, the relevant mass is that of the whole structure, which is an order of magnitude more massive than the BSM. Thus accelerations attributable to the BSM will be well below 10 micro-g.

7.4 Components & Declared Lists

7.4.1 Declared Components List (DCL)

The Mechanical declared parts list is maintained as a project configured document, AD10. Additional electronic components are declared in AD12

The combined DCL will be supplied as part of the Acceptance Data Pack for each of the BSM deliverable models.

7.4.2 Motor coils

The BSM motor coils are adapted from the PACS design, and will be supplied as space-rated items by Zeiss, via MPIA. Per RD13 the motor construction is:

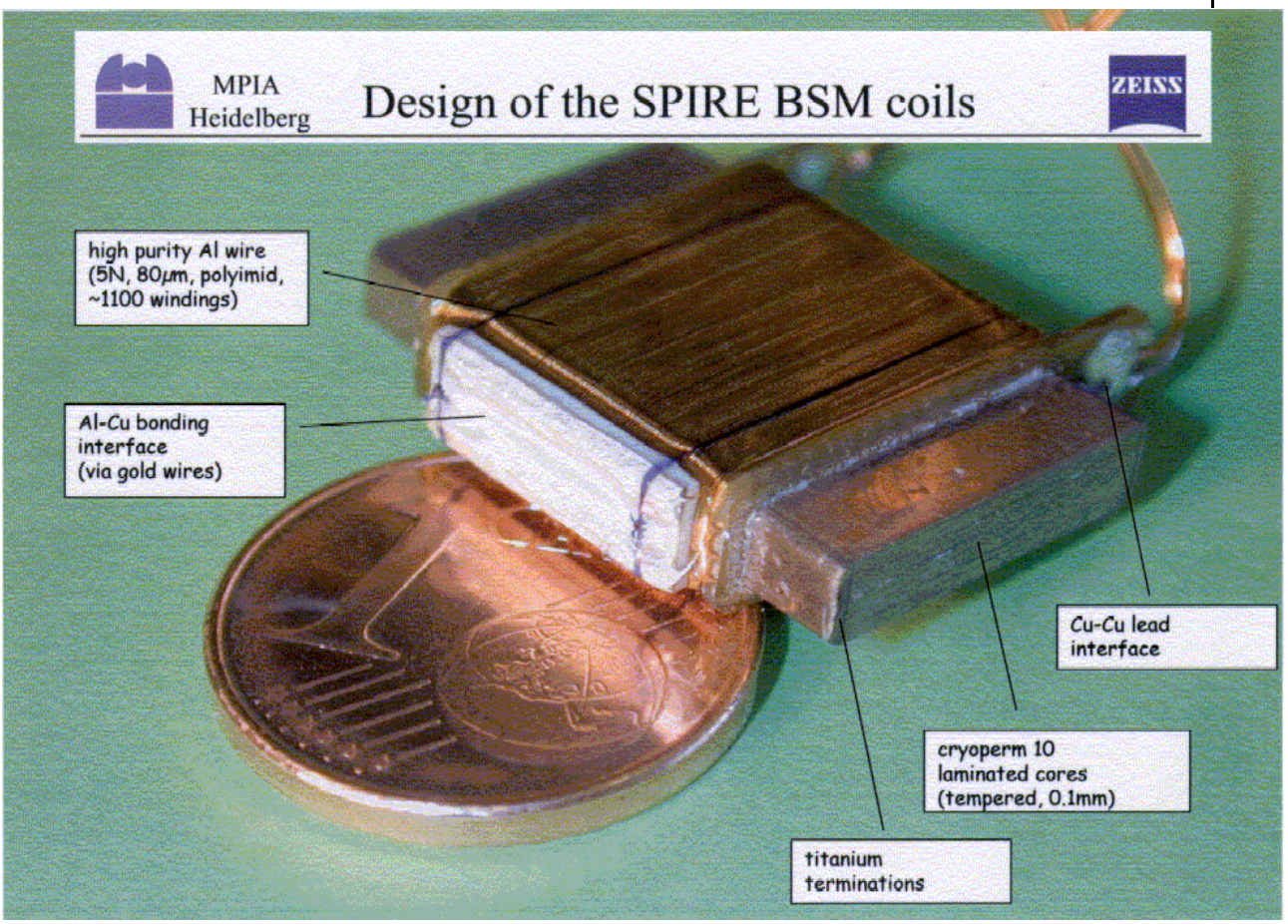

Figure 15 Zeiss/PACS coils, courtesy MPIA

The core material is Cryoperm 10 (Vakuumschmelze) with high permeability ($\mu_r > 10^5$) and high saturation fields ($B_s > 0.9T$), both at temperatures around 4K. This is laminated with ~112 sheets each at 0.1mm, glued and encapsulated with Stycast 1266 in layers of approximately 10µm thick. After vacuum degassing the laminates are milled to size and prepared for windings. A titanium termination provides a rounded winding surface and improved thermal path. The winding comprises 80µm 5N aluminium (1100 windings).

The aluminium wires are terminated via an intermediate gold strip on a ceramic pad, and feed out to copper wires which provides a standard Cu-Cu solder lead tab.

7.4.3 Fasteners

All fasteners will be a cryogenic grade (i.e. austenitic) stainless steel. Fasteners will all be locked to withstand vibration. This is achieved by one of three methods:

- use of a locking insert in the tapped hole (preferred). The smallest locking inserts readily available are M2.5, and this is hence the generally preferred BSM fastener size. the advantage of universal usage of these fasteners is that in general any obviously tight screw will be locked by default. Inspection of the tapped component at manufacture must verify that locking inserts have been assembled in to the component.
- Torque control is important in ensuring a locked connection, and providing sufficient pre-load to avoid loosening of an Al-SS joint on cooldown.
- To avoid vacuum welding of cleaned metal-metal components in vacuum conditions, all screw threads will be treated with a lubricant. This will also reduce pre-load scatter. The baseline lubricant will be MoS_2. (TBC - action in progress at RAL/MSSL to define SPIRE lubrication procedure).
- For M2.5-0.45 threads the recommended preloads are discussed in RD14, nominally 500Nmm (lubricated), 1000Nmm (un-lubricated). Torque measurements are complicated by the presence of locking factors, and appropriate procedures will be determined experimentally (TBD)
- The SPIRE optical bench thread sizes are UNC to match an elliptical closure insert favoured by the SPIRE structure supplier, MSSL. MSSL will provide these fasteners.
- Where smaller thread sizes than M2.5 are required, a controlled amount of adhesive (Stycast – TBC) will be used under the fastener head. This provides a visual indication that the fastener is locked.

Fastener torque's are important and must be sufficient to ensure adequate lock up of joints, but not over-torqued where damage to the mounted components and the fastener or the thread may occur. Guidelines on fastener torque will be added to assembly drawings, and will be verified during prototype assembly.

Thread lock will not be used in the BSM, mainly as subsequent verification by inspection is difficult.

7.4.4 Materials

The declared materials list is maintained as a project configured document, AD11.

The DML will be supplied as part of the Acceptance Data Pack for each of he BSM deliverable models.

7.4.5 Declared Processes

The declared processes list is maintained as a project configured document, AD9

The DPL will be supplied as part of the Acceptance Data Pack for each of he BSM deliverable models.

8. Thermal Control

8.1 Thermal Path

The BSM block diagram is shown in Figure 16 below.

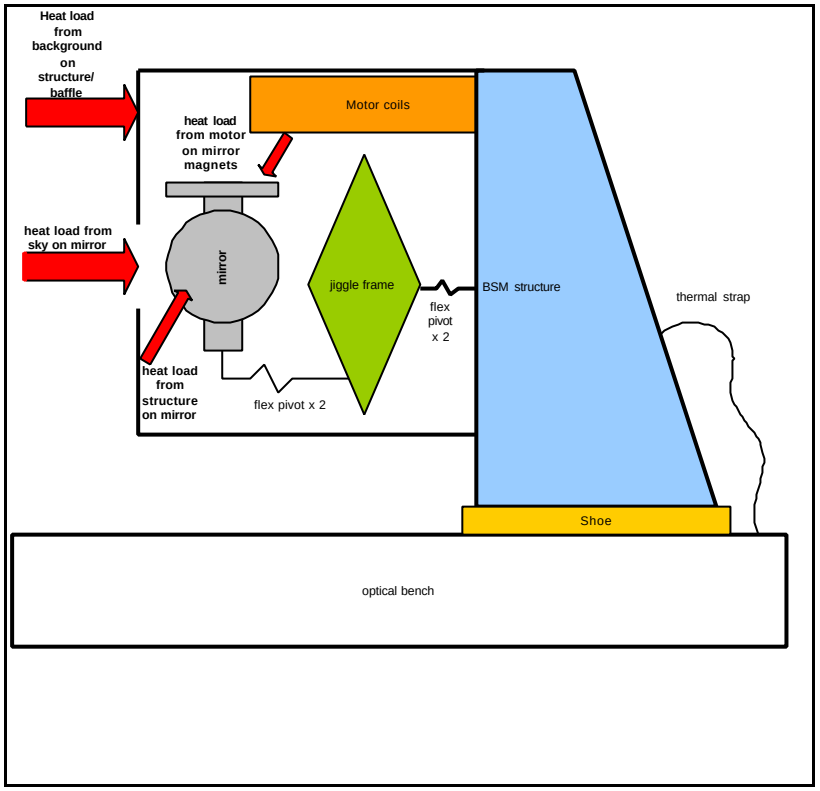

Figure 16 BSM thermal block diagram

8.1.1 Strap Connection

A provision has been made on the BSMs structure for a thermal strap connection against the eventuality that thermal straps are required in addition to bolting to the SPIRE optical bench. These may be required in particular if the interface 'shoe' provides too high a thermal resistance, or if the optical bench sees heat loads from other mechanisms.

A clearance hole for M4 is nominally provided on the rear BSMs 'shelf' to take a nut and bolt clamping a thermal wick end-tab. The position, thermal strap end details and hole size are indicated on interface drawings SPIRE-BSM-021-001, sheet1.

8.1.2 Heat Path to Mirror

One area of concern is thermal path through to the mirror, which includes two sets of flex pivots, five bolted joints and two adhesive or clamp-fit (TBC) joints.

Calculations (appendix 6) indicate that the chop axis flex pivots restrict the thermal path (i.e. are significantly less than all bolted joints and/or of material sections downstream).

As the specified instrument cooling rate is to be no more than 20K/hour the thermal shock and differential expansion issues are minimised. However, a remaining issue - more so for ground based tests at ATC than for the integrated instrument, is that thermal load on the

mirror from cryostat background radiation is significant compared to the ability to dissipate the load via the pivots.

Results of calculations (appendix 6) are shown in the chart below, and indicate that with cryostat background temperatures of >30K the thermal specification that the mirror 'not exceed the BSMs temperature by >1K' would not be met.

For tests, this may require that a thermal IR filter be fitted to the test cryostat radiation shield, or that the temperature validation tests are performed with the radiation shield aperture closed.

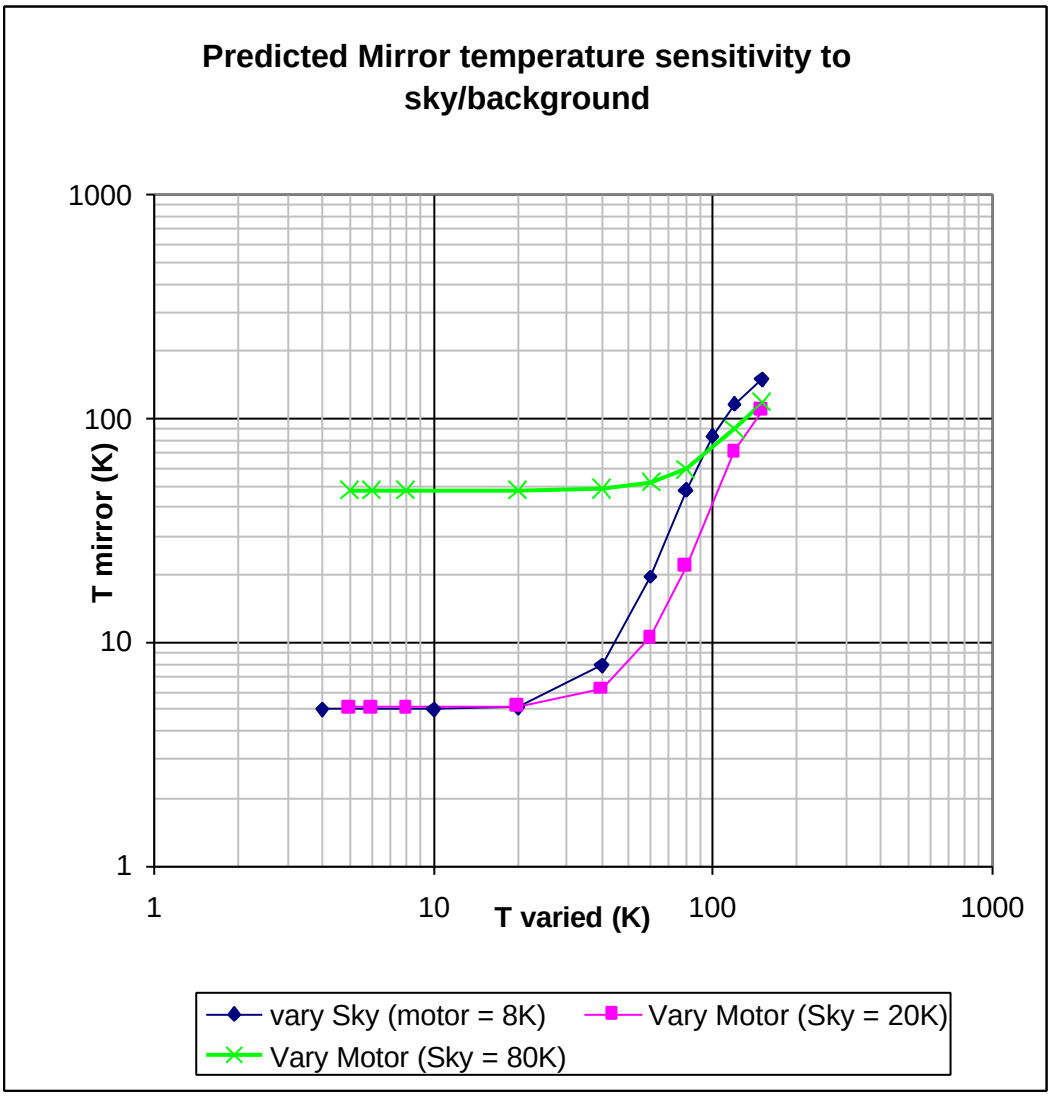

Figure 17: predicted mirror temperature at varying background radiation loads. The Sky or Motor coil temperature is varied (x-axis) and the predicted mirror temperature shown (y-axis). The local radiation from motor copils is shown to be a small effect

The jiggle stage sensor cables will provide some thermal path, though they will not be locally heat sunk. A change to CuBe pivots would significantly enhance the thermal path..

An option exists to improve cooling path - during cooldown the chop and jiggle stages will be driven to the end of travel, (or against the deployable end stop, TBD) where the end-of travel end stop will be designed to provide some thermal contact for cooling. Thus, in the baseline

design (TBC) a thermal end-stop will be adopted as with the PACS chopper [RD 13] provide an additional cooling path.

8.1.3 Heat Path to Motors

A second concern is that the motor coils may overheat, causing either life reduction or a thermal hot spot visible to the detectors. To minimise eddy current losses the motors are housed in an aluminium mounting with a G-10 end cap providing a non-metallic closure.

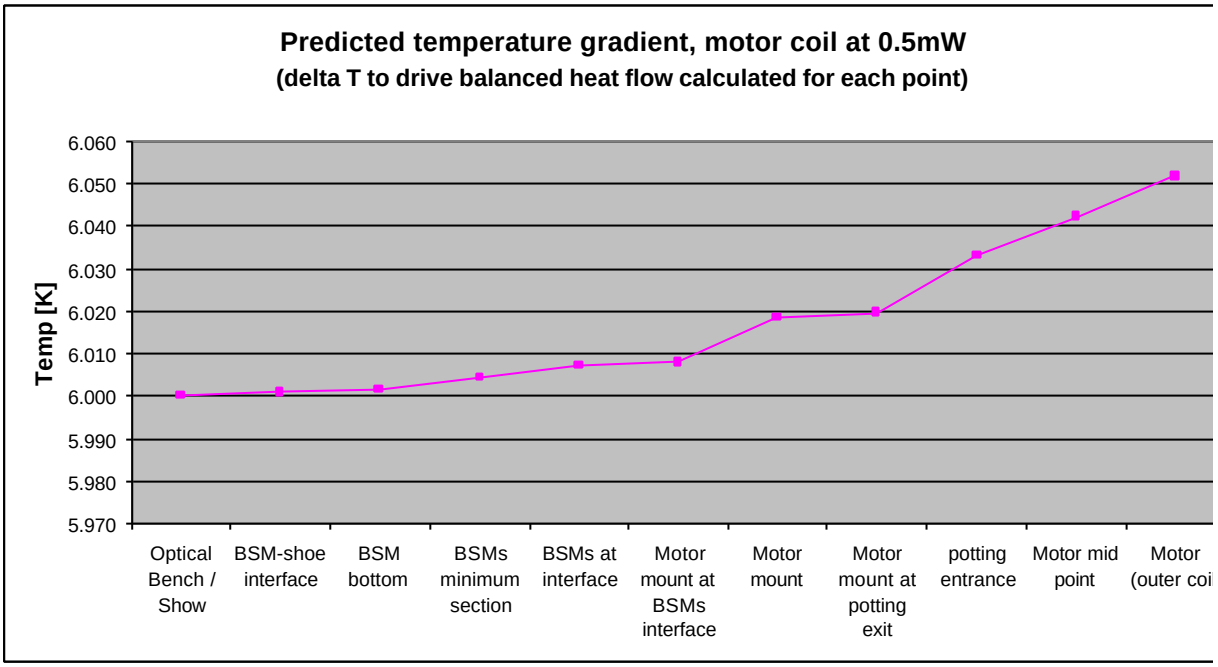

Figure 19: Cooling of motors : heat flow balanced along thermal path at 0.5mW.

The temperature curve indicates temperature required to drive heat flow of 0.5mW. Radiation from the motors is considered, assuming a 'sky' temperature of 6K, but radiation from the structure is ignored. The main restrictions on thermal path are at the motor-mount to structure bilted joint, and at the potting layer which holds the motor in (thermal properties of Stycast 1266 used). The motor core is assumed to have conductivity similar to mild steel, In practice it is a NiFe/Stycast sandwich with Ti strips down each side. The analysis suggest background temperature would remain in specification (<1K above structure)

The possibility of local hot spots may remain, and is dealt with by a combination of a local baffle around the motors, combined with heat sinking of this local shield to Aluminium parts of the structure.

8.1.4 Flex Pivot Thermal Stresses

Given the restricted thermal path of the pivots, concerns exist for flex pivot stresses induced during cooldown. 2 axis prototype data, using stainless steel flex pivots, indicates worst case differentials of

chop stage (225K) - jiggle stage (186K) = 39K
jiggle stage (260k) - structure (100K) = : 160K

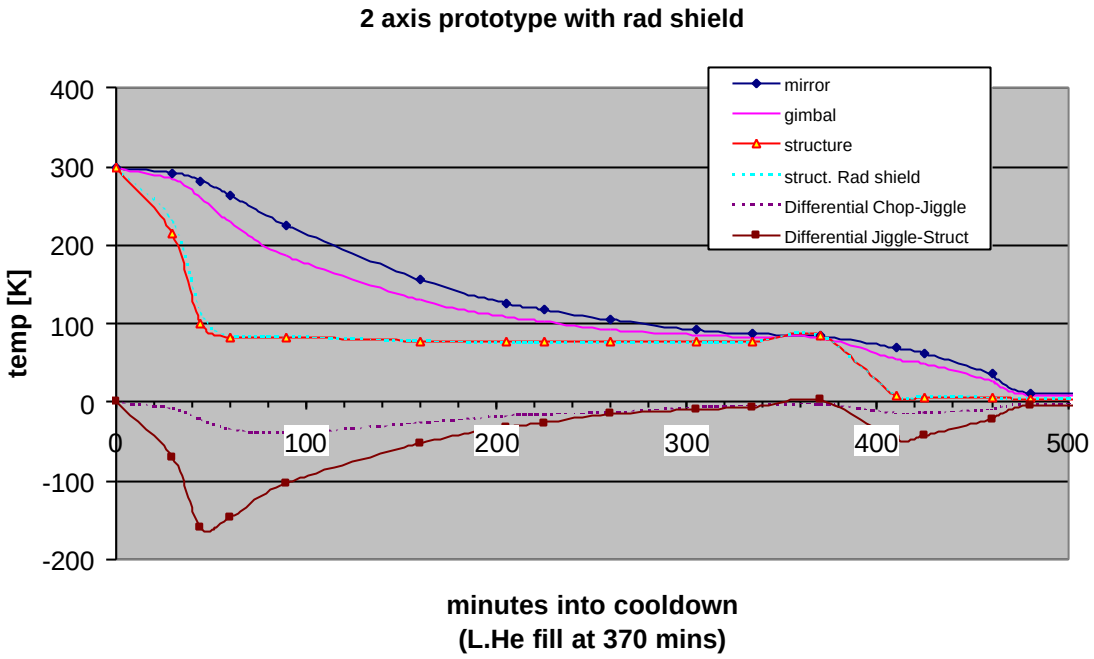

Figure 20 : Actual cooldown datea (2 axis prototype)

The worst case differential equates to a compression of the jiggle axis by 0.22mm, however stresses on the flex pivots are minimised by the inherent flexibility of the jiggle frame. The Stiffness of each pivot in compression is ~3100 N/mm, the frame at ~0.9N/mm (based on manual approximation that each jiggle frame arm is a simple beam). This keeps the total axial forces down to ~0.2N.

In the chop axis case, the central axis is stiff but again the jiggle axis flexibility limits the loads. The peak differentials on the chop and jiggle stages occu well spaced in time, which ensures the jiggle axis can provide the required flexibility first in one direction, then the other.

8.1.5 Magnetic shielding

Strong stray magnetic fields around the motor coils would be undesirable if they interfered with the BSM magneto-resistive sensors or the instrument detectors. No EMC requirement has yet been set by the SPIRE systems team, and it is assumed that the local BSM requirement dominates.

The ideal magnetic shield enclosure would be similar to those discussed for local heat shields above. However, magnetic shielding is generally achieved by thin sheets of a magnetically soft material (e.g. mu-metal) built up in layers. This would be difficult to achieve around the BSM motor assemblies within the compact space envelope currently envisaged. In contrast a heat shield may be of monolithic construction, making fabrication and fastening easier.

Basic lab tests (appendix 9) indicate no problems with the magneto-resistive sensors even when deliberately placed close to the operating BSM motors, which has lead the BSM design to de-emphasise full magnetic shields.

The ATC needs to collaborate further with MPIA to establish what the effects of material selection and BSM housing design are.

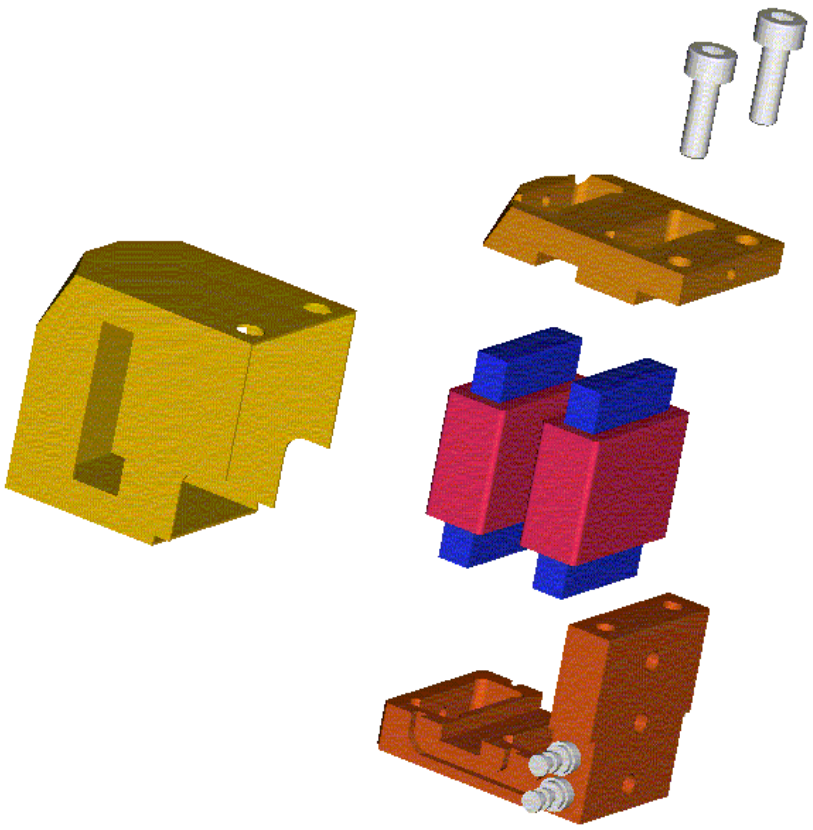

Figure 21 Assembly of a shielded motor assembly (SPIRE-BSM-020-005) with heat shielding

Drawing SPIRE-BSM-020-005 , illustrated in Figure 21 above shows the motor block assembly. The option exists to use the outer thermal shield (-005) to incorporate magnetic shielding directly by plating the inside with Niobium (super conducting and hence magnetic shielding below 9K). The baseline however is to fit no magnetic shielding (TBC).

The motor housing details require re-design in detail to accommodate the revised Zeiss coils, but the concept remains unchanged

8.2 Thermometers

The operating temperature of the BSMm will be 4-6K and the mirror or structure is to rise by no more than 1K from the nominal operating temperature.

The temperature of the BSMm will be monitored using a Lakeshore Cernox 1030 sensor, illustrated in Figure 22 below. This component is in fact more precise, and operates at lower temperatures (to 1.4 mK) than required by the BSM. However, to simplify spacecraft electronics and software architecture a common thermistor – driven by the requirements of the SPIRE cooler – is adopted.

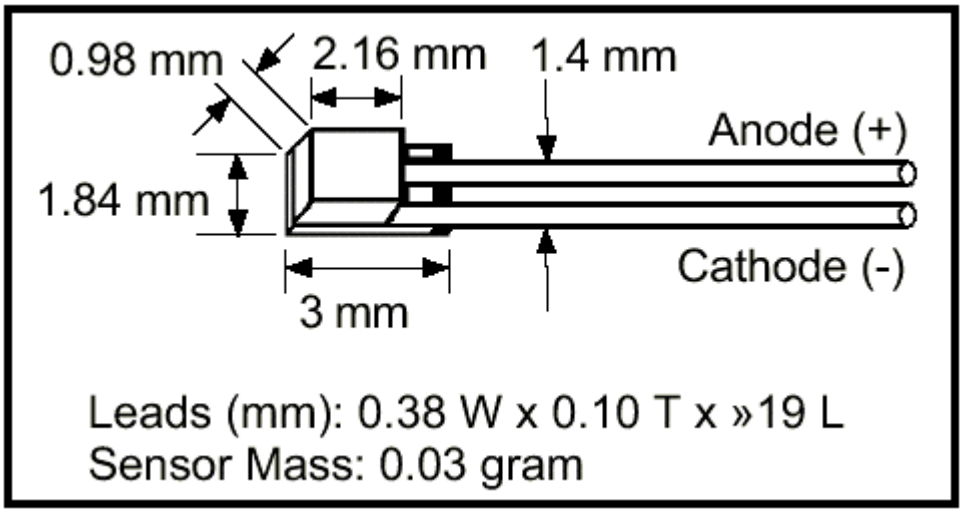

Figure 22 Cernox 1030 sensor (SD package)

CX-1030-CU copper canister , Figure 23 below, incorporates the above sensor, and provides for greater ease of mounting.

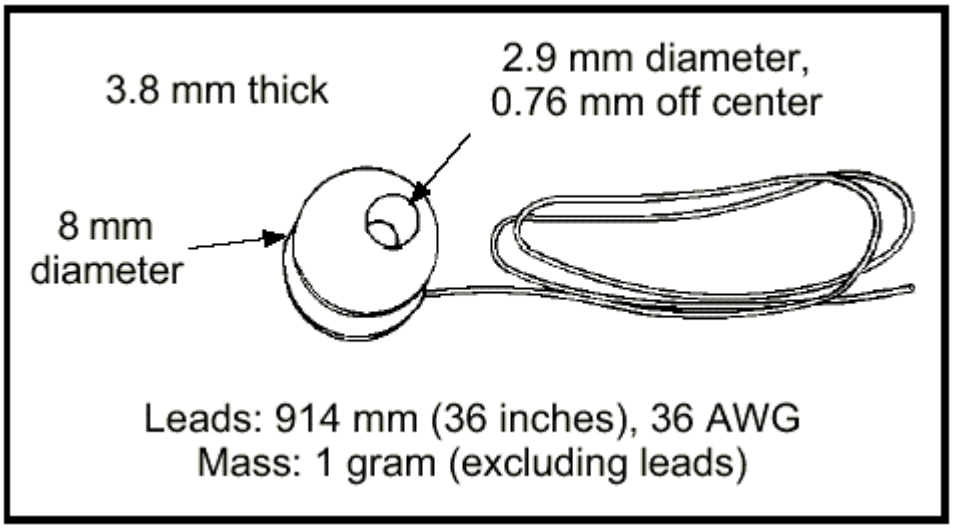

Figure 23 Cernox 1030-CU package

This device is sensitive over the 1.4K to 325K region. For cost reasons, flight rated but uncalibrated sensors will be procured centrally (e.g. by RAL) and calibrated against a calibrated sensor.

The maximum temperature rating is 325K, as shown in the data sheet Appendix 6, but as the specified soldering temperature exceeds this, no particular concerns are identified for bake-out at 353K.

The thermometers will be mounted to the BSMs – and a convenient location is identified as being in the front ‘pocket’ underneath the mechanism. This location allows space for mounting and for running the thermometer wires, and is will provide a representative temperature of the motor and flex pivot-mounting environment, but could not be used to isolate heating or friction in a particular component.

During ATC testing a wider range of local positions will be explored (e.g. on mirror surface, on baffle). The ATC preferred thermistor is the lakeshore DT-470, which has compatible mounting interfaces (care will need to be taken to tag non-flight thermistors to prevent confusion) .

8.3 Coatings

No coating requirements have been specified by SPIRE.

ATC assumes the BSM will be :

- widely gold-coated to control emissivity, and enhance thermal contacts at bolted joints, or
- Alachrom 1200 finished where no emissions control requirements exist but where corrosion control is required

Gold plating of aluminium components will typically require a post-machining polishing process (mechanical or chemical), a copper flash, a nickel plating layer and a final gold plating. In some cases the intermediate Nickel coat may be omitted. Plating details and process parameters for each component drawing are TBC

8.4 Surface Finish

Surface finish will be specified on component drawings as required.

8.5 Mass budget

The overall BSM mass budget, including the prime and redundant cryogenic harness is specified as less than 1100 gm, including harness. A full mass budget breakdown is given in Annex B, and illustrated below. The structural interface is the bulk of the mass, and could be addressed further to find additional light-weighting, though at additional cost.

BSM MASS BREAKDOWN BY FUNCTION (%)
Total 1120gm incl contingency

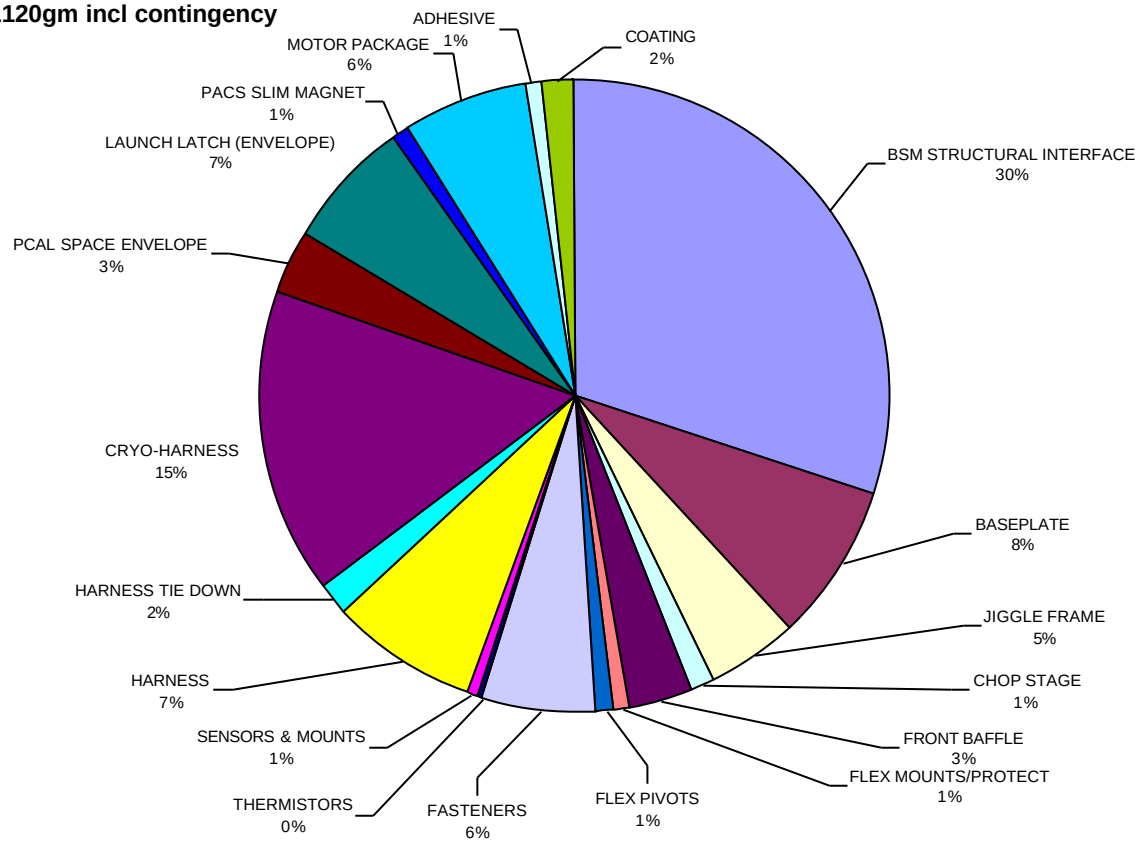

9. Optics

9.1 General

The BSM is a critical part of the overall SPIRE optical design (AD4). The BSM, designated CM4 in the optical scheme, allows for chop and jiggle motion to ensure full sampling of the instrument arrays without the overhead of moving the entire spacecraft. Fine pointing corrections may also be provided.

Requirements of the optical design (LAM) and stray light and baffling control (RAL) drive the BSM mirror design. Optical beam space envelopes, based on 20% oversize photometer and spectrometer beams are presented to ATC by RAL in the form of IGES surfaces and the BSM space envelope based around this.

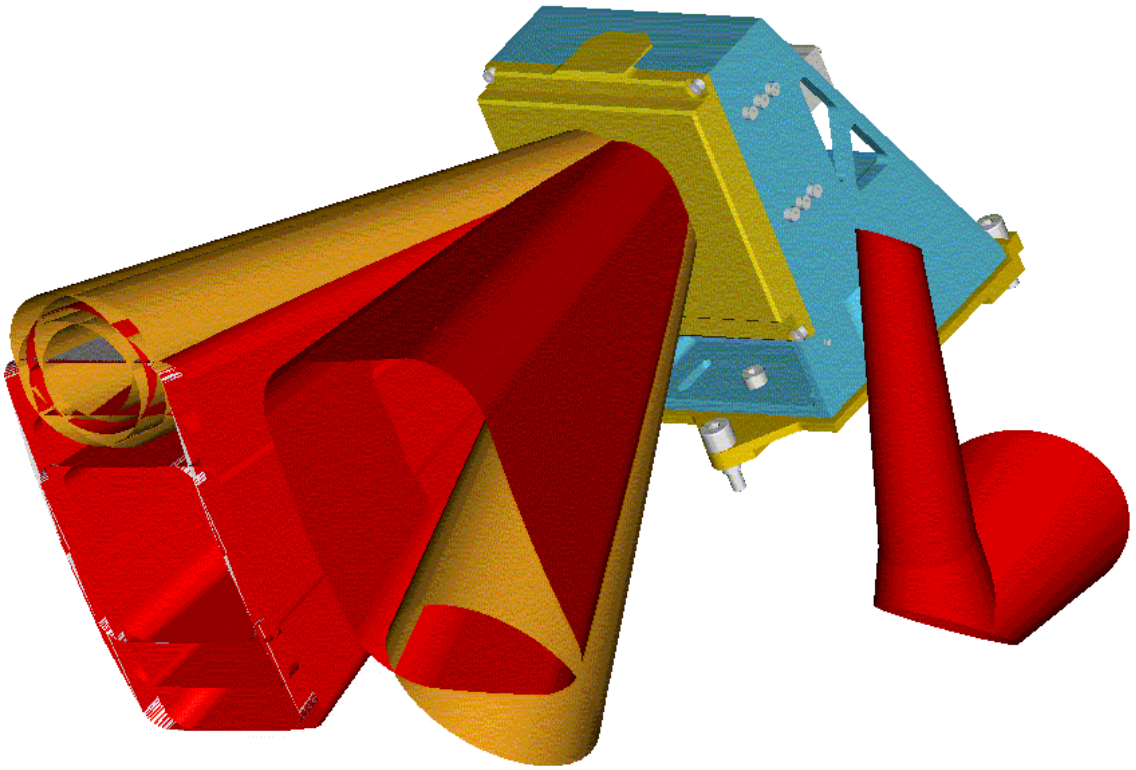

Figure 24: BSM with optical beam (20% oversized)space envelopes provided by RAL

The requirements of the optical design are encapsulated in the BSM specification document and it is to these purely mechanical parameters that the BSM is designed.

9.2 Mirror

The required (AD1) minimum mirror diameter is 32 mm. These requirements are derived from RD7 – Spire optics diffraction description.

The BSM design incorporates a 32.5mm diameter mirror. The monolithic mirror is incorporated into the chop axis and light-weighted from behind. The mirror is produced in aluminium 6061 alloy, thermally stabilised, as per ATC stabilisation procedure (RD8) , and diamond machined (MCD turned) to an optical finish.

The mirror surface of the BSM is required to

- Be flat to <100nm P-V to allow for optical testing. This is a tighter specification than the 1µm rms. (2µm WFErms.) which is required for functioning of the instrument.
- Have a surface roughness of <10nm (rms).
- The reflectivity of the mirror surface >99% in the wavelength range 200 - 670 µm. This will not be measured; it is assumed that this will be satisfied by machined aluminium 6061. (The emissivity of the mirror surface <1% in the wavelength range 200 - 670µm.)

For the purposes of interferometric testing at 633nm this surfaces specification will be adequate for testing of the surface form. At this wavelength the reflectivity will be approximately 80% which is more than sufficient.

These surface requirements are readily met by standard diamond machining techniques.

No requirement is placed on the BSM for any post-machining mirror surface coating. The mirror will be stored in a dry environment to prevent deterioration.

The BSM is required to have a central aperture, nominally of 2.8mm minimum diameter, to accommodate the PCAL source 'light pipe'. Various options for the size of the central aperture have been proposed to allow for masking of the telescope secondary mirror, and for stray light control (RD9,10). These range from hole sizes of ~4 to 6 mm diameter, with some possibilities for offsets in x or y by up to 0.5mm or slightly elliptical profiles. As the optimum option has not been determined, *the baseline BSM aperture remains 2.8mm diameter*. A larger diameter of up to 8mm may be accommodated before significantly impacting the mirror rib structure. It may be necessary to put a black coating on the mirror in an annulus around the 2.8mm hole rather than increasing its diameter. *It is RAL's responsibility to specify the size of the hole or black annulus*. Final sizing TBC of the hole will be determined by RAL once the telescope secondary design has been fixed.

9.3 Baffle

The baseline design has no baffle, just a pierced plate over the structure with the aperture sized to pass the oversized beams. The aperture size is derviced by first cutting the solid model with the beams provided, and then 'tidying up' by applying next-largest size radii to facilitate machining. Precision location of the baffle is not required. Given the comfortable 20% optical oversizing, the requirement on location would be driven by the need to avoid mechanical fouls. Dowel pins on the flanges could serve for location if required.

For this to be acceptable no part of the BSM structure must be hotter than 1K above the ambient temperature, and there must be no part of the structure clipping the 20% oversized beams. The motors will be sufficiently well heat sunk and shielded not to be seen as hotter than one degree above ambient.

The alternative is a complex machined partial baffle intruding into the mechanism, described in what follows. It should be noted that no baffling scheme that can be implemented on the current design and allowing for a 20% oversized beam would completely hide the structure of the BSM from being seen by the detectors.

The baffle or plate mounts to the BSMs front surface via 4 off M2.5 self-locking screws. The flanges at the top and bottom serve primarily to block the jiggle-frame flex pivot apertures, preventing contamination ingress and reducing light leakage paths

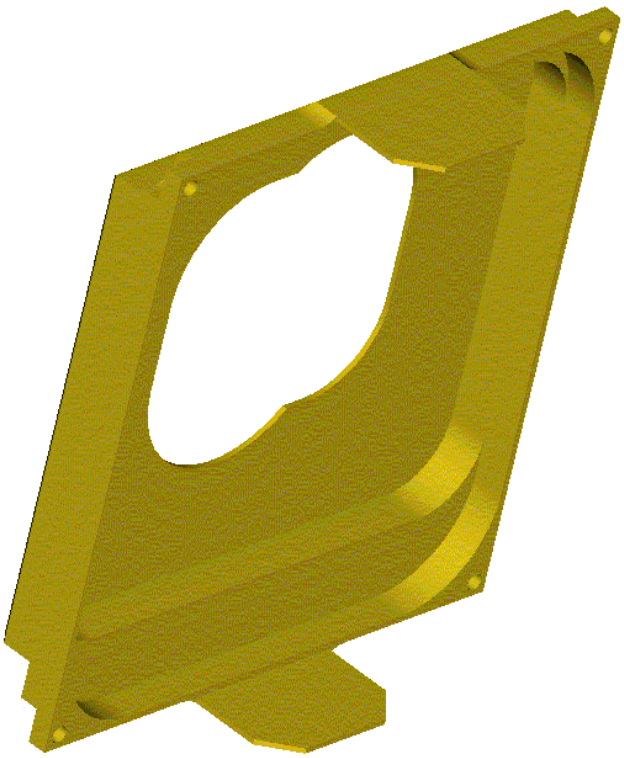

Figure 25: BSM baffle. The end 'tabs' provide debris closure of the flex-pivot apertures.

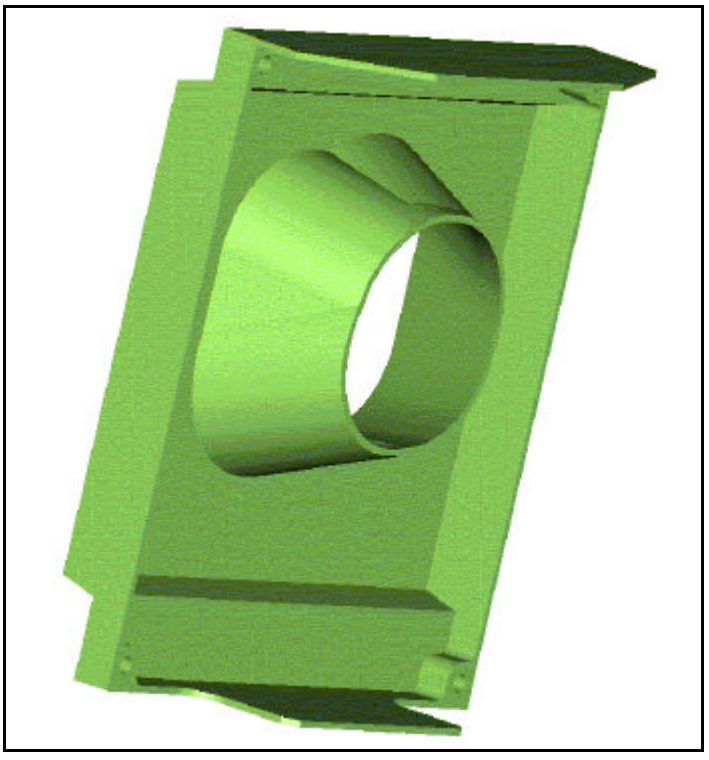

Figure 26: BSM 'conformal' baffle. This alternate concept fully wraps the beam (except for a ~1mm gap around the edge). It is not adopted at this point as it is not required if all visible BSM parts are <1K above the structural temperature.

9.4 Light Tight Enclosure

There is no firm requirement on light tightness placed upon the BSM. This matter should be considered part of the baffling.

9.5 Harness Feed-Through

The BSM wiring harness to the motors require the mechanism enclosure to be pierced in 8 (TBC) places for motor wiring feed through. These openings are at the rear of the BSM, which faces away from all optical elements of the SPIRE design. If required, a gland type (TBD) feed through would be used to prevent stray light leakage.

9.6 Alignment

Alignment tolerances for the optical train are given in RD11, Spire optical alignment verification plan. These require that the BSM be positioned to ±0.1mm in x, y and z, with a total angular precision that would allow for the maximum total angular alignment error of the mirror, in the event of failure, to be ±0.18º.

Although the BSM provides for steering corrections and offsets, it remains desirable to provide precise location on the desired optical path such that a failure of the drive motors would leave the BSM in the failsafe position within ±0.18º of the nominal (0,0) position.

Rough calculations[3] show that direct mounting of the BSM to the optical bench would require that holes were placed with approximately +/- 0.1mm precision, and that the BSM rest position toleranced to +/- 0.14 degrees. The hole position tolerance is achievable, but the BSM rest angle may prove more problematic (as it will be attitude dependent) and an overly tight tolerance will increase assembly costs exponentially.

To allow additional latitude in the BSM assembly precision shoulder bolts will be used to locate on the optical bench a mounting 'shoe' with three machined pads, as commonly used in ATC cryogenic mechanisms. The BSMs proper will mount to this shoe, with the precise location (and the provision for one-off corrective machining) provided by mounting against the pads.

For alignment, the shoe would be placed upon the SPIRE optical bench and actual positions measured via CMM. The as assembled BSM rest position and BSMs dimensions will have been characterised at ATC and the relevant offsets required would then be calculated. The shoe would be removed from the bench and machined to provide pitch roll and yaw adjustment, then re-positioned.

The shoe, (drawing SPIRE-BSM-020-001-002) has been drawn to nominal size, but would be produced with +1mm oversized thick pads to allow for machining.

This scheme also allows removal of the BSM from the optical bench for trouble-shooting during AIV without loss of alignment.

9.7 OGSE

For alignment of the SPIRE optical train, a fixed mirror replaces the BSM whilst other systems are aligned (e.g. using a laser). The fixed mirror would be 'Optical Ground Support Equipment' – OGSE and would be supplied by ATC. The fixed mirror is required because the BSM is susceptible to vibrations when not damped or served to the (0,0) position powered. The resulting vibrations would make alignment work difficult, and the BSMe would not be connected/powered up during initial alignment.

The BSM OGSE has not yet been designed. It will probably comprise a mounting structure similar to the BSMs with a fixed, standard commercial optical quality, flat mirror mounted to it.

[3] Maximum mount hole pitch approx. 110mm. Allow BSM assembly to have errors of 0.14 degree, leaving 0.11 degrees for mount holes (RSS calc). Tan(0.11)x110 = 0.21mm, but allocate across 3 holes = sqrt(0.21^2/3) = 0.12mm

There is an option to make the fixed mirror compliant with the 'standard' SPIRE mirror mounting scheme – this would also allow use of the standard CMM spherical mounting tool which will be used for other SPIRE mirrors (see **SPIRE Alignment Tools Specification** and RD11– Spire optical alignment plan) . This might incur extra cost, so is not the baseline.

The BSM OGSE would be mounted to the spire mount shoe as described for the BSM alignment. The OGSE would need to replicate any offset of the BSM rest position, which could be achieved by shimming of the fixed mirror or machining of the structure.

10. BSM Electronics & Controls

10.1 Control System Design

The control system for the BSM is based on a nested velocity and position loop scheme. In the case of the Chop axis, an additional loop is used to limit the mechanism acceleration to prevent instability due to limited current loop slew rate.

The required velocity and acceleration signals are obtained from the system position and torque demand signals using a second-order observer for the mechanism. The observer is essentially a model of the mechanism, and includes flex joint spring rate and inertia. Though the model can never be exact, internal error correction feedback ensures an accurate estimation of the required parameters.
All control functions are implemented in software, allowing considerable flexibility – for example, in the event of some faults, such as a broken flex joint or loss of position signal, some degree of control can still be obtained, though of course performance is not to full specification.

Section 10.5 describes the simulation of the mechanism, electronics and software in Matlab-Simulink.

The electronics required to implement the control scheme is fairly simple, and limited to
a) Pre-amplification of the position signal from the magneto-restive sensor
b) Power amplification of the motor drive signal
c) A-D and D-A conversion to and from the software controller

The testing of the development models uses similar Simulink models to those described in this section. The relevant parts of the block diagrams (i.e. the control loops) are compiled into code using the same type of 'dSPACE' prototype development system that is also used by LAM. This code is then run on the Digital Signal Processor (DSP) that operates in the hardware part of the dSPACE system. The dSPACE system allows the necessary connections to the test hardware using A-D and D-A converters. This allows rapid prototype development of the software part of the BSM system. It is possible to alter code parameters while the hardware system is running to immediately evaluate the effects on performance.

10.2 Parameters

Normally, the control parameters are fixed and require no adjustment. However, all parameters used in the control algorithms can be changed if required, for example in the event of a fault. Each axis has 28 parameters for servo control.

In addition, there is a lookup table for step response profiling, to enable a minimum-power step movement to be realised. Additional lookup tables are used for linearisation of the position sensor outputs.
.

By use of flags and switches in the software, the structure of the controller can also be changed (in particular to suit fault conditions) by setting appropriate parameters as required.

10.3 Dynamic Analysis

See section 7.2.2.3 (Mechanism mechanical analysis)

10.4 Simulink Model

Check with Brian for updates this section.

The Matlab-simulink model used to predict performance and establish control parameters includes all the significant linear and non-linear effects. With regard to the following figure, the main model elements are described.

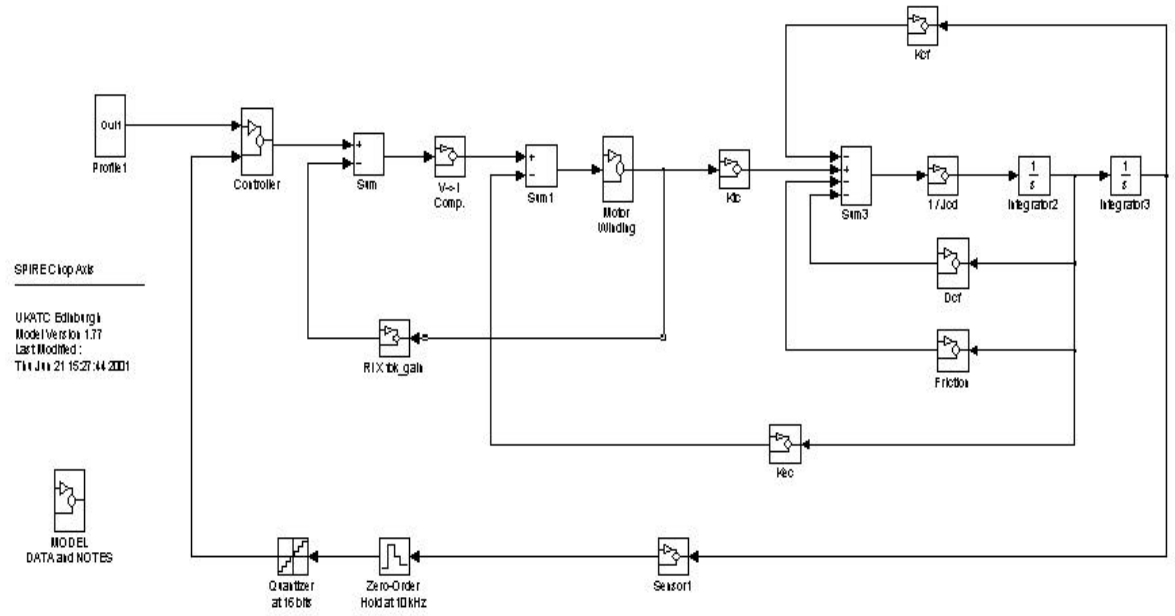

Figure 27 Simulink model

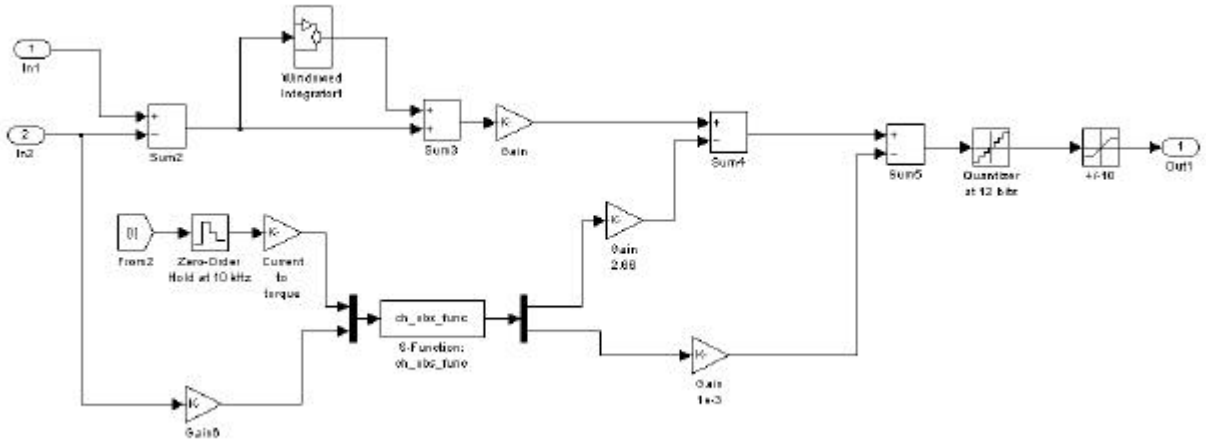

Figure 28 Controller

The controller includes a ‘windowed’ integrator, to ensure zero position error, the state observer, implemented as a matlab ‘S-function’, and the A-D converter.

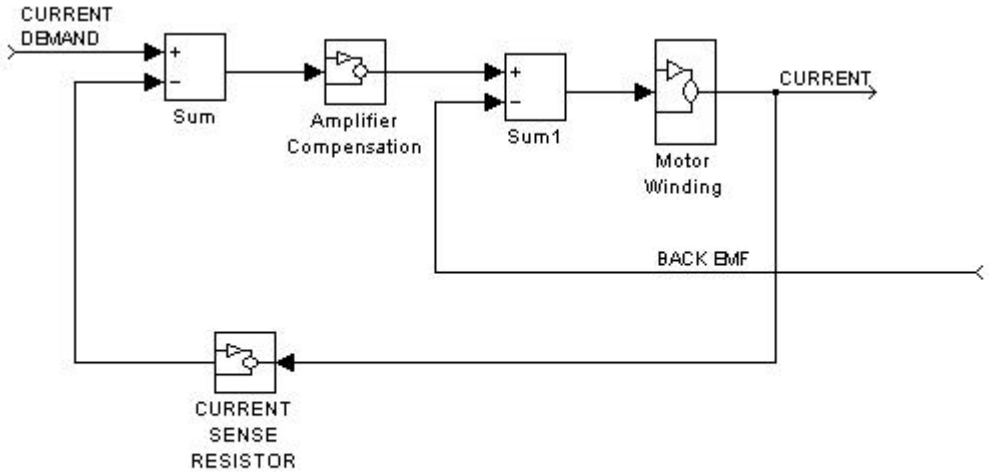

Figure 29 Power Amplifier

The power amplifier model includes voltage limiting in the elctronics and limited bandwidth.

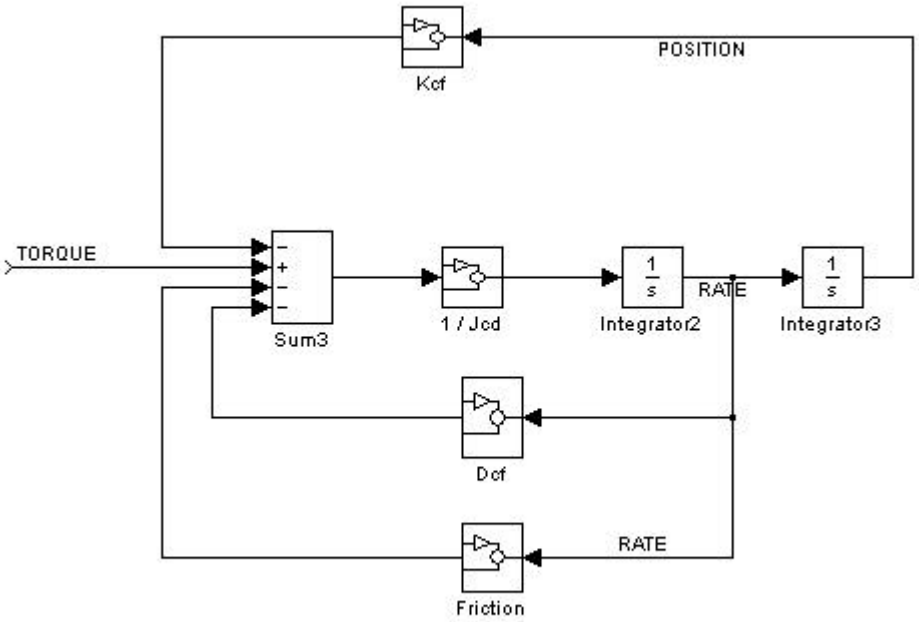

Figure 30 Mechanism

The mechanism model includes the flex joint spring force, the flex joint mechanical damping, and friction block which used only when modelling the fault condition with a broken joint.

10.5 Predicted Performance

10.5.1 Power Dissipation

System power calculations have been produced as follows.

The calculations are made using the mathematical modelling package 'Mathcad 7.0'.

The BSM comprises two motors and two position sensors. The motors are composed of stators wound from either aluminium or copper wire, and rare earth permanent magnets. The position sensors are regarded as fixed resistors for the purposes of this analysis, though in use this resistance changes slightly, say +/- 10%.
The BSM mirror is constrained by low friction torsional springs, which require a constant force for a constant angle – this relationship is linear.

In operation, the mirror quickly slews between two fixed points, and stops for a relatively long time period, here called 'stare'. Power is calculated for the slew and stare movement phases, though due to the much longer period spent at the fixed locations, this phase dominates the average power calculations.
The stare power is caused by the constant force required to hold the angle against the support springs.

The power dissipation is calculated using the relationship
$P = I^2R$
where
P = power (watts)
I = current (Amps)
R = Resistance (Ohms)

The step movement is in fact a controlled sinusoidal edge, so the step time specification is converted into an equivalent frequency to calculate power.
That is, if the mirror were moved sinusoidally back and forth between two fixed angles A and B, from A to B to A would take one cycle, so half of one sine period (e.g. from A to B) would take the specification step time.
This allows calculation of the maximum acceleration, and using the known spring constants, the total torque required from the motor.

The power dissipation calculations include a duty cycle factor to produce an average power from the peak acceleration powers.
However, as the total power over time is dominated by the required spring force in the stare or static mode, the acceleration power has relatively little effect.

The effects of eddy current losses during axis movement are difficult to predict without detailed magnetic analysis, but as the duty cycle of the system is only 5%, the mirror position is static for 95% of the time. Therefore these losses are not expected to be significant. Analysis by MPIA is in hand using the MAFIA analysis package to quantify this further.

Angle Step Time, Chop $tsc := 0.015$

Angle Step Time, Jiggle $tsj := 0.05$ (Goal)

$\omega c := \frac{2\cdot\pi}{2\cdot tsc}$ $\omega c = 209.44\,s\,\frac{rad}{s}$ $\omega j := \frac{2\cdot\pi}{2\cdot tsj}$ $\omega j = 62.832\,s\,\frac{rad}{s}$

Inertias $Ich := 2.7\cdot 10^{-6}\cdot kg\cdot m^2$

$Iji := 48\cdot 10^{-6}\cdot kg\cdot m^2$

Step angles (2.5 deg chop, 0.6 deg jiggle)

$\theta ch := 0.044\cdot rad$

$\theta ji := 0.0105\cdot rad$

Spring torques
(to be confirmed ..)

$Ksch := \frac{0.044\cdot N\cdot m}{rad}$ $Ksji := 0.44\cdot\frac{N\cdot m}{rad}$

$Tsch := \theta ch\cdot Ksch$ $Tsch = 1.936\times 10^{-3}\,N\cdot m$

$Tsji := \theta ji\cdot Ksji$ $Tsji = 4.62\times 10^{-3}\,N\cdot m$

Peak acceleration $\alpha ch := \omega c^2\cdot\theta ch\cdot\frac{rad}{s^2}$ $\alpha ch = 1.93\times 10^3\,s^{-2}$

$\alpha ji := \omega j^2\cdot\theta ji\cdot\frac{rad}{s^2}$ $\alpha ji = 41.452\,s^{-2}$

Therefore acc. torque $Tach := Ich\cdot\alpha ch$ $Tach = 5.211\times 10^{-3}\,N\cdot m$

$Taji := Iji\cdot\alpha ji$ $Taji = 1.99\times 10^{-3}\,N\cdot m$

Peak torque required is (acceleration + spring/4) for 0 to max angle step,
for (-max angle) to (+max angle) it is (acceleration - spring/2)

0 deg to Max : $Tch := Tach + \frac{Tsch}{4}$ $Tch = 5.695\times 10^{-3}\,N\cdot m$

$Tji := Taji + \frac{Tsji}{4}$ $Tji = 3.145\times 10^{-3}\,N\cdot m$

-Max to +Max :

$$Tach - \frac{Tsch}{2} = 4.243 \times 10^{-3}\ N\cdot m$$

$$Taji - \frac{Tsji}{2} = -3.203 \times 10^{-4}\ N\cdot m$$

Therefore make required motor torque = 0.01 N-m for chop and jiggle

POWER DISSIPATION

Assuming the MPIA 'small' motors were used, with a 20 deg.C resistance of 520 ohms, and R(hot)/R(cold) = 500:1 (800:1 in PACS) using pure aluminium conductors

Motor resistance

$Ra20 := 520\cdot ohm$

$Ra4k := \frac{Ra20}{500}$ $\quad Ra4k = 1.04\ ohm$

Motor Torque Constants (these are to be confirmed ...)

$Ktc := 0.08\cdot \frac{N\cdot m}{A}$ $\quad Ktj := 0.12\cdot \frac{N\cdot m}{A}$

Duty Cycle

$D := 0.05$

Current

$Ich := \frac{Tsch + D\cdot Tach}{Ktc}$ $\quad Ich = 0.027\ A$

Power at 20 deg.C :

$Pchop\_20 := (Ich)^2\cdot Ra20$ $\quad Pchop\_20 = 0.392\ W$

Power at 4 deg.K :

$Pchop\_4k := (Ich)^2\cdot Ra4k$ $\quad Pchop\_4k = 7.84 \times 10^{-4}\ W$

Jiggle Current $Iji := \frac{Tsji + D \cdot Taji}{Ktj}$ $Iji = 0.039\,A$

Power at 20 deg.C :

$Pjig\_20 := (Iji)^2 \cdot Ra20$ $Pjig\_20 = 0.804\,W$

Power at 4 deg.K :

$Pjig\_4k := (Iji)^2 \cdot Ra4k$ $Pjig\_4k = 1.609 \times 10^{-3}\,W$

Total BSM Power is calculated by adding powers for sensors and motors

Total sensor power is 2 * [1mA * 1 mA * 400 ohm (max)] = 0.8 mW

$Sensors := 0.8 \cdot 10^{-3} \cdot W$

$Pt\_20 := Sensors + Pchop\_20 + Pjig\_20$

Total power at 20 deg.C : $Pt\_20 = 1.197\,W$

$Pt\_4k := Sensors + Pchop\_4k + Pjig\_4k$

Total power at 4 deg.K : $Pt\_4k = 3.193 \times 10^{-3}\,W$

The total power estimated of 3.2mW is within the specification value of 4.0 mW, however this is highly dependant on the motor torque constant (itself dependant on precise mechanical alignment) and the axis flex joint spring torques.

The Simulink model has also been used to estimate the BSM dynamic power performance.

The power dissipation of the BSM is dominated by the torque required to keep the axes at fixed non-zero positions against the spring force. Acceleration forces are of comparatively short duration. The figure below illustrates this.

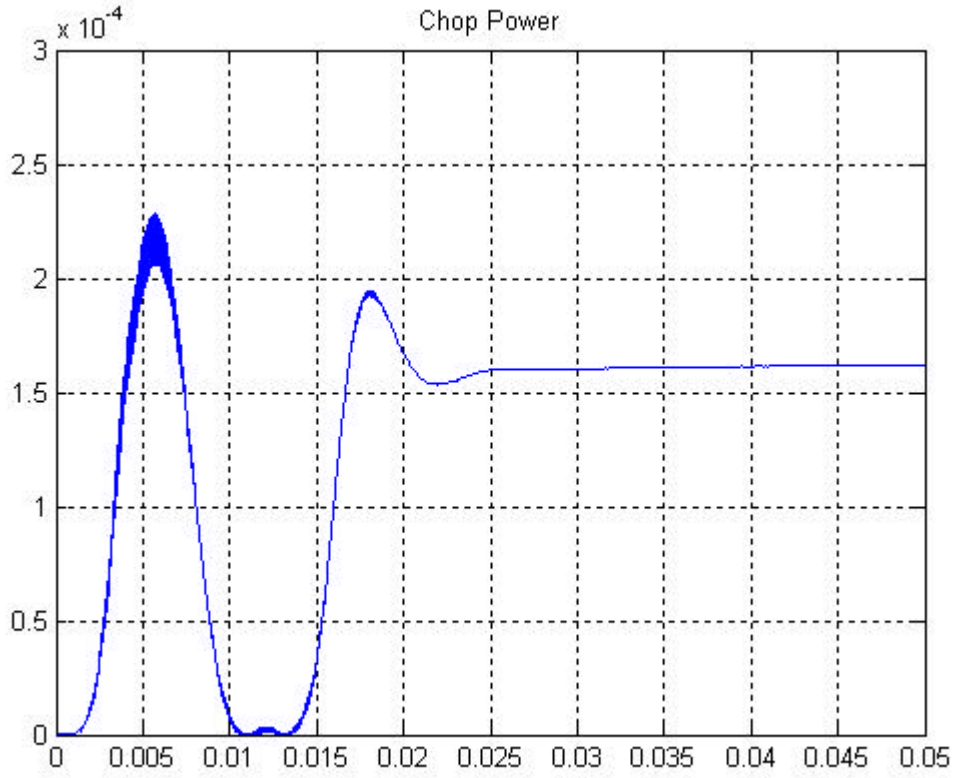

Figure 31 Predicted power (chop stage)

10.5.2 Rise Time

The position rise times are within specifications for both axes (Simulated 15 mS Chop, 40 mS Jiggle, for specification 20 and 50 mS respectively)

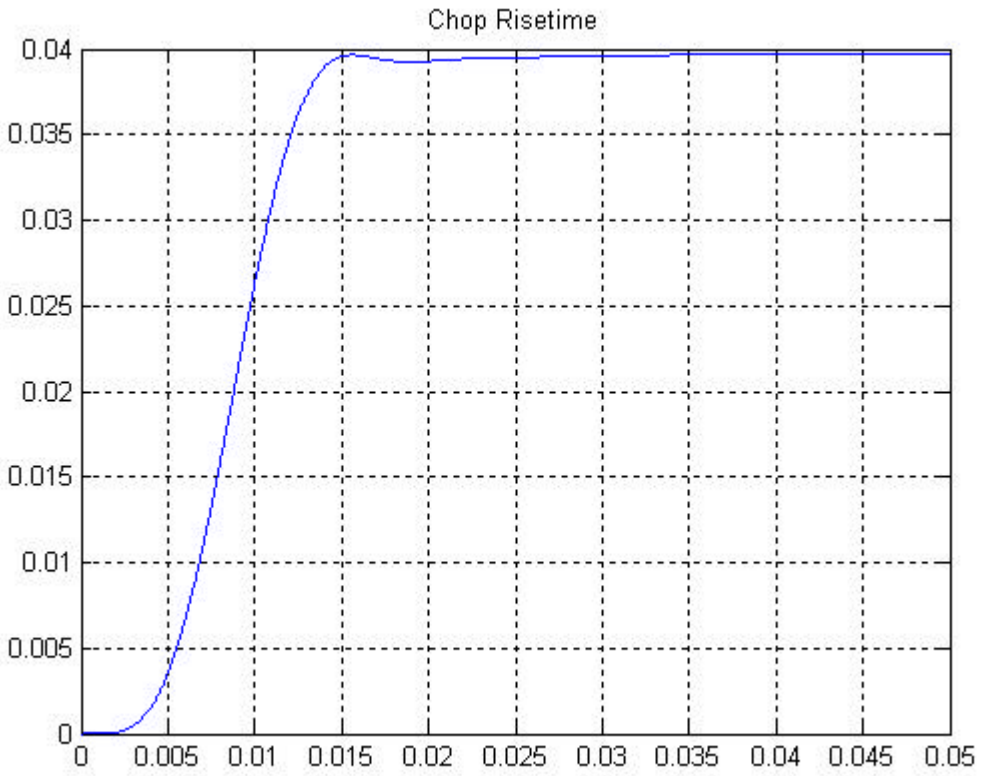

Figure 32 : Predicted chop stage risetime

10.5.3 Positional Stability

Tests on the two-axis prototype show that stability meets the specification requirements at room temperature. Cold testing should show improved stability as the temperature is fixed.
Currently the angle measurement system drifts by approximately the same amount as the required specification figure over a period of 1 hour. Long term stability will therefore be verified by optical methods.

10.5.4 Gain and Phase Margins

System gain and phase margins are described in the document 'BSM Control Systems Analysis', which indicates robust stability margins for the BSM control loops, allowing reasonable parameter variations without significantly affecting BSM performance.
Some resonance search testing on the two axis prototype using a sinewave drive to the power amplifiers and observing the position outputs using a Transfer Function Analyser has shown no significant resonance problems. The main flex joint support resonance is at approximately 15 Hz, consistent with theory, with minor structural modes at 663 and 830 Hz. Higher frequencies are not testable using this simple method.

10.6 BSMe Electronics

The Electronics specified by UKATC designed by LAM takes the following form.

10.6.1 Block Diagram

In simplified form, this illustrates the interconnects between the BSM and its electronics.
The BSM mechanism motors and launch latch are powered from the Warm Electronics. The BSM position sensors are preamplified by the Warm Electronics.
The A-D and D-A functions, and the controlling code, operate within the LAM MAC board.
Finally, data and commands are exchanged via the MAC board to the SPIRE system.

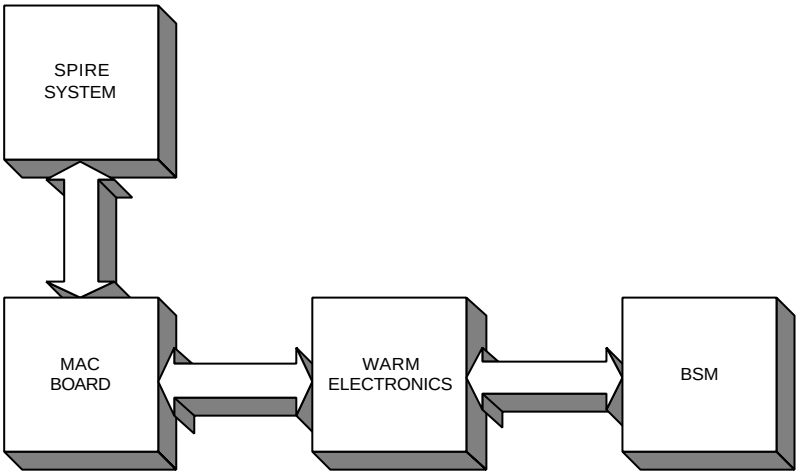

Figure 33 : Warm electronics overview

10.6.2 Position Sensors (Current Source)

The current sources use precision voltage sources (AD584) and voltage-to-current amplifiers.

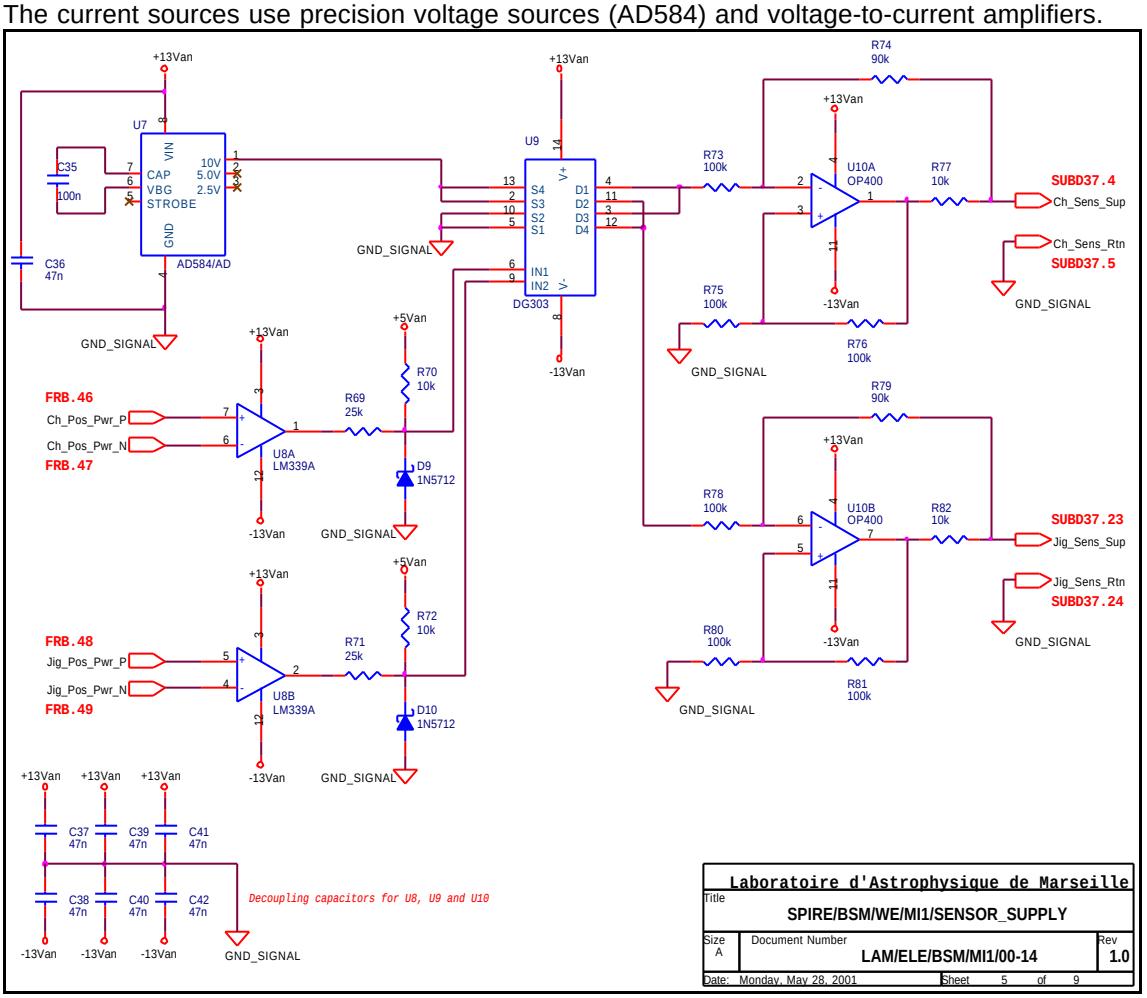

Figure 34 sensor supply

10.6.3 Position Sensor Read-Out Circuit

The position sensor outputs are differentially amplified to reduce noise pickup using monolithic instrumentation amplifiers.

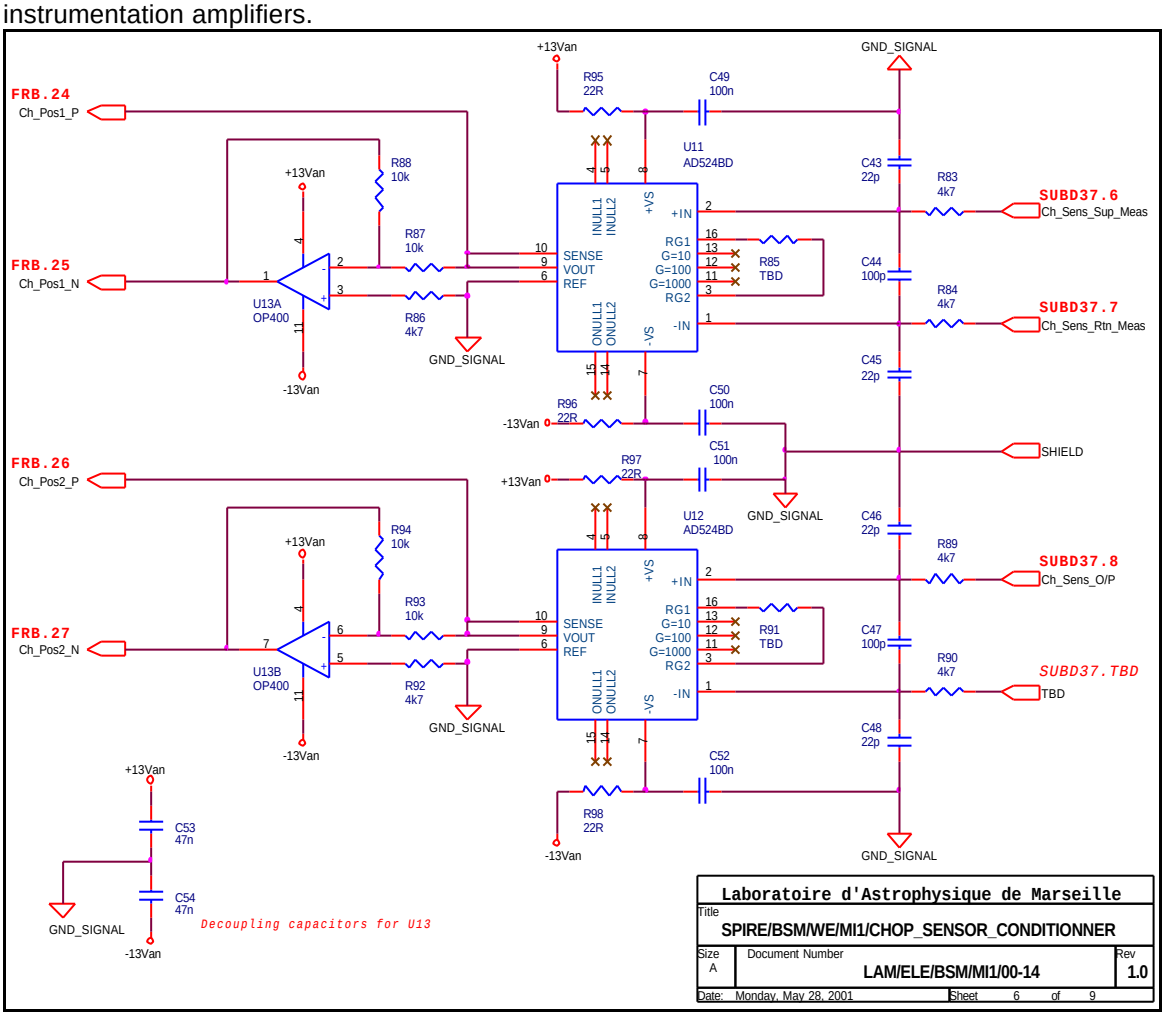

Figure 35 Chop sensor conditioner

10.6.4 Motor Power Amplifiers

The motors are driven by voltage-to-current amplifiers, which as well as reducing the effects of motor electrical time constant on the control loop, ensure stable operation with the large changes in motor resistance between cryogenic and ground test temperatures.

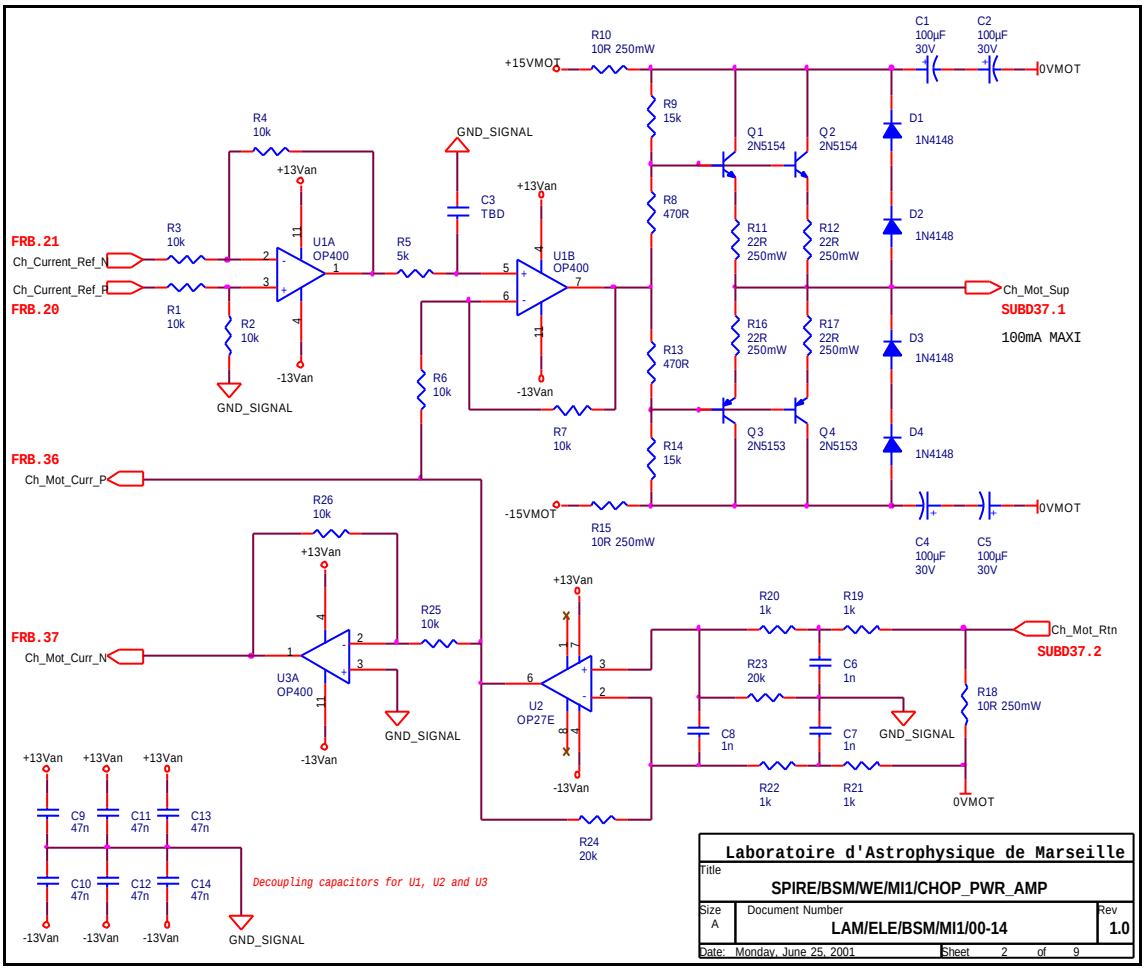

Figure 36 Chop Power Amp

10.6.5 Launch Latch

The launch latch is driven by separate 'engage' and 'dis-engage' signals, and has an integral position sensor to indicate latch status to the driving system.
The driving circuitry is shown in the figure below. Additional logic ensures that 'engage' and 'disengage' are not simultaneously driven.

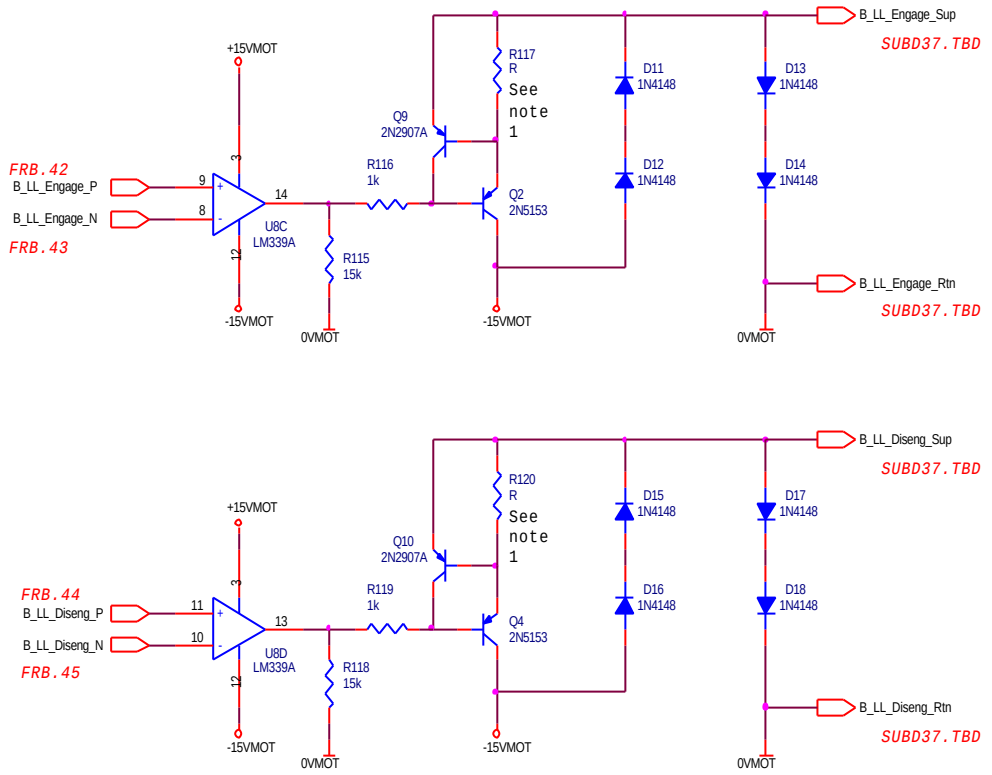

NOTE 1: R=33 Ohms for I=25 mA
R=22 Ohms for I=35 mA

Laboratoire d'Astrophysique de Marseil		
Title: SPIRE/BSM/WE/MI1/LAUNCH LATCH		
Size: A	Document Number: LAM/ELE/BSM/MI1/00-14	
Date: Monday, May 28, 2001	Sheet 8 of 9	

Figure 37: Launch Latch Driving Circuitry

10.6.6 Thermometry

Standard Cernox 1030 thermometers are used to sense local temperature on the BSM.

10.6.7 Power Supply

Power Supplies are standard +/- 15V and +5V supplies suitable for analogue electronics and digital electronics respectively.

10.6.8 Grounding Scheme

The grounding scheme ensures no electrical contact with the BSM structure, with the exception of overall screens on harness wire bundles from connectors, that should connect to chassis. Inner screened wires will terminate at the required component without any connection – however, the end at the warm electronics will be terminated to the local electrical ground for EMC screening.
Overall electronics screening and grounding policy is agreed between UKATC, LAM and SPIRE systems.

10.6.9 Harness/Cables

Electronic/Electrical

The BSM wiring harness is designed to minimise EMC and cross-talk by suitable screening, and is described in detail in the UKATC BSM Electronic Interface document, AD 8.

The mechanically critical harness link between the Jiggle axis and the fixed structure will use a custom flexible tape with printed wires and screening, to produce minimum spring torque load.

The EMC effects of the harnesses are difficult to predict theoretically due to the strong dependence of layout on the capacitances between wires. As all wires also have braid screens connected to 0V, it means crosstalk should be at the practical minimum. It is therefore not considered useful to analyse this further, unless problems arise during test

Mechanical

The BSM prime and redundant harness are separate. Each harness includes the motor, sensor, thermometry and PCAL cables and interfaces via a fully populated 37-way MDM connector, as specified in AD5. The harness is run to the BSM as described in AD6, with a total length of 415 (TBC) mm.

The approximate harness runs are shown below (OBSOLETE figure - new design in preparation)

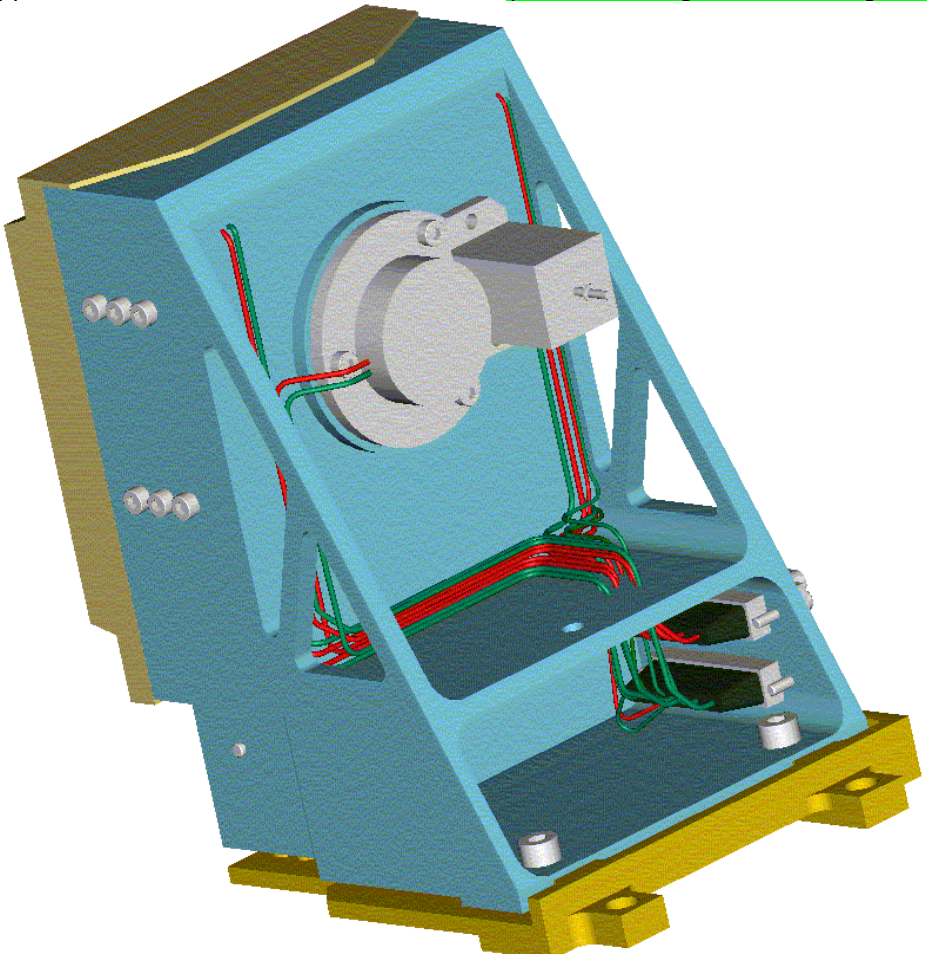

Figure 38 BSM on-board harness run (concept) showing prime and redundant harness runs

Figure 38 above shows a conceptual local harness routing on the rear of the BSM. The prime harness (red) and redundant harness (green) follow a similar path , though the above concept has not been optimised to allow the removal of a single harness without having to disturb the other.

Key issues to be incorporated in developing this harness concept are to:

1) provide apertures for the wiring to pierce the structural members.
2) Avoid light leaks, if required (TBD)
3) Provide for stake out of the harness, via P-clips, lacing and adhesive. (note that p-clips will require locking fasteners)

10.6.10 Interface to Digital Controller

The A-D and D-A interfaces, which are within the LAM MAC board, using SEi 78705 ALPRP 16-bit and Sei 7846 RP 16 bit converters respectively, ensure in particular an accurate position signal conversion, which is essential for BSM angle stability and accuracy.

The noise contribution from these devices is negligible. The most sensitive component is the A-D, which only produces a noise of 0.002% of full scale, equivalent to 0.0001 deg.

10.6.11 Motor Function & Wiring

A brief outline of motor wiring is described here. Mechanically, two coils are packaged together on each end of the chop and jiggle lever arms. However, electronically, a 'motor' consists of one coil at each side, as illustrated below.

Motor Function Schematic

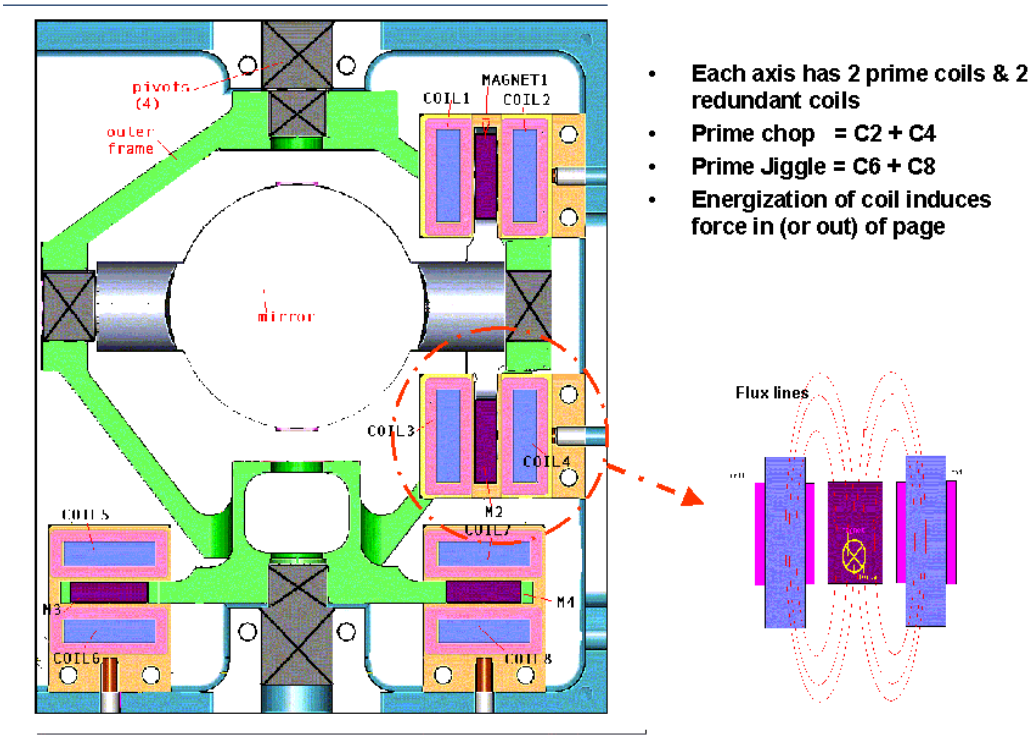

Figure 39 Motor Function Schematic

The wiring to each coil consist of a sense and voltage supply to each coil, and a single bridging wire between the two coils. Mechanically, the sense and voltage wires are run together (possibly within a common screened cable TBC). The bridging wire is run back behind the mechanism cavity, and joined by an ESA approved crimp joint (TBC). See the figure below.

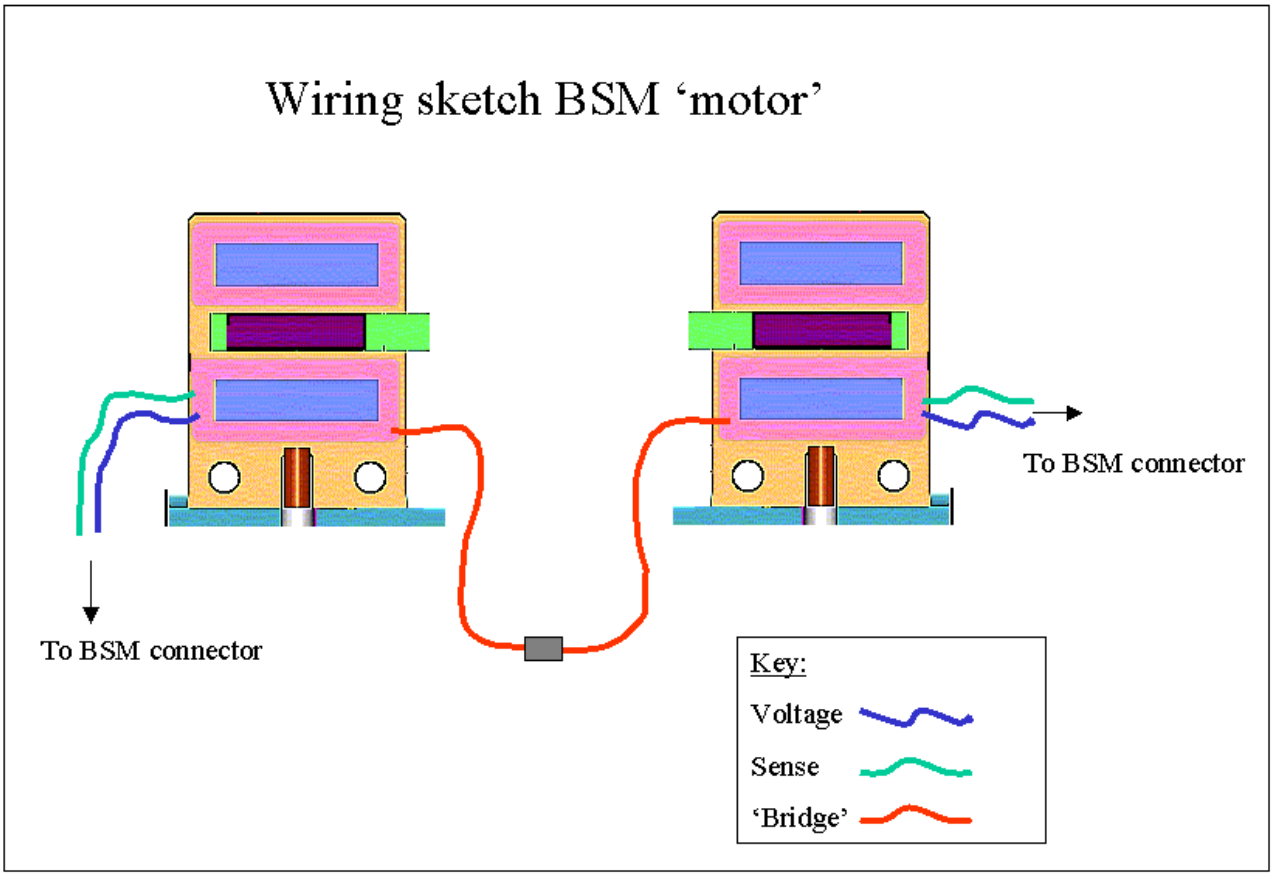

Figure 40 Wiring schematic for BSM motor

10.7 Components & Declared Lists

10.7.1 Component List

The detailed component list for components on the BSMm is provided in AD12, those in the BSMe are provided by Lam as part of the MCU DCL.

Generally, pre-space models will use MIL-STD parts, and space-rated models will use ESA/SCC parts obtained through the SPIRE common parts procurement system, for all electronics associated with the BSM, that is the BSM mechanism, Warm Electronics and MAC board.

Parts for the Warm Electronics and the MAC board are being ordered by LAM.

10.7.2 Processes Soldering

UKATC wiring and assembly personnel are being trained at approved agencies in sufficient time for BSM assembly of space-rated parts. Therefore the soldering process used will conform to the required ESA standards

10.7.3 Processes Crimping

UKATC wiring and assembly personnel are being trained at approved agencies in sufficient time for BSM assembly of space-rated parts. Therefore the crimping process used (if any) will conform to the required ESA standards

10.8 Electronics Systems Interfaces

10.8.1 MCU

The BSM does not interface directly with the MCU, however the DSP controller (MAC board) that runs the BSM control code also communicates with the MCU, so there is an indirect interface that is jointly defined by UKATC and LAM.

10.8.2 Command Modes

The BSM has the following main operating modes.

1. LAUNCH
The BSM is un-powered, but the launch latch can be activated and the motor coils are shorted.

2. OFF
The BSM is un-powered, the launch latch is de-activated

3. ON - POINTING
The BSM is powered, and the position loop is active

4. ON - DIAGNOSTIC
As mode 3, but data is stored for subsequent transfer to the MCU for downloading via telemetry.

5. UPDATE
The MAC board accepts new control parameters from the MCU.

10.8.3 Command List

1. LAUNCH

SIGNAL	FUNCTION	STATE
Launch Latch Activate	Close Launch Latch, Short coils	HI = Activate
Launch latch Deactivate	Open Launch Latch	HI = Deactivate

2. OFF

None

3. ON - POINTING

SIGNAL	FUNCTION	STATE
Chop position demand	Chop position loop input	
Jiggle position demand	Jiggle position loop input	

4. ON - DIAGNOSTIC

SIGNAL	FUNCTION	STATE
TBD		

5. UPDATE

SIGNAL	FUNCTION	STATE
TBD		

10.8.4 EGSE

The BSM mechanism is tested using the dSPACE system.
The control software can be modelled in real-time, or the BSM mechanism and associated electronics can be emulated for testing the software.
The dSPACE system emulates the following Simulink model of the BSM mechanism (one axis shown).

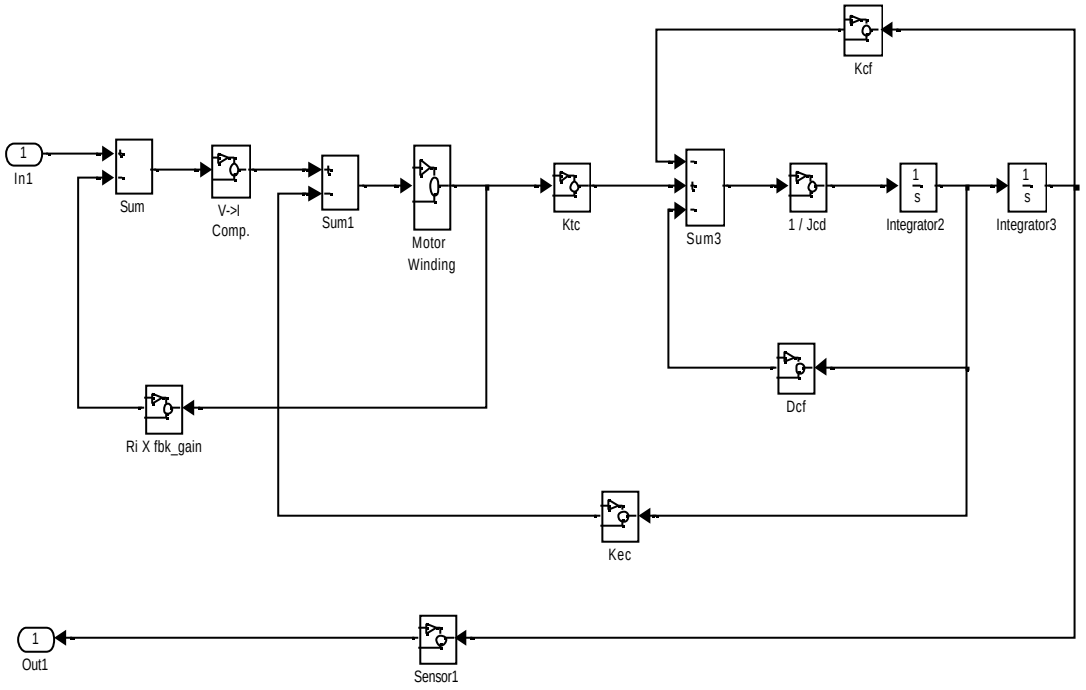

Figure 41: The model includes the mechanism with its inertia, flex joint spring and damping, and the motors, power amplifiers and position sensors.

11. Reliability & Redundancy

In the BSM design redundancy principles have been implemented so as to avoid single point failures, and the propagation of failures to other subsystems, by means of dedicated redundancy and specific protection devices. Where redundancy can not be realised the architecture is designed to limit the effects of a failure.

The BSMe consists of two complete separate circuits (situated on the same double Eurocard, but supplied by separate connectors to the BSMm). This provides complete parallel redundancy, with main and redundant position sensors and motors, driven by separate main and redundant analogue boards, which are in turn supported by separate main and redundant MACs and DPUs as shown in Figure 42 below. A common backplane connector is however advised by LAM for the MCU interface, for packaging reasons. The harnesses, both warm and cryogenic, are also maintained as separate systems.

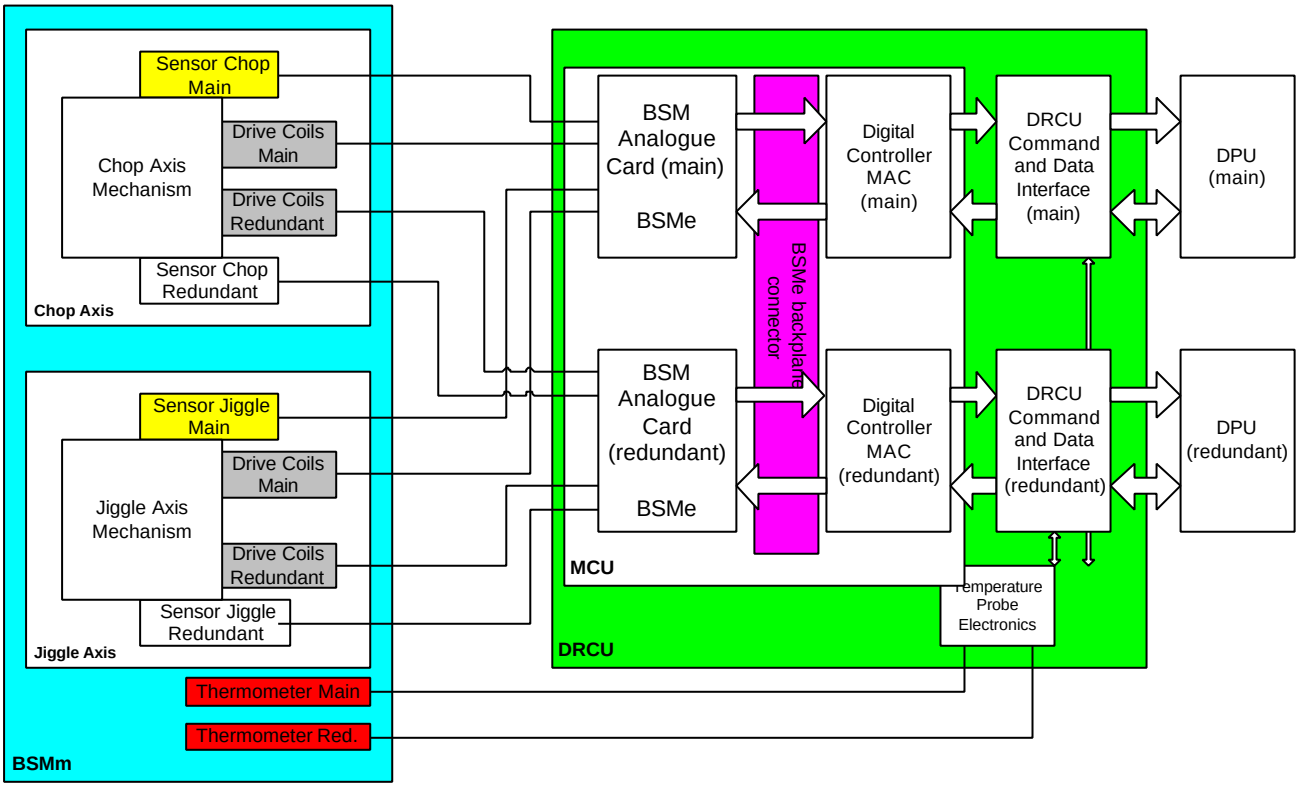

Figure 42 : BSM electronics architecture showing parrallel redundancy

The BSMe redundancy scheme will not be able to operate independently of the SMEC mechanism. A failure in the primary system of either mechanism results in both switching to the redundant schemes. Equally, the PCAL and thermometry units carried aboard the BSMs would be required to switch at the same time.

The BSMs and BSMm mechanical design incorporates little redundancy. The structural parts are in general over-designed from a strength viewpoint in order to give adequate stiffness. The structures are maintained at very low stress levels during launch and even lower stresses during orbit. The primary sources of stress will be those induced on assembly and thermal cooldown. The components are manufactured from space-proven materials with good fatigue and stress corrosion cracking properties. The design includes the ability to limit the motion of the BSM during launch, to protect the flexures, and physical limits to the motion in the event of a component failure.

The design of the BSMs and BSMm should be such that the BSM will meet the reliability requirements for SPIRE as set out in the IRD (AD-1). In summary this is that a failure of the BSM should not lead to a total loss of the instruments ability to do science, albeit with loss of efficiency due to the need to use a backup observing mode. If for some reason the BSM were unable to move in either axis at all, then science could be obtained using the scan mapping mode - although there would be a serious loss of efficiency/sensitivity. The jiggle axis would provide some limited ability to modulate signal in event of a catastrophic failure in the chop axis and much worse than expected 1/f noise. In order to ensure that SPIRE can obtain data in the event of a BSMm failure, the mechanism must fail such the field of view of the FTS is still available, and that large or unpredictable offsets of the photometer field are not required.

This is achieved by ensuring *by design* that in the event that there is no drive signal reaching the BSM the mirror will be within +/- 0.18 degrees of the nominal bore-sight, and that in the event of a complete mechanical failure the mirror will be within +/- 1 degree of its nominal position.

11.1 Reliability Block Diagram

A reliability block diagram is presented in AD7. Key results are summarised here.

11.2 Single Point Failures

1. The wiring harness is a potential Single point failure, unless both the BSMe 'half' boards have an individual cable harness with it's own connectors.
2. The BSM structure and jiggle frame are SPF's. No surprise, but it reinforces the requirement for analysis of these structures for survival, and possible additional tests (e.g. to verify the FEA).
3. Assuming we have a launch damper (shorted motor coils). In the primary operations mode the launch damper 'unlatch' command must unlatch the primary mode motor coil, BUT MUST ALSO unlatch the cold redundant motor coils latching circuit. Vice versa for the redundant mode. This is discussed in the BSME schematic Subsystem Specification Document (Beam Steering Mechanism, Figure 4).
4. The same comment as (1) applies for the cables which send the unlatch command - they should remain separate and parallel.
5. The common connector at the BSMe board is undesirable but is advised by LAM on the grounds of space constraints and the problem that alignment tolerances could lead to an over stress of components if a single board is to be mated via two back-plane connectors simultaneously. Clearly, fully redundant connectors and boards would be preferred, and is being investigated by LAM

11.3 FMECA

A failure modes, effects and criticality analysis (FMECA) has been performed, AD7.

The FMECA ‘viewpoint’ is that of normal operation, with the observing mode being assumed to require combined chop and jiggle motion of the BSM.

A FMECA for the other states – off, standby, thermal cooldown, launch, have not been performed. For the first two the main implications are understood to be electronic. Cooldown and Launch failures have been folded into the main FMECA, as this is more pragmatic than creating a duplicate analysis.

For each element of the reliability block diagram, a number of failure modes and their implications are considered. The analysis is limited to considering a single component failure at any one time, except for cold redundant components where the operation is exposed only after a prime mode has failed.

The principal recommendations resulting from the FMECA are :

11.3.1 Control Software

1. We need to guard against a software command to unlatch when we don't want to.
2. Observation Definition Software needs to be robust handling chop/jiggle requests (i.e. not forgetting them or sending wrong one, or out of range value .....)
3. The bistable deployable end stop relay may have an indeterminate state, in which case the MCU must be robust against it.
4. MCU needs voltage limiter on analogue outputs, and software needs similar check to prevent the system from being driven out of range.
6. need to set invalid sensor range flags in WE (MCU) software

11.3.2 Electronics :

1. for latch solenoid, must be able to turn off power to launch latch solenoid with good redundancy. leaving a solenoid switched on would boil of all the cryogens fast.
2. Single connector at BSMe backplane undesirable. The trade is between a single but rugged backplane connector and two less rugged single connectors. LAM to advise.
3. The short circuit case for the DRCU should be carefully considered in the MCU FMECA concerning propagation to the DPU.
4. Propagation of shorts between separate boards of the BSMe and the internal protection should also be considered. in the MCU FMECA

11.3.3 Mechanical :

1. Mirror surface should be tested for print through of light weighting
2. Good process control on magnet adhesive is required
3. The flex pivot mounting is critical.
4. End stops must be well characterised.

11.4 Critical Components Identification

We assume that items which require declaration here are those which "fail to meet the project requirements" for *failure tolerance*, or undetectable loss of redundancy.

As discussed above for SPIRE the failure tolerance is total loss of science - i.e. a failure of the BSM which would result in (a) large pointing offset for the photometer or/and (b) inability to take data with the FTS due to loss of its field of view. i.e. critical components would be those whose failure would result in the BSM failing to meet the required fail safe positions defined in SPIRE-ATC-PRJ-000460, 4.2.13 and 4.2.14.

No such components were identified, but the design must ensure that the fail-safe positions are met should one or more flex pivots or motors fail.

12. Interface Control Documents

12.1 ICD Philosophy

The BSM interfaces with other subsystems in the SPIRE instrument. The interface to each sub-system is specified in the relevant Interface Control Document. For each ICD there will be:

- An ICD document.
- Where required, an ICD drawings (or equivalent electronic design information) with distinct drawing numbers. A copy of the drawings will be included within the document, probably in postscript or PDF format.

All these ICD's are collated as single document, AD 8.

12.2 BSM ICD Master Reference Table

This section presents a table showing:

- which institute UK ATC interfaces to,
- the relevant documents the interfacing institute is supplying to the rest of SPIRE,
- which UK ATC documents their ICD information is fed from.

Whenever UK ATC update and release interface information with any party we will update the relevant annex and the master table, as well as the design description document.

Although this may leads to multiple updates of the design description, this is felt essential in order to ensure the design and interfaces are kept in lock-step.

Table 7: BSM interface master reference table

ID	Sub-System	Organisation responsible [4]	External ICD document	Internal ATC ICD document	Internal ATC ICD drawing/ file
1	BSM-SPIRE	RAL	Instrument Requirements Document (IRD). SPIRE-RAL-PRJ-000034 v0.30 May.00	SPI-BSM-PRJ-0713-a	SPIRE-BSM-021-001-001
2.1	Structure – BSM	MMSL	ICD Structure - Mechanical I/F MSSL/SPIRE/SP004.11 29.Nov.01	SPI-BSM-PRJ-0713-b	SPIRE-BSM-021-002-001
2.2	Structure – BSM	MMSL			SPIRE-BSM-021-002-002 (IGES file)
2.3	Thermometry	RAL	TBD		SPIRE-BSM-021-002-003
3	Photometer Calibration Source - BSM	UoW, Cardiff	TBD	SPI-BSM-PRJ-0713-c	SPIRE-BSM-021-003-001
4	Launch Latch – BSM	LAM (TBC)	Spectrometer mirror mechanism design description LAM.SPI.PJT.NOT.200008 Ind 3	SPI-BSM-PRJ-0713-d	SPIRE-BSM-021-004-001
5.1	Optics – external finish	LAM	Optical System Design Description SPIRE-LAM-PRJ-000447 Draft 1 18.Dec.00	SPI-BSM-PRJ-0713-e	SPIRE-BSM-021-005-001
5.2	Optics – BSM	RAL	TBD		SPIRE-BSM-021-005-002
5.3	Baffles – BSM	RAL	TBD		SPIRE-BSM-021-005-003
6	Cryo-Harness	RAL / MSSL	SPIRE Harness Definition. SPIRE-RAL-PRJ-000608 Issue: 0.3 30.May.01 Harness routing : TBD (MSSL)	SPI-BSM-PRJ-0713-?	SPIRE-BSM-021-006-001

[4] .i.e. responsible for feeding ICD info upwards to SPIRE system design

ID	Sub-System	Organisation responsible [4]	External ICD document	Internal ATC ICD document	Internal ATC ICD drawing/ file
7.1	MCU-BSM	LAM	Agreement by both parties on ATC design description and Annex G	SPI-BSM-PRJ-0713-f	SPIRE-BSM-021-007-001
7.2	On Board Software - BSM	LAM	TBD		SPIRE-BSM-021-007-002
8	Photometer Bolometer Arrays - BSM	MSSL	ICD Structure - Mechanical I/F SPIRE-MSS-MSSL/SPIRE/SP004.11_29.Nov.01	SPI-BSM-PRJ-0713-b	
9	Spectrometer Bolometer Arrays - BSM	MSSL	ICD Structure - Mechanical I/F SPIRE-MSS-MSSL/SPIRE/SP004.11_29.Nov.01	SPI-BSM-PRJ-0713-b	
10	FPU Simulator - BSM	TBD	TBD	SPI-BSM-PRJ-0713-g	
11	Instrument Simulator - BSM	TBD	TBD	SPI-BSM-PRJ-0713-h	

13. Assembly, Integration & Verification

13.1 General

AIV requirements are primarily programmatic, and met through the product assurance plan (AD3), the test plan and development plan (RD5). These programmatic issues are not discussed in the design description

However, there are several design implications and features of relevance, which are discussed below.

13.2 Assembly

The BSM design is compatible with assembly in a class 1000 clean room. Volatile materials are avoided, and all components are capable of immersion/cleaning with isopropyl alcohol or in an ultrasonic bath.

The development and product assurance plan requires that parts are fully traceable for build configuration control on deliverable models, and where test data forms part of the qualification process. For all components of adequate size the design drawing identifies a location to permanently mark the component drawing number, revision and serial number. Components of small size will either be marked with the serial number alone (which shall be unique for all components and cross-referenced to drawing number, revision and manufacturing lot). Below a certain size of component (e.g. small fasteners, P-clips) the components will be 'bagged and tagged', with the packaging identifying the part numbers.

The method of marking each component is TBD, and will usually be based on engraving or etching. Where components are subject to high stress levels the design drawing will ensure that marking will not act as a stress raiser.

The BSM design is inevitably comprised of small components within a tightly packed assembly. Consideration has been given to access for fasteners and wiring harness, and additional lessons learnt from prototyping will be incorporated into the design via the change-control process. The BSM comprises several sub-assemblies and the tight alignment tolerance leaves the design vulnerable to tolerance stack up if not correctly approached. The following design features and assembly aids are incorporated into the design:

13.2.1 Flex pivot protection sleeves:

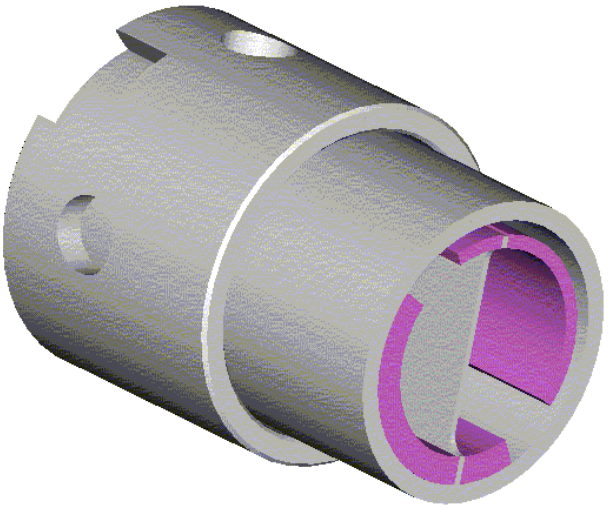

Figure 43 flex pivot mounted in protection sleeve (note holes for adhesive- this allows glue to be added after assembly and reduces risk of adhesive being placed on moving parts)

The flex pivots are sized as a light push fit, avoiding buckling loads on the flexures during installation. To ensure survival of warm vibration and maintain position during build, the pivots are fixed with a cryogenic space rated adhesive - Eccobond or Stycast (TBD). The pivots are not marked for identification, but the flex pivot sleeves may be identified externally as they are required in handed pairs. A discussion drawing (SPIRE-022-001) is produced to demonstrate correct alignment technique on subsequent integration.

13.2.2 Mirror handling

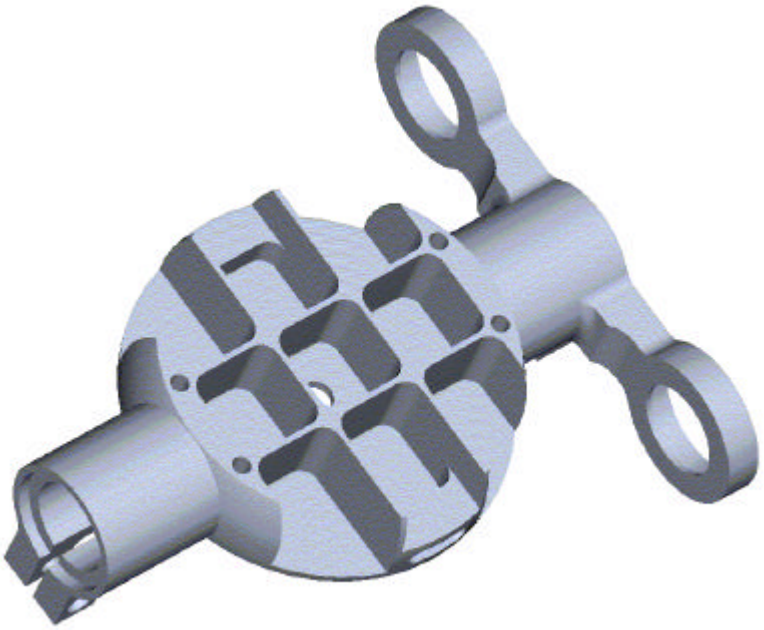

Figure 44 underside of mirror showing light-weighting and 4-off tapped holes for process mounting

The chop stage and mirror have four tapped holes on the mirror backing structure. These provide a clamping facility for optical machining, and are useful in subsequent processes. Inserts are not placed in the threads to avoid print through at cryogenic temperatures.

13.2.3 Chop Stage (drawing SPIRE-BSM-020-004)

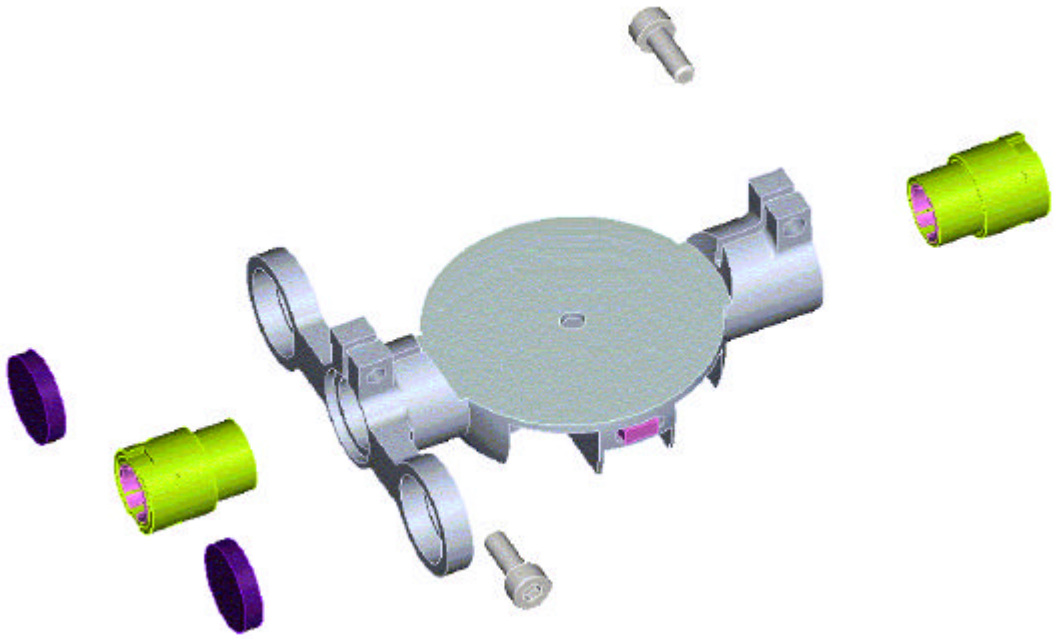

Figure 45 Chop stage assembly showing sensor cores (pink), magnets (purple) and flex-pivots (green)

The insertion of flex pivots into the chop stage is facilitated by an open fit, clamped up by a screw after assembly and alignment.

The sensor cores are pushed into the bottom of their pockets, facilitating positioning, and glued in place.

The magnets are currently a slight push fit, again seating in the bottom of a pocket and retained by a fillet of adhesive. The magnets are relatively brittle components and the fit may need to be opened out if problems are found in prototype and development model builds (TBC).

13.2.4 Motor Assemblies (drawing SPIRE-BSM-020-005)

Alignment of the motor air gaps is a critical design parameter - both to optimize torque performance and to avoid the possibility of fouls.

A design aim is to avoid shimming or adjustment of the assemblies, as with 4 off motor assemblies per BSM model there will be strong advantages to interchangeability.

The motor assemblies be bolted together with the coil cores as a loose fit in their pockets (0.25-0.5mm gap). An assembly jig (BSM-022-002) will locate the motor coils with high precision with respect to the coil bracket mounting face and hold them in place whilst the adhesive cures. This will produce an assembly with high precision (25-50 microns) repeatability on mounting.

After assessing the Zeiss motor dimensional repeatability, it may be possible to assemble based on supplied interface dimensions, but this is TBC.

13.2.5 Jiggle assembly (drawing SPIRE-BSM-020-003)

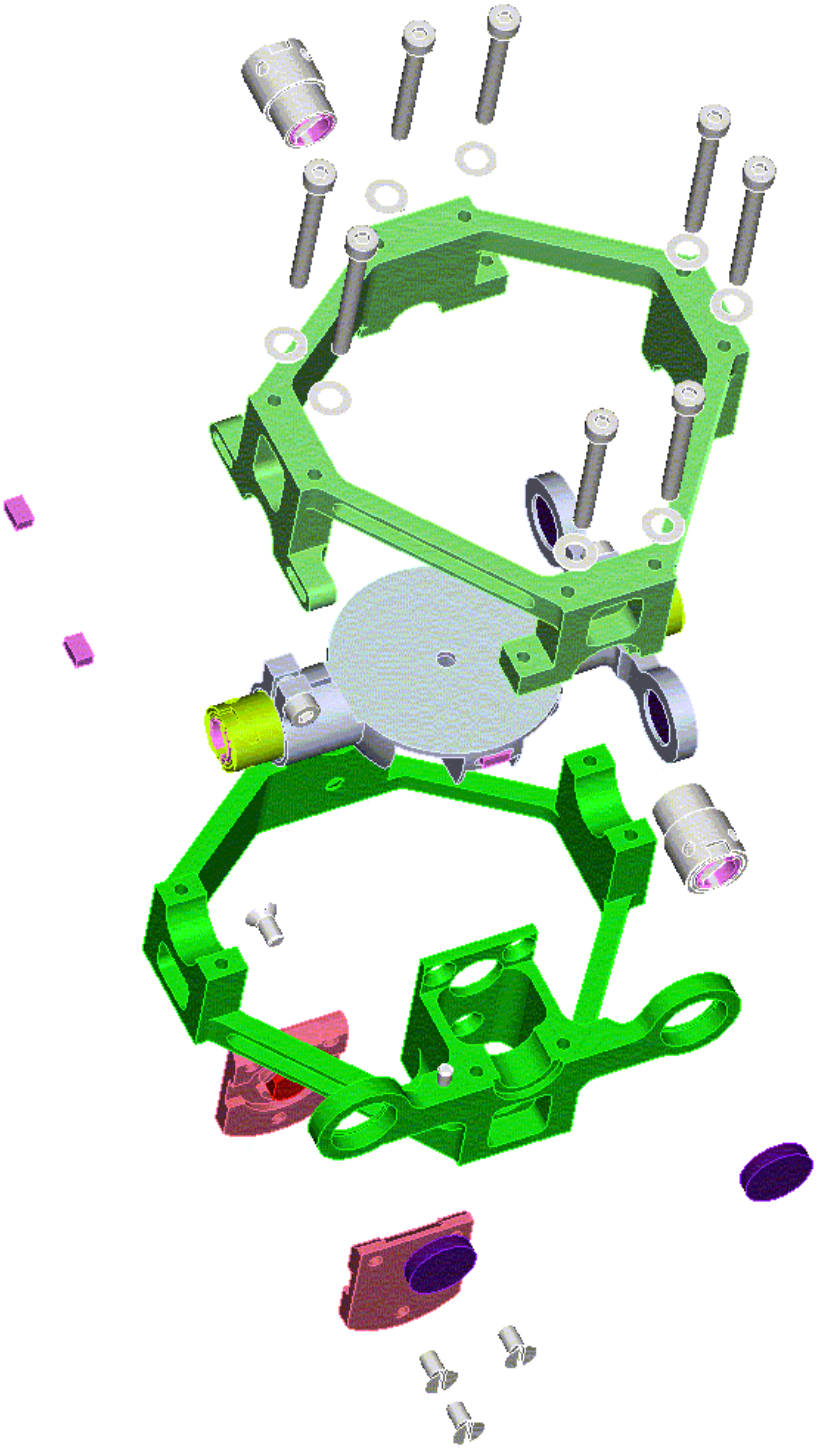

Figure 46 Jiggle stage assembly showing jiggle frame (green), sensor cores (pink), Infineon sensors (red)

Alignment of the mirror at the correct geometric location is important,

- to minimise optical alignment of the BSM on integration to SPIRE
- to ensure that the distance between the chop axis magnet lever-arms and the jiggle axis bores is correct, to prevent fouls between the magnet lever-arms and the drive motor assemblies.

- the mirror must be located flat within the jiggle frame so that it's rest position will be within the fail-safe tolerance.

This task is complicated because

- the flex pivots will easily take a small pre-load during the assembly process, and thus spring back to an undesired position when done.
- The presence of strong magnets attracted to local objects creates offsets or lack of control,
- The need to fit the 'lower' chop axis motor housing during the build of this assembly adds a dead weight to one lever arm.

Consequently an assembly jig is envisaged. This would (TBC)

- Hold the lower jiggle frame flat and facing upwards
- Provide a set of mounting holes to position the motor assembly in place
- Provide a spigot to locate the mirror centroid and a reference face to align the mirror face to.

The assembly would be freed from the jig, and the rest position of the mirror checked. Pending prototype and development model experimentation it remains possible that a small preload will occur and the process might need to be repeated until the tolerance were met. (It is anticipated that some process parameters such as the torque-up pattern of the eight jiggle frame screws will need to be worked out).

13.2.6 Jiggle frame to structure assembly

The complete 2 axis gimbal mount and remaining three motor assemblies are installed at this stage. Due to the use of assembly jigs for the gimbal and motor assemblies, and CNC machining of the structure, the tolerance stack up is limited (as compared to the 10+ components which would contribute to stack up if jigging were not used). Therefore the motor air-gaps are achievable to tolerance without adjustment on assembly.

To meet the jiggle axis rest position tolerance a further jig is envisaged assist in setting the jiggle frame angle. This will use the rotation slots in the jiggle flex-pivot sleeves to assist in rotating the jiggle frame.

13.2.7 Harness routing

The motors and sensors will have flying leads soldered to them at the sub-assembly stage. These flying leads will then be routed through apertures in the BSMs bulkheads and staked down as appropriate. The attachment of the flying leads into the on-BSM connectors will require soldering/crimping operations on an assembly which will be 'clean' at that point.

The BSM and PCAL may be protected by covering/enclosure (with only the flying lead exposed) and the soldering operation could then be performed outside the ATC clean room (or indeed inside, if local extract facilities can be made available without contaminating the clean room).

13.3 Integration

All components are capable of withstanding bake out to 80 deg C (note however that this is close to the magnet material specified limit and close control of the bake out process will be required).

The PCAL interface provides for a toleranced hole and mounting face, and no mechanical problems are envisaged.

The alignment issues of integration to the SPIRE optical bench are discussed elsewhere in this document (section 7 Mechanical and section 9, Optical)

13.4 Verification

Verification / test plans for the design is outlined in RD 5

13.5 Transport & Storage

The BSM will be transported in a sealed container, purged with dry nitrogen. As postal service vibration loads are well known to be more rigorous than launch loads, the device will be hand carried where at all possible.

A transport lock may be provided (TBD), and if so will be 'red flagged' for removal before use and identified as such in the ADP.

The transport container will provide for storage facilities also. Components and sub-assemblies will be stored in dry Nitrogen environments where required. For corrosion control and protection during handling, components will in general be gold plated, Alachromed or sealed/potted as applicable.

13.6 Handling

No special handling requirements are envisaged, beyond normal clean room care and attention.

13.7 Test Programme & Test Matrix

The Verification / test plans for the design are outlined in RD 5

This page left intentionally blank

Document Ends

List of Appendices

This page intentionally left blank

Document Ends.

Appendix 1
v1.0

Mechanical Design Drawing Pack

Contents

1. Bill of Materials
2. Pro/E drawings (development model), latest release.
3. Interface Control Drawings
4. Process Instructions

1. Bill of Materials

ASSEMBLIES :-						
Model Name	**Drawing Number**	**Description**	**Rev.**	**Ver.**	**Release Level**	**Quantity**
atc-brg-flex-001.asm	n/a	Lucas flex pivot 5010-600	1	12	Review	2
atc-brg-flex-002.asm	n/a	Lucas flex pivot 5010-800	1	0	Released	2
spire-bsm-020-001.asm	SPIRE-BSM-020-001	beam steering mirror assembly	3	0	Released	1
spire-bsm-020-003.asm	SPIRE-BSM-020-003	Gimbal Assembly (Jiggle + Chop stages)	3	0	Released	1
spire-bsm-020-004.asm	SPIRE-BSM-020-004	BSM chop axis assembly	3	0	Released	1
spire-bsm-020-005.asm	SPIRE-BSM-020-005	COIL ASSEMBLY	2	0	Released	4
spire-bsm-020-007.asm	SPIRE-BSM-020-007	SENSOR ASSY	2	0	Released	4
spire-bsm-020-008.asm	SPIRE-BSM-020-008	Shielded flexure assy (jiggle top)	2	0	Released	1
spire-bsm-020-009.asm	To Be Drawn	Harness Routing Assembly (prime)	1	6	Released	1
spire-bsm-020-010.asm	To Be Drawn	Harness Routing Assembly (redundant)	1	4	Released	1
spire-bsm-020-012.asm	SPIRE-BSM-020-012	Shielded flexure assy (jiggle bot)	2	0	Released	1
spire-bsm-020-015.asm	SPIRE-BSM-020-015	Shielded flexure assy (chop LH)	1	0	Released	1
spire-bsm-020-016.asm	SPIRE-BSM-020-016	Shielded flexure assy (chop RH)	1	0	Released	1

PARTS :-						
Model Name	**Drawing Number**	**Description**	**Rev.**	**Ver.**	**Release Level**	**Quantity**
37way_conn.prt	n/a	37 pin connector MDM	1	5	Released	2
atc-brg-flex-001-001.prt	n/a	Sleeve	1	6	Review	8
atc-brg-flex-001-002.prt	n/a	Core	1	6	Review	4
atc-brg-flex-001-003.prt	n/a	Outer flexure	1	7	Review	8
atc-brg-flex-001-005.prt	n/a	Core	1	5	Review	4
atc_brg_flex-001-004.prt	n/a	centre flexure	1	6	Review	4
cap-hd-screw-ss-m2-5x12.prt	n/a	CAP HD SCREW SS M2x12	1	0	Released	4
cap-hd-screw-ss-m2-5x21_8.prt	n/a	CAP HD SCREW SS M2.5x21.8mm	1	1	Released	4
cap-hd-screw-ss-m2-5x24.prt	n/a	CAP HD SCREW SS M2.5x24mm	1	1	Released	4
cap-hd-screw-ss-m2-5x6.prt	n/a	CAP HD SCREW SS M2.5 x 6mm	1	1	Released	10
cap-hd-screw-ss-m2-5x7.prt	n/a	CAP HD SCREW SS M2.5x7mm	1	2	Released	17
cap-hd-screw-ss-m2-5x7_75.prt	n/a	CAP HD SCREW SS M2.5X7.75	1	0	Released	10
cap-hd-screw-ss-m2x10.prt	n/a	CAP HD SCREW SS M2X10	1	1	Released	4
cap-hd-screw-ss-m4x10.prt	n/a	CAP HD SCREW SS M4x10	1	0	Released	3
csk-hd-screw-ss-m2-5x5.prt	n/a	CSK HD SCREW SS M2.5X5	1	0	Released	6
cx-1030-cu.prt	n/a	CERNOX THERMISTOR, Cu CANISTER MOUNT	1	1	Released	2
disc-spring-id-3_2.prt	n/a	DISC SPRING SS 3.2mm ID	1	1	Released	12
dowel_8x2.prt	n/a	DOWEL SS 2mm dia x 8mm	1	1	WIP	6

PARTS :-						
Model Name	**Drawing Number**	**Description**	**Rev.**	**Ver.**	**Release Level**	**Quantity**
		lg.				
spire-bsm-020-001-001.prt	SPIRE-BSM-020-001-001	BSM Structural Interface	2	0	Released	1
spire-bsm-020-001-002.prt	SPIRE-BSM-020-001-002	BASEPLATE	2	0	Change	1
spire-bsm-020-001-003.prt	SPIRE-BSM-020-001-003	Jiggle axis flexure clamp lower	2	0	Released	1
spire-bsm-020-001-004.prt	SPIRE-BSM-020-001-004	PCAL SPACE ENVELOPE	1	6	Released	1
spire-bsm-020-001-005.prt	SPIRE-BSM-020-001-005	Jiggle axis flexure clamp upper	2	0	Released	1
spire-bsm-020-001-007.prt	SPIRE-BSM-020-001-007	BSM LAUNCH LATCH SPACE ENVELOPE	1	3	Released	1
spire-bsm-020-001-009.prt	SPIRE-BSM-020-001-009	FRONT BAFFLE	1	3	WIP	1
spire-bsm-020-003-001.prt	SPIRE-BSM-020-003-001	Jiggle Frame Bottom	3	0	Released	1
spire-bsm-020-003-002.prt	SPIRE-BSM-020-003-002	Jiggle Frame Top	2	0	Released	1
spire-bsm-020-003-003.prt	SPIRE-BSM-020-003-003	PACS slim magnet	1	3	Released	4
spire-bsm-020-004-001.prt	SPIRE-BSM-020-004-001	Chop Stage	3	1	Released	1
spire-bsm-020-004-004.prt	SPIRE-BSM-020-004-004	sensor actuator	2	0	Released	4
spire-bsm-020-005-001.prt	SPIRE-BSM-020-005-001	COIL BRACKET	2	0	Released	4
spire-bsm-020-005-002.prt	SPIRE-BSM-020-005-002	COIL RETAINER	2	0	Released	4
spire-bsm-020-005-003.prt	SPIRE-BSM-020-005-003	COIL	1	2	Released	8
spire-bsm-020-005-005.prt	SPIRE-BSM-020-005-005	HEAT SHIELD	2	0	Released	4
spire-bsm-020-006-002.prt	SPIRE-BSM-020-006-002	SENSOR	1	0	Released	4
spire-bsm-020-007-001.prt	SPIRE-BSM-020-007-001	SENSOR HOUSING	2	0	Released	4
spire-bsm-020-008-001.prt	SPIRE-BSM-020-008-001	Flex Pivot Protective Shield	1	6	Released	4
spire-bsm-020-009-001pcal.prt	To Be Drawn	Wiring Routing, PCAL (prime)	1	4	Released	1
spire-bsm-020-009-002llat.prt	To Be Drawn	Wiring Routing, Launch Latch (prime)	1	4	Released	1
spire-bsm-020-009-003jigl.prt	To Be Drawn	Wire Routing, Jiggle Motor Left (prime)	1	1	Released	1
spire-bsm-020-009-004jigr.prt	To Be Drawn	Wire Routing, Jiggle Motor Right (prime)	1	1	Released	1
spire-bsm-020-009-005chol.prt	To Be Drawn	Wire Routing, Chop Motor Left (prime)	1	2	Released	1
spire-bsm-020-009-006chor.prt	To Be Drawn	Wire Routing, Chop Motor Right (prime)	1	2	Released	1
spire-bsm-020-009-007senc.prt	To Be Drawn	Wire Routing, Chop Sensor (prime)	1	1	Released	1
spire-bsm-020-009-008senj.prt	To Be Drawn	Wire Routing, Jiggle Sensor (prime)	1	1	Released	1
spire-bsm-020-009-009ther.prt	To Be Drawn	Wire Routing, Thermistor (prime)	1	3	Released	1
spire-bsm-020-009-010.prt	To Be Drawn	cable boot	1	0	WIP	1

PARTS :-						
Model Name	**Drawing Number**	**Description**	**Rev.**	**Ver.**	**Release Level**	**Quantity**
spire-bsm-020-010-001pcal.prt	To Be Drawn	Wire Routing PCAL (redundant)	1	1	Released	1
spire-bsm-020-010-002llat.prt	To Be Drawn	Wire Routing Launch Latch (redundant)	1	1	Released	1
spire-bsm-020-010-003jigl.prt	To Be Drawn	Wire Routing Jiggle Motor Left (redundant)	1	1	Released	1
spire-bsm-020-010-004jigr.prt	To Be Drawn	Wire Routing Jiggle Motor Right (redundant)	1	1	Released	1
spire-bsm-020-010-005chol.prt	To Be Drawn	Wire Routing Chop Motor Left (redundant)	1	2	Released	1
spire-bsm-020-010-006chor.prt	To Be Drawn	Wire Routing Chop Motor Right (redundant)	1	2	Released	1
spire-bsm-020-010-007senc.prt	To Be Drawn	Wire Routing chop sensor (redundant)	1	2	Released	1
spire-bsm-020-010-008senj.prt	To Be Drawn	Wire Routing Jiggle sensor (redundant)	1	2	Released	1
spire-bsm-020-010-009ther.prt	To Be Drawn	Wire Routing thermistor (redundant)	1	1	Released	1
spire-bsm-020-010-010.prt	To Be Drawn	cable boot space envelope (redundant)	1	0	Released	1
terminal_pin_571-4015.prt	N/A	TERMINAL PIN	1	0	WIP	16

The drawing release status is as per the release scheme described in the BSM PA Plan.

2. Pro/E drawings (development model), latest release.

This page left intentionally blank

3. Interface Control Drawings

This page left intentionally blank

4. Process Instructions

This page left intentionally blank

This page left intentionally blank

This page left intentionally blank

Document Ends.

Appendix 2
V1.0

Electronic Design Drawing Pack

2.1 Contents

2.2 *Table* of *Figures*

2.3 General

The following diagrams show the BSM Warm Electronics circuit diagrams. The BSM wiring is described in the document ‘BSM Electronics Interface’.

The processor board (LAM MAC board) is described in separate LAM documentation. These circuit diagrams are best viewed in Microsoft Word with 'Zoom' set to 200%, or printed.

2.4 Circuit Diagrams

Figure A2-1 POSITION SENSOR PREAMPLIFIER (CHOP AND JIGGLE SAME)

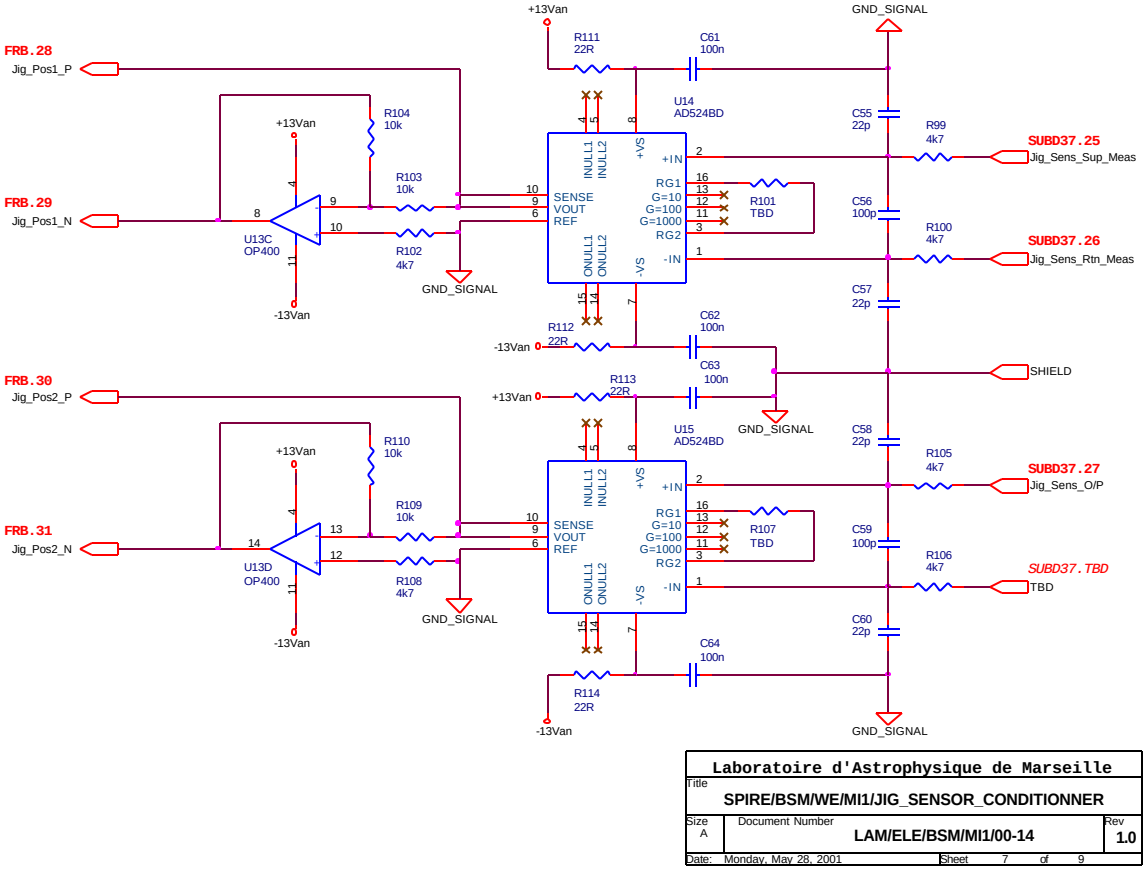

Figure A2-2 POSITION SENSOR CURRENT SUPPLY

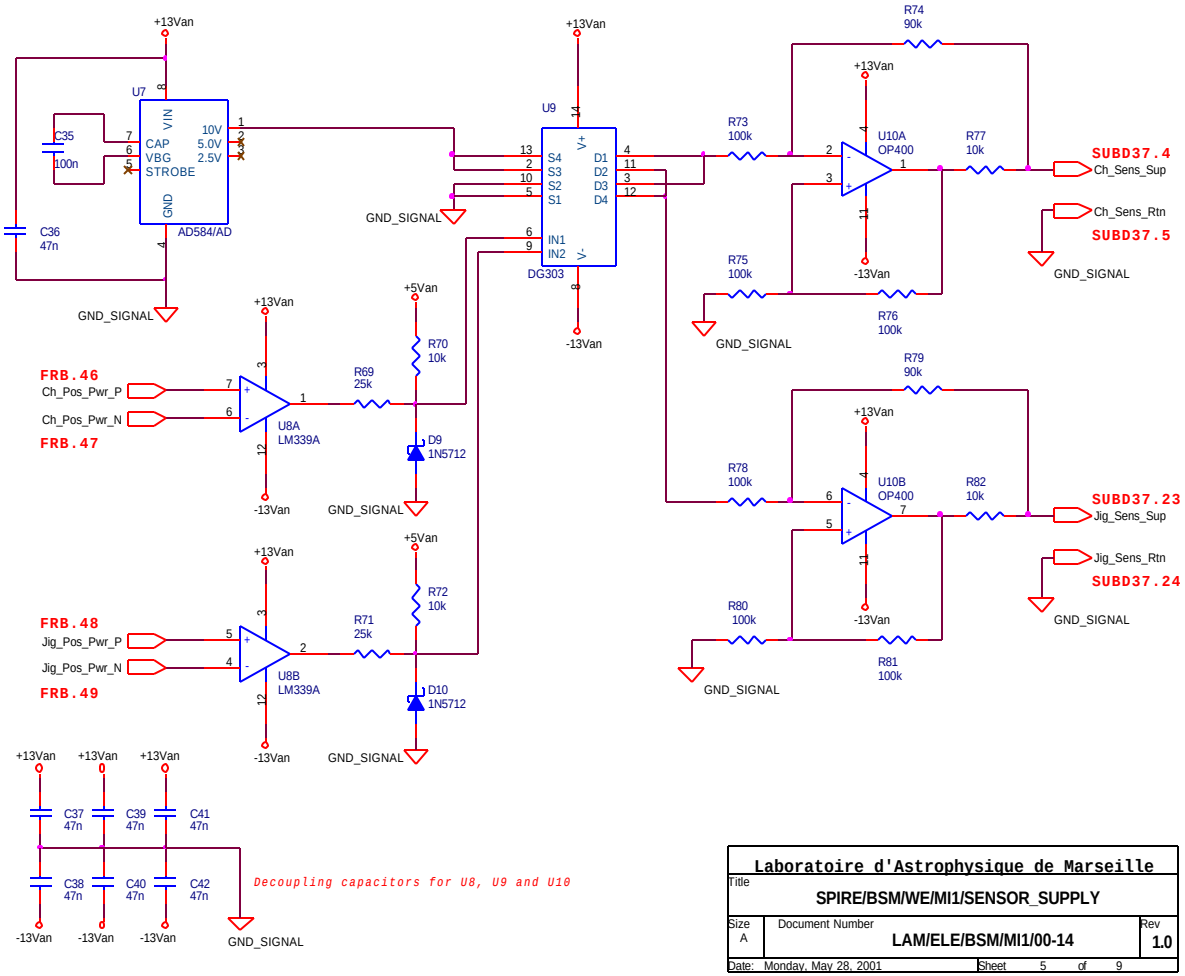

Laboratoire d'Astrophysique de Marseille		
Title: SPIRE/BSM/WE/MI1/SENSOR_SUPPLY		
Size: A	Document Number: LAM/ELE/BSM/MI1/00-14	Rev: 1.0
Date: Monday, May 28, 2001	Sheet 5 of 9	

Figure A2-3 MOTOR POWER AMPLIFIER (CHOP AND JIGGLE SAME)

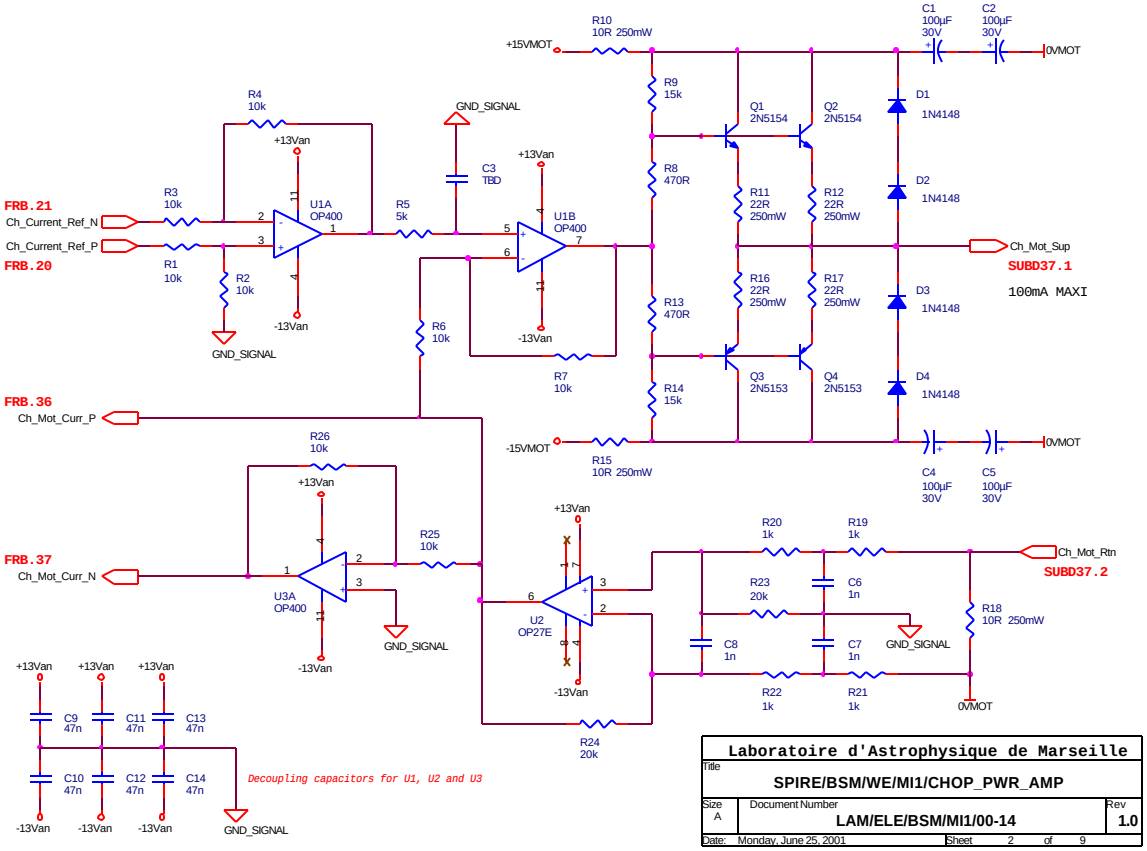

Figure A2-4 BSM LAUNCH LATCH INTERFACE

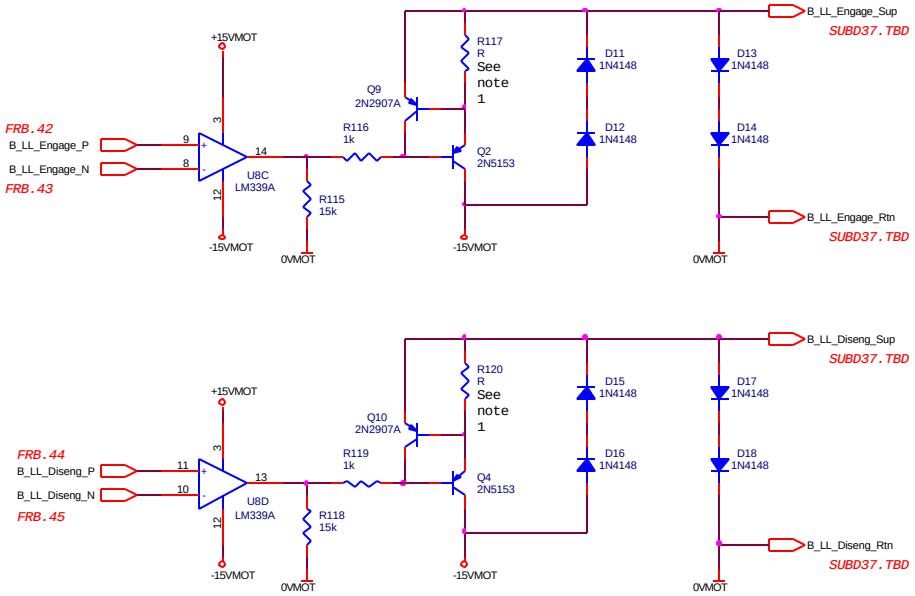

NOTE 1: R=33 Ohms for I=25 mA
R=22 Ohms for I=35 mA

Laboratoire d'Astrophysique de Marseille		
Title: SPIRE/BSM/WE/MI1/LAUNCH LATCH		
Size: A	Document Number: LAM/ELE/BSM/MI1/00-14	Rev: 1.0
Date: Monday, May 28, 2001	Sheet 8 of 9	

Figure A2-5 LAUNCH LATCH STATUS INTERFACE

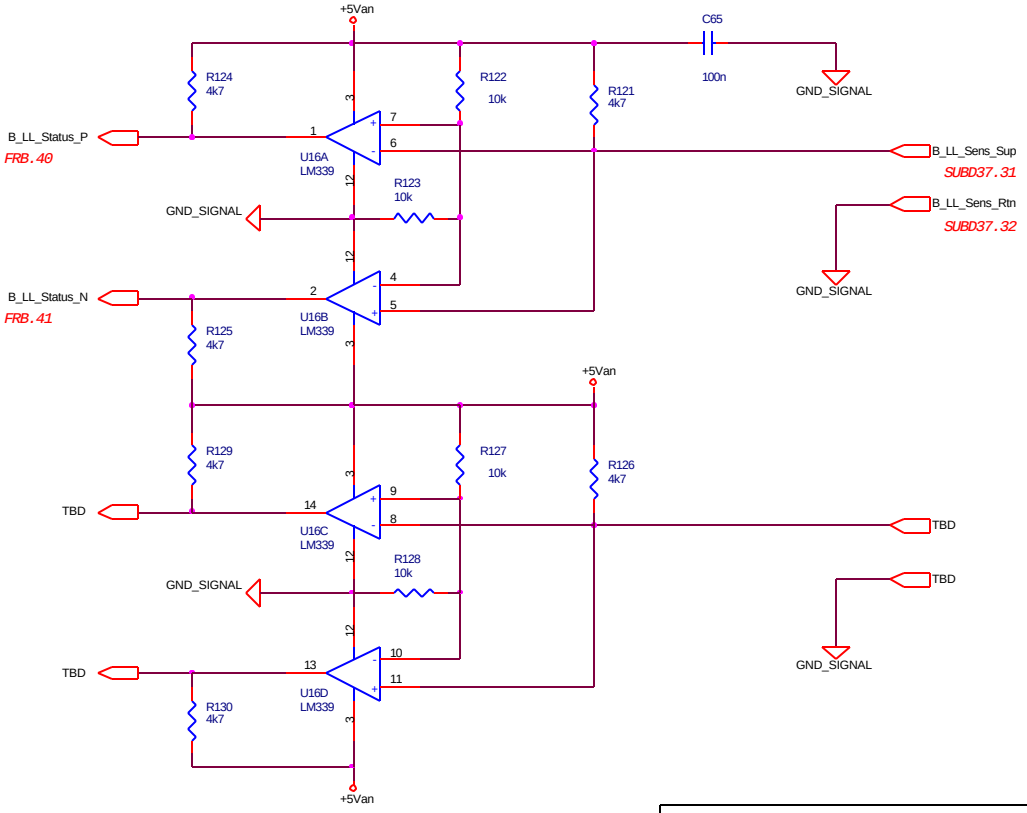

Laboratoire d'Astrophysique de Marseille		
Title: SPIRE/BSM/WE/MI1/LAUNCH LATCH STATUS		
Size: A	Document Number: LAM/ELE/BSM/MI1/00-14	Rev: 1.0
Date: Monday, May 28, 2001	Sheet 9 of 9	

Figure A2-6 ***MOTOR BACK EMF SENSOR (CHOP AND JIGGLE)***

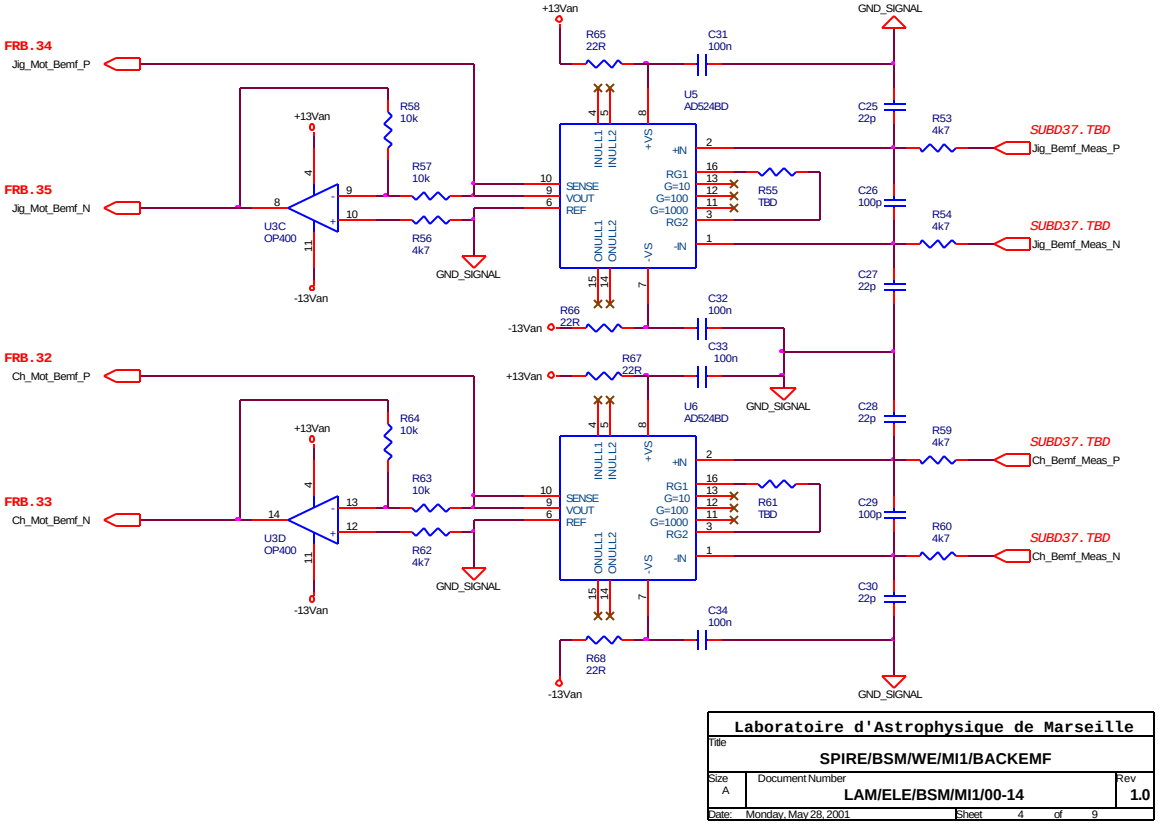

Document Ends

Appendix 3
v1.0

3A: Dynamic Analysis Of The BSM

Document No:	BSM_DESIGN_DESCRIPTION_V4.1_appendix_3_v1.0.doc
Status:	Draft
Version:	8
Modified by:	Alison Tonï
Modified date:	27 February 2002 4:15 a15/p15
Author:	Ian Pain
Created date:	4 May 2000 5:04 PM
Category:	
Type:	
Generated with:	Microsoft Word 8.0

1 BSM Design

The SPIRE Beam Steering Mirror has been modelled for finite element analysis as a simplified representation of the Pro/E solid model shown below.

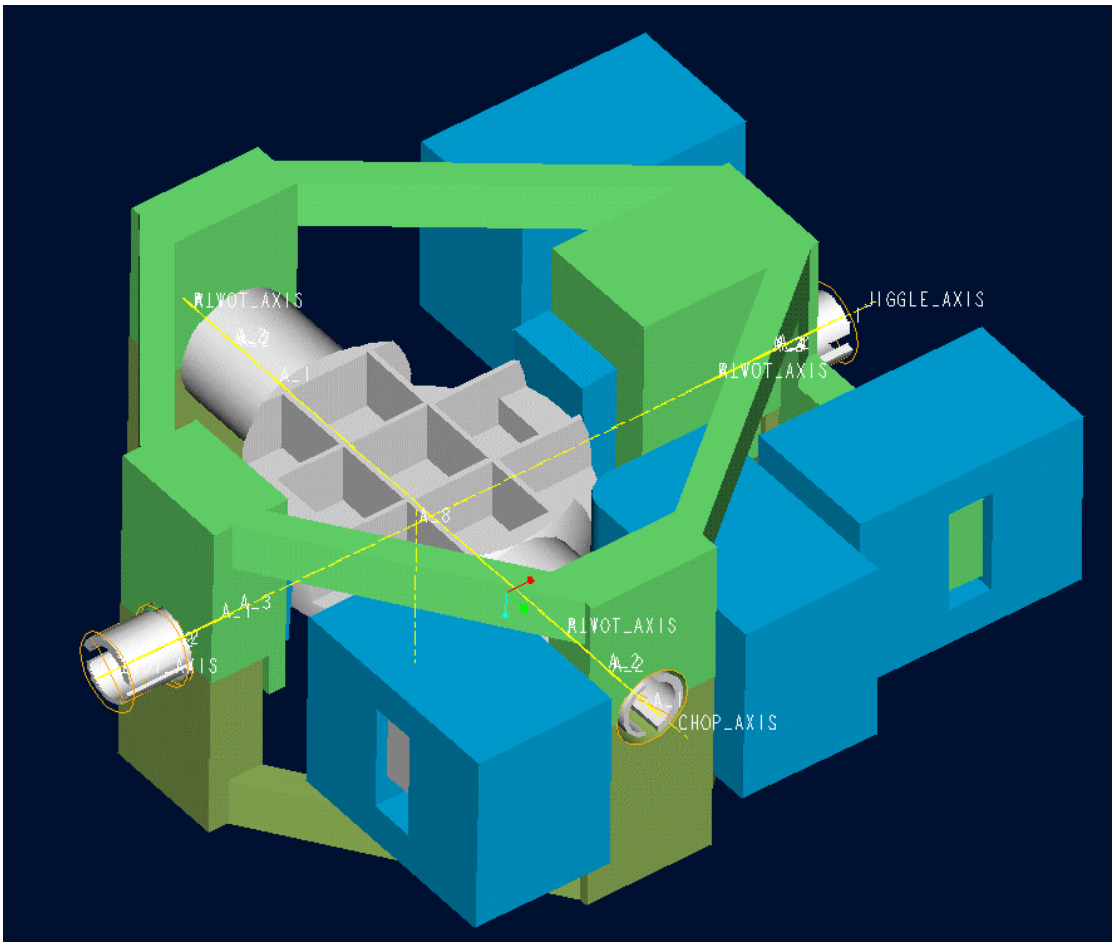

- The chop stage is monolithic. The underside of the mirror is lightweighted and has pockets for the iron plates for the sensors.
- The jiggle stage is split and clamps together around the flex pivots.
- Space envelopes for the coils and sensors (potted) are shown in blue.
- The outer rings of the flex-pivots are not shown for clarity.
- In this revision Lucas 5010-600 pivots have been used for the jiggle axis and 5010-800 for the chop axis. These have torsional stiffnesses of 0.0286 and 0.0036 lb.in/degree respectively.

2 FEA Model

2.1 Modelling

- The jiggle stage structure has been represented by thin shell elements;
- The chop stage has been represented by a tube of solid elements together with lumped masses (shown red in the illustration below) to give the same mass and moments of inertia as the solid model;
- The flex pivots have been modelled using a combination of solid and shell elements.

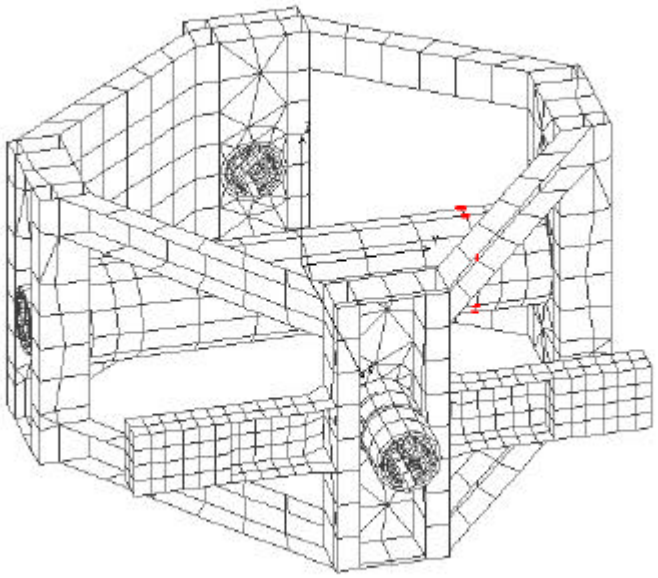

- The jiggle stage framework between the flex-pivot housings has been modelled as 5mm x 5mm x 0.5mm channel section.
- The pivots have been moved as far as reasonably practical towards the mirror to minimise the inertia and maximise the stiffness. To clear the coils this leads to an asymmetric arrangement.
- To balance the jiggle stage the framework in the opposite corner to the coils has been made solid. This also increases the stiffness of the structure. Due to the use of lumped masses which do not give the correct products of inertia and also because the jiggle stage has not been dynamically balanced their will be some inaccuracy in modelling coupling of the stages.

2.2 Load cases

The following analyses have been made:

- 50 g static load in X,Y and Z directions
- Frequency response analysis for excitation of the chop and jiggle stages by couples of 1 Newton forces at the centre of the drive magnets (equivalent forces for the chop stage.)

3 Results

3.1 Static stress analysis

The three load cases (50g in X, Y and Z) lead to stresses in the flexures of similar magnitude.

The highest stress, 265 MPa, occurs in the jiggle axis flex-pivots. The 0.2% proof and ultimate tensile stresses and of 420S29 equivalent to the stainless steel used for these items are 555 MPa and 755 MPa respectively so the design appears relatively safe. It should be noted however that the model is a simplified representation for dynamic analysis and would need refinement for accurate stress calculation.

The load capacity of each of the pivots is 245 N (55 lb) and the weight of the jiggle and chop stages at 50g is 27 N.

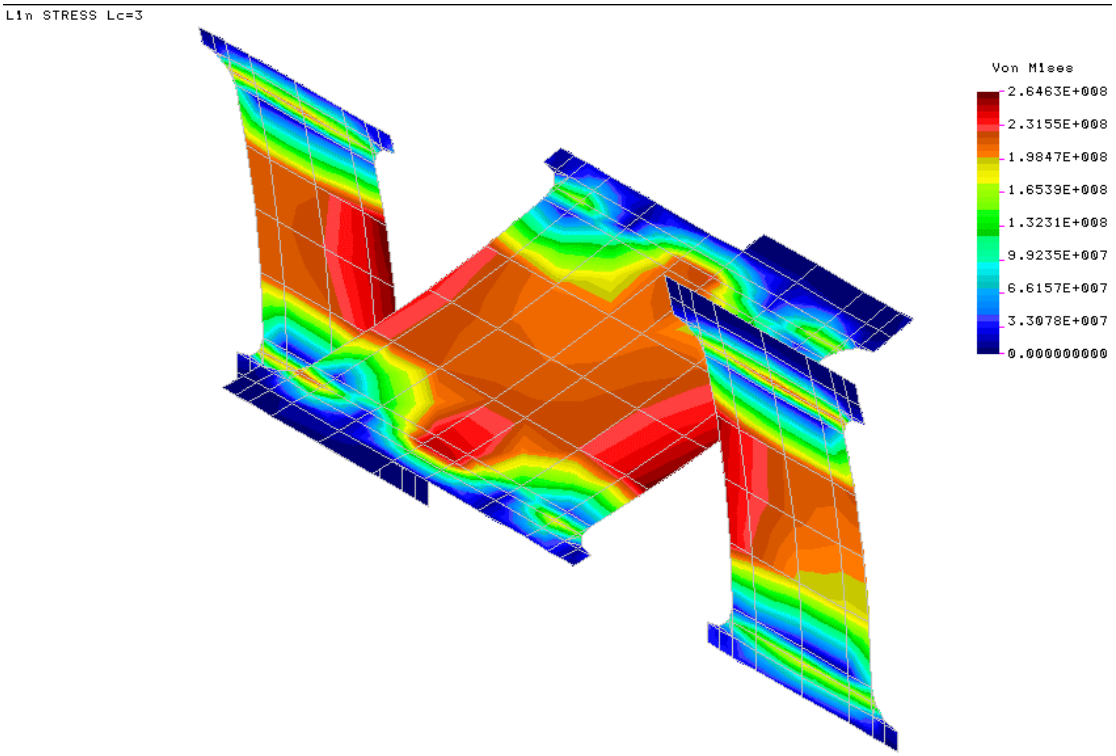

3.2 Dynamic Analysis

3.2.1 Frequency analysis

The model was analysed to obtain the first 50 natural frequencies. The resonant frequencies of the chop and jiggle stages are 23 and 18 Hz respectively.

The first parasitic resonance occurs at 729 Hz.

FREQUENCY NUMBER	FREQUENCY (RAD/SEC)	FREQUENCY (CYCLES/SEC)	PERIOD (SECONDS)
1	.1142200E+03	.1817867E+02	.5500952E-01
2	.1454493E+03	.2314898E+02	.4319844E-01
3	.4577739E+04	.7285698E+03	.1372552E-02
4	.5822649E+04	.9267033E+03	.1079094E-02
5	.7800567E+04	.1241499E+04	.8054781E-03
6	.9250813E+04	.1472313E+04	.6792036E-03
7	.1019618E+05	.1622772E+04	.6162294E-03
8	.1030486E+05	.1640069E+04	.6097305E-03
9	.1129106E+05	.1797028E+04	.5564743E-03
10	.1459196E+05	.2322382E+04	.4305923E-03

3.2.2 Damping

The damping ratio for the near rigid-body modes (chop and jiggle) were set to 0.0004 based on data in the Lucas flex-pivot catalogue. For the higher frequency where the flexure of the jiggle-stage framework is significant the ratio was set to 0.02 which is typical of a well engineered bolted structure.

Set no.	First Mode	Last Mode	Damping Ratio
1	1	2	.4000E-03
2	3	50	.2000E-01

3.2.3 Chop axis excitation

Forces were applied equivalent to a couple of 1Newton forces acting at the chop magnet radius (15mm from the axis).

Below the resonance the response tends to the static case; a rotation of 0.086 radian.

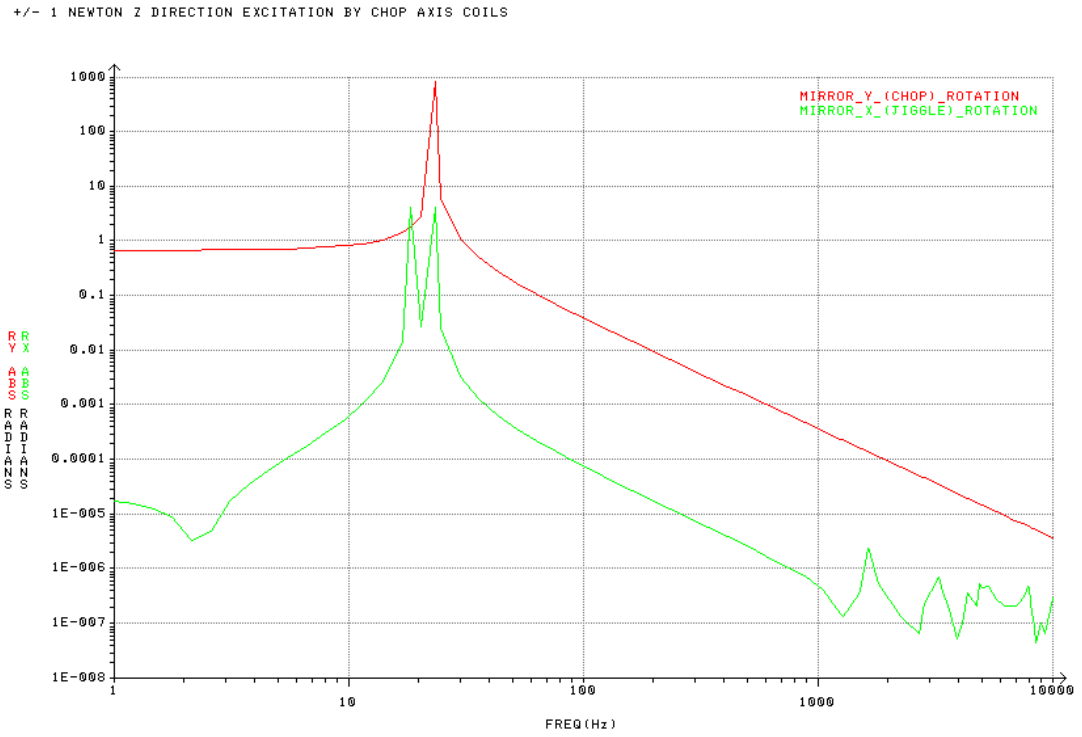

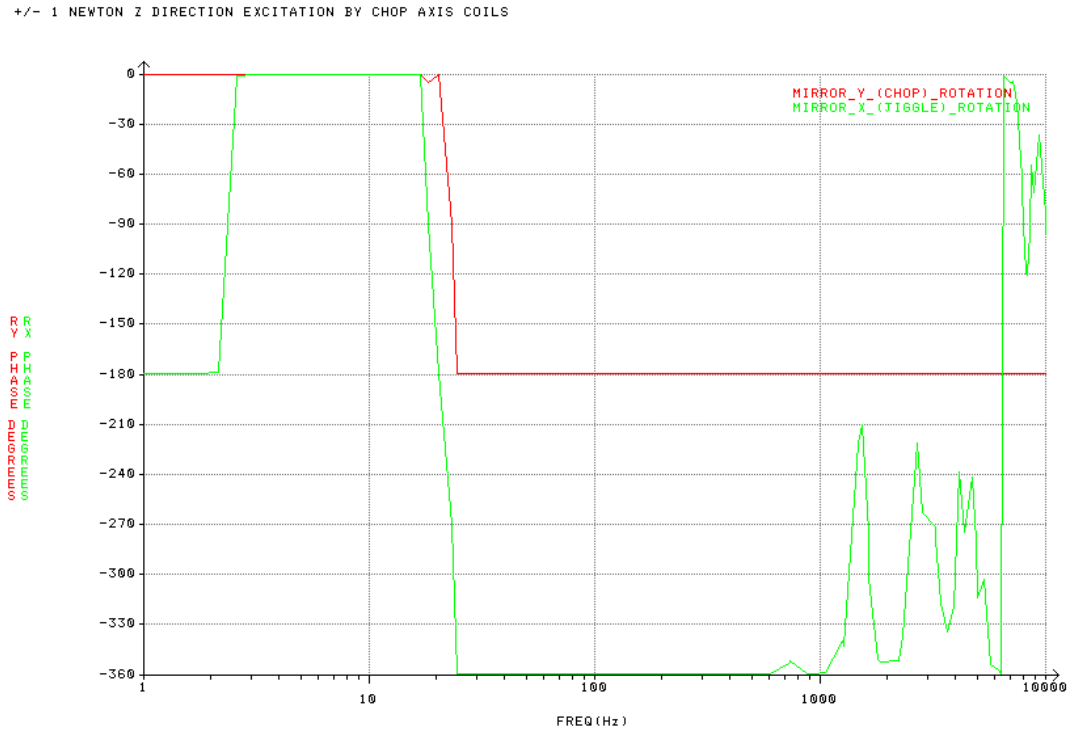

3.2.4 Jiggle axis excitation

A couple of 1Newton forces acting at the centre of the jiggle magnets. Below the resonance the response tends to the static case; a rotation of 0.14 radian.

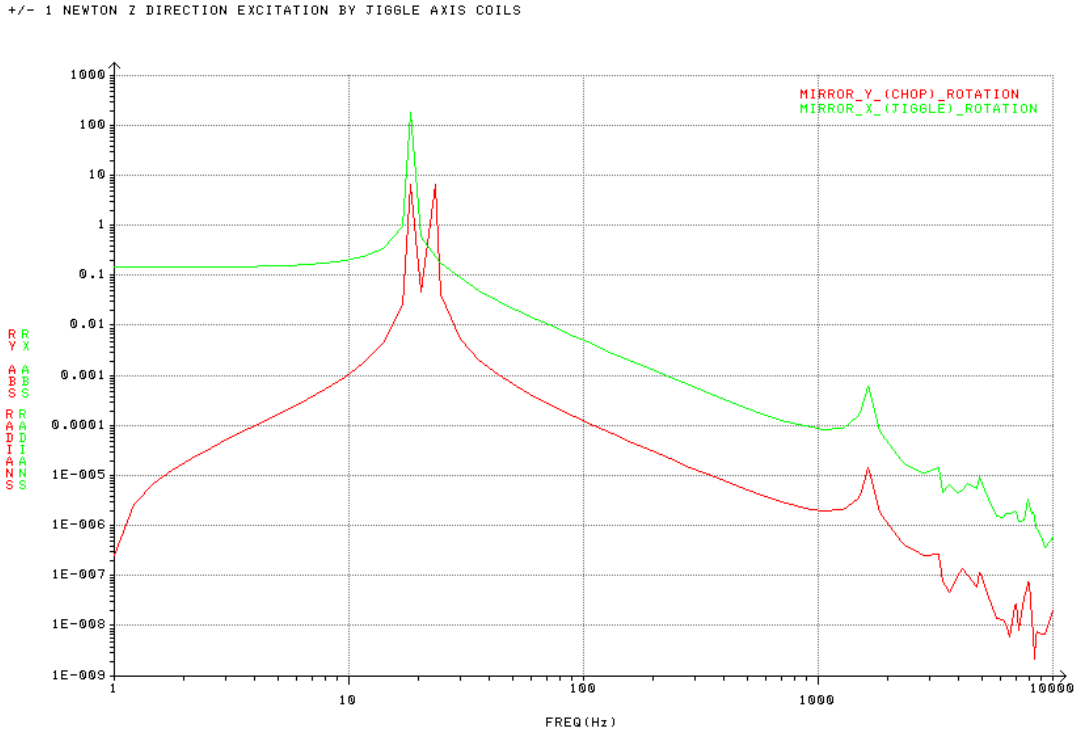

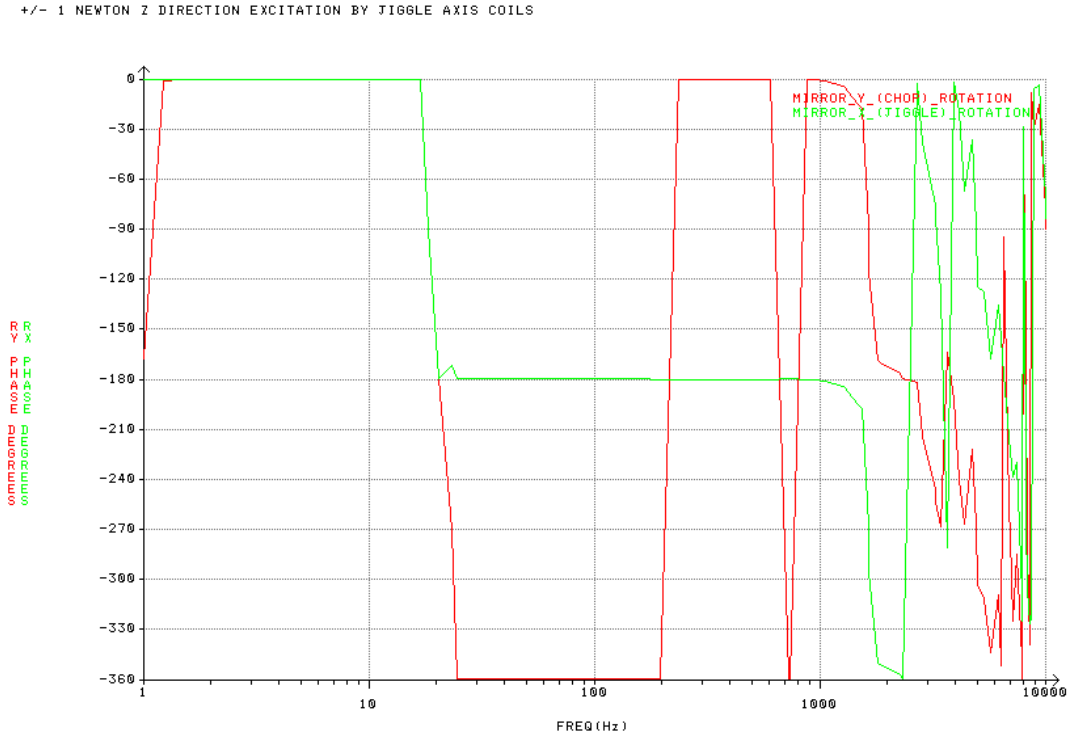

4 References

4.1 Mass properties

The following parameters are derived from the FEA model. The section dimensions used will be fed back into the solid model and more accurate values obtained in due course.

Stage	Parameter	Value
Chop	Mass	0.018 Kg
	Moment of Inertia	2.1 Kg.mm^2
Jiggle	Mass	0.054 Kg
	Moment of Inertia	27 Kg.mm^2

Appendix 3B: Structural Interface FEA Results

1 Scope

This document records a Finite Element Analysis performed on the SPIRE Beam Steering Mirror structure component,

2 Model

2.1 Design

The model is based on Pro/Engineer drawing number BSM-02-001-001 dated Rev 1 (WIP) 29.May.01.

2.2 FEA representation

The FEA was performed as a solid model in integrated Pro/Mechanica. Multi-pass adaptive meshing was used, with convergence set at 10%. Small fillets and holes were generally suppressed, with the exception of connector pin and base mounting features. Material was assigned as Aluminium 6082

2.3 Software

- Pro/Engineer 2000i2
- Pro/MECHANICA STRUCTURE Version 22.3(305) (integrated mode)

3 Results

3.1 50 G acceleration load case

3.1.1 Deflection results

Maximum displacement is predicted at 43 microns under this load case, with prime deflections occurring in a twisting mode (from the side loading) and a pistoning mode around the front mounting hole (from vertical and fore-aft loads).

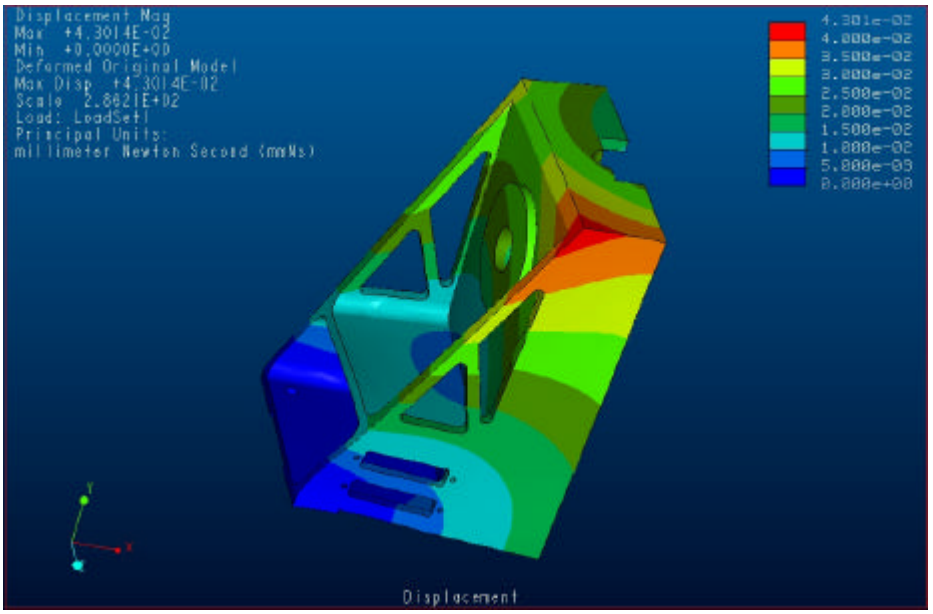

Figure 1 : displacement results (millimetres)

3.1.2 Von Mises Stress results

stresses peak at 36 MPa.

Permissible is per BS8118 (IP's design log no 9, p57)

For fatigue with FoS of 1.0

- 67 MPa friction grip bolted zones (not strictly applicable here as loads are not construction level friction grip)
- 96MPa for re-entrant features
- 76MPa small holes (dia < 3t)

For parent plate
240 MPa with suggested load factor of 2.5, ie a target of 96 MPa in this case

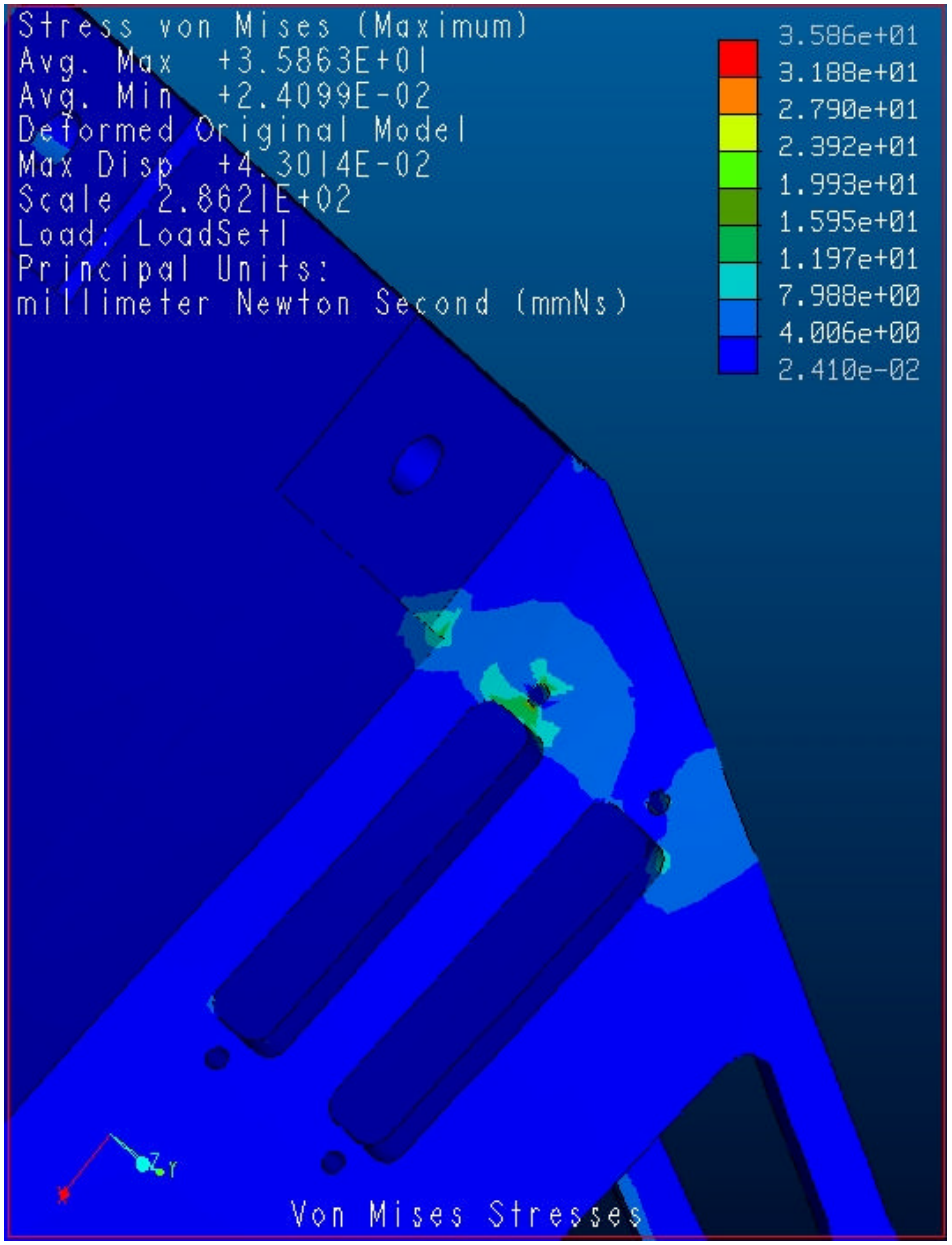

Figure 2 stress distribution around connector cut out and mounting feet

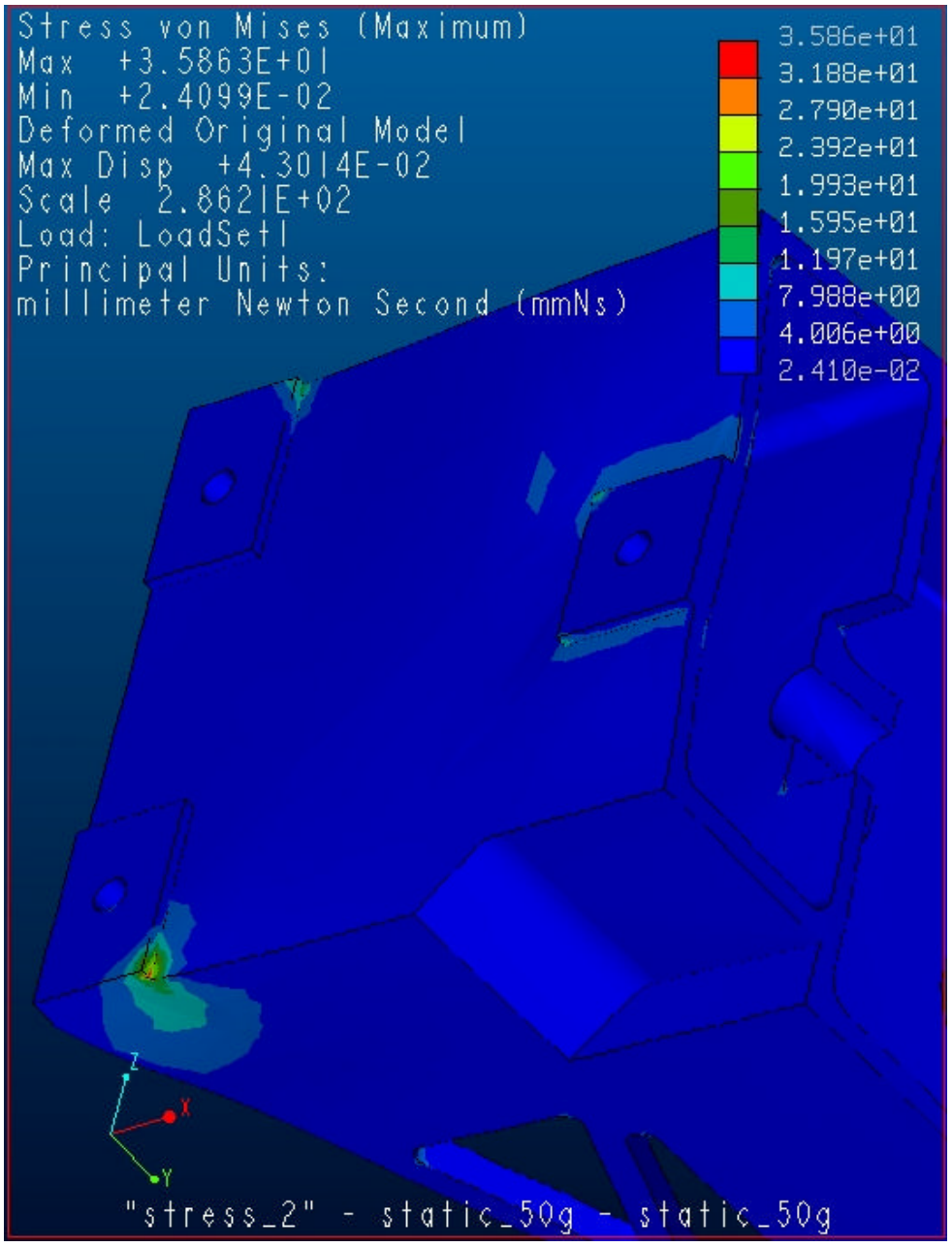

Figure 3 stress distribution around rear mounting foot

3.1.3 Analysis report (extracts)

```
---------------------------------------------------------------
Pro/MECHANICA STRUCTURE Version 22.3(305)
Summary for Design Study "static_50g"
Mon Jun 04, 2001   19:10:01
---------------------------------------------------------------
No errors were found in the model.

Pro/MECHANICA STRUCTURE Model Summary

  Principal System of Units: millimeter Newton Second (mmNs)

  Length:         mm
  Force:          N
  Time:           sec
  Temperature:    C

  Model Type: Three Dimensional

  Points:      1146
  Edges:       5435
  Faces:       7465

  Springs:       0
  Masses:        0
  Beams:         0
  Shells:        0
  Solids:      3189

  Elements:    3189

---------------------------------------------------------------

Standard Design Study

Description:
  50G loads applied in x,y,z

Static Analysis "static_50g":

  Convergence Method: Multiple-Pass Adaptive
  Plotting Grid:     4

  >> Pass  1 <<

        Total Number of Equations:    3330
        Maximum Edge Order:              1

        Elements Not Converged:       3189
        Edges Not Converged:          5435
        Local Disp/Energy Index:     100.0%
        Global RMS Stress Index:     100.0%
>> Pass  2 <<

        Total Number of Equations:   19418
        Maximum Edge Order:              2

Elements Not Converged:       1956
        Edges Not Converged:          4627
        Local Disp/Energy Index:     100.0%
        Global RMS Stress Index:      84.8%
  >> Pass  3 <<
        Total Number of Equations:   63723
        Maximum Edge Order:              4
        Elements Not Converged:       1639
        Edges Not Converged:          2628
        Local Disp/Energy Index:     100.0%
        Global RMS Stress Index:      80.9%

  >> Pass  4 <<
        Total Number of Equations:  117789
        Maximum Edge Order:              5
```

```
        Elements Not Converged:       815
        Edges Not Converged:          207
        Local Disp/Energy Index:    100.0%
        Global RMS Stress Index:     36.4%

>> Pass  5 <<
        Total Number of Equations:  174100
        Maximum Edge Order:           6
        Elements Not Converged:       146
        Edges Not Converged:          0
        Local Disp/Energy Index:     54.9%
        Global RMS Stress Index:     13.1%

>> Pass  6 <<
        Total Number of Equations:  199893
        Maximum Edge Order:           6
        Elements Not Converged:       22
        Edges Not Converged:          0
        Local Disp/Energy Index:     30.1%
        Global RMS Stress Index:     12.0%

     RMS Stress Error Estimates:

     Load Set         Stress Error  % of Max Prin Str
     ---------------  ------------  -----------------
     LoadSet1          4.56e-01      1.3% of  3.63e+01

** Warning: Convergence was not obtained because the maximum
        polynomial order of 6 was reached.

  The analysis did not converge to within 10% on
  edge displacement and element strain energy.

  Total Mass of Model:  2.943847e-04

  Mass Moments of Inertia about WCS Origin:

    Ixx:  1.41233e+00
    Ixy: -2.35807e-01  Iyy:  3.84633e-01
    Ixz: -4.52996e-03  Iyz:  1.01220e-03  Izz:  1.29888e+00

  Principal MMOI and Principal Axes Relative to WCS Origin:

         Max Prin          Mid Prin          Min Prin
       1.46399e+00       1.29874e+00       3.33110e-01

  WCS X:  9.76566e-01       2.74581e-02       2.13461e-01
  WCS Y: -2.13377e-01      -5.97632e-03       9.76952e-01
  WCS Z: -2.81010e-02       9.99605e-01      -2.26723e-05

  Center of Mass Location Relative to WCS Origin:
              ( 1.02862e+01,  4.89316e+01, -5.38177e-02)

  Mass Moments of Inertia about the Center of Mass:

    Ixx:  7.07486e-01
    Ixy: -8.76379e-02  Iyy:  3.53484e-01
    Ixz: -4.69293e-03  Iyz:  2.36968e-04  Izz:  5.62882e-01

  Principal MMOI and Principal Axes Relative to COM:

         Max Prin          Mid Prin          Min Prin
       7.28123e-01       5.62755e-01       3.32974e-01

  WCS X:  9.73328e-01       2.64026e-02       2.27892e-01
  WCS Y: -2.27705e-01      -9.92492e-03       9.73680e-01
  WCS Z: -2.79695e-02       9.99602e-01       3.64820e-03

  Constraint Set: ConstraintSet1

  Load Set: LoadSet1

    Resultant Load on Model:
```

in global X direction: 1.451317e+02
in global Y direction: 1.451317e+02
in global Z direction: 1.451317e+02

Measures:

Name	Value	Convergence
max_disp_mag:	4.301418e-02	0.8%
max_disp_x:	3.048651e-02	0.8%
max_disp_y:	-1.805561e-02	0.9%
max_disp_z:	2.839908e-02	0.8%
max_prin_mag:	3.626618e+01	3.8%
max_stress_prin:	3.626618e+01	3.8%
max_stress_vm:	3.586344e+01	0.2%
max_stress_xx:	2.019206e+01	15.5%
max_stress_xy:	1.101872e+01	15.7%
max_stress_xz:	7.227989e+00	0.5%
max_stress_yy:	3.609924e+01	2.9%
max_stress_yz:	-7.932948e+00	0.6%
max_stress_zz:	-1.609714e+01	0.5%
min_stress_prin:	-3.532419e+01	1.2%
strain_energy:	9.345811e-01	0.6%

3.1.4 Verification

Reaction loads

- need checking

Manual verification

- required,

3.2 Modal Analysis

3.2.1 Modal Analysis Results

To limit run time, the maximum number of modes to sweep for was set to 12. The results were:

Mode	Frequency
1	6.881738e+02
2	8.638142e+02
3	1.780816e+03
4	2.715497e+03
5	3.058290e+03
6	3.283797e+03
7	3.344646e+03
8	3.614443e+03
9	3.957047e+03
10	4.096691e+03
11	4.676689e+03
12	5.185199e+03

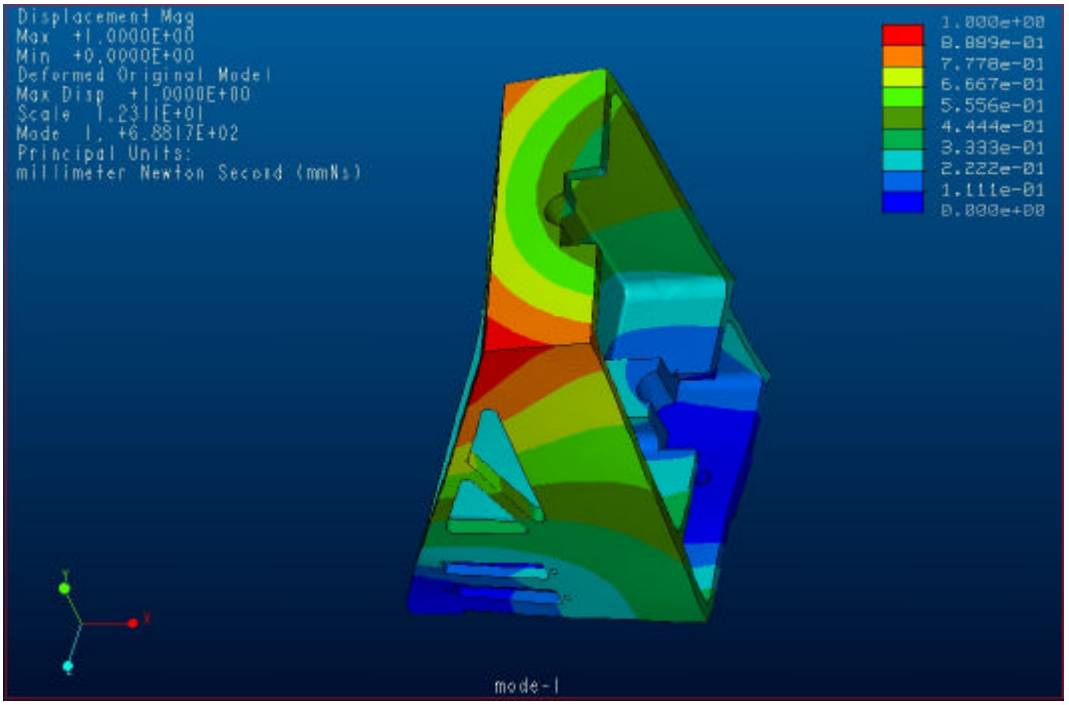

Figure 4 First resonant mode, twisting of entire structure, 688 Hz

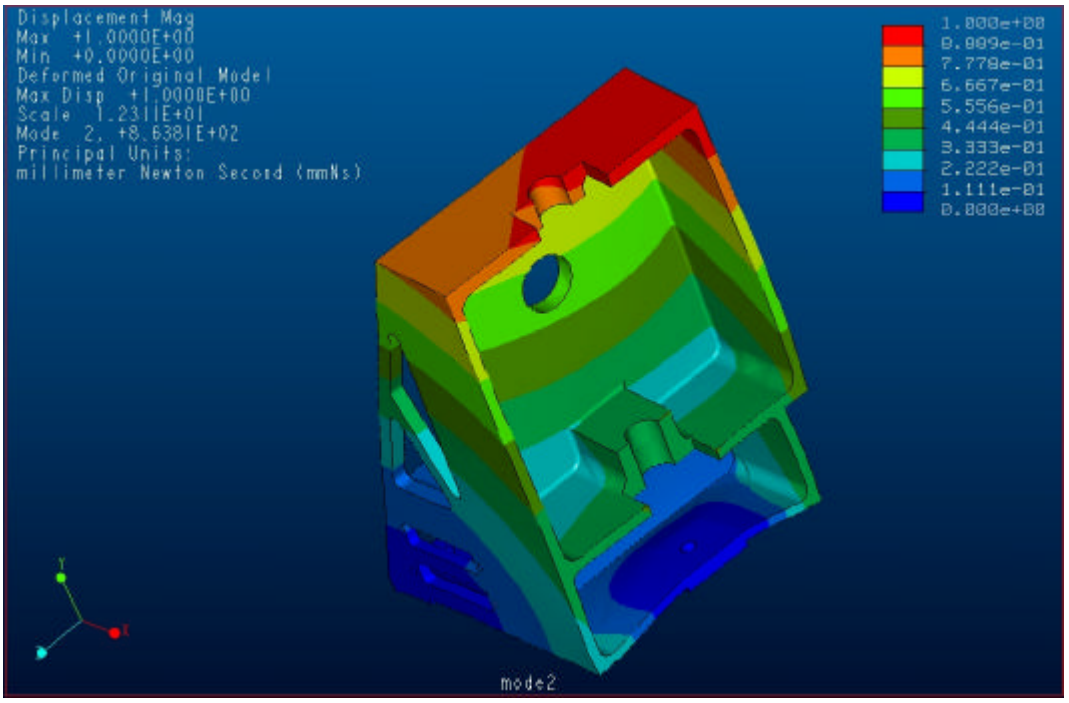

Figure 5 mode 2 , 864Hz. Piston and twist of whole structure

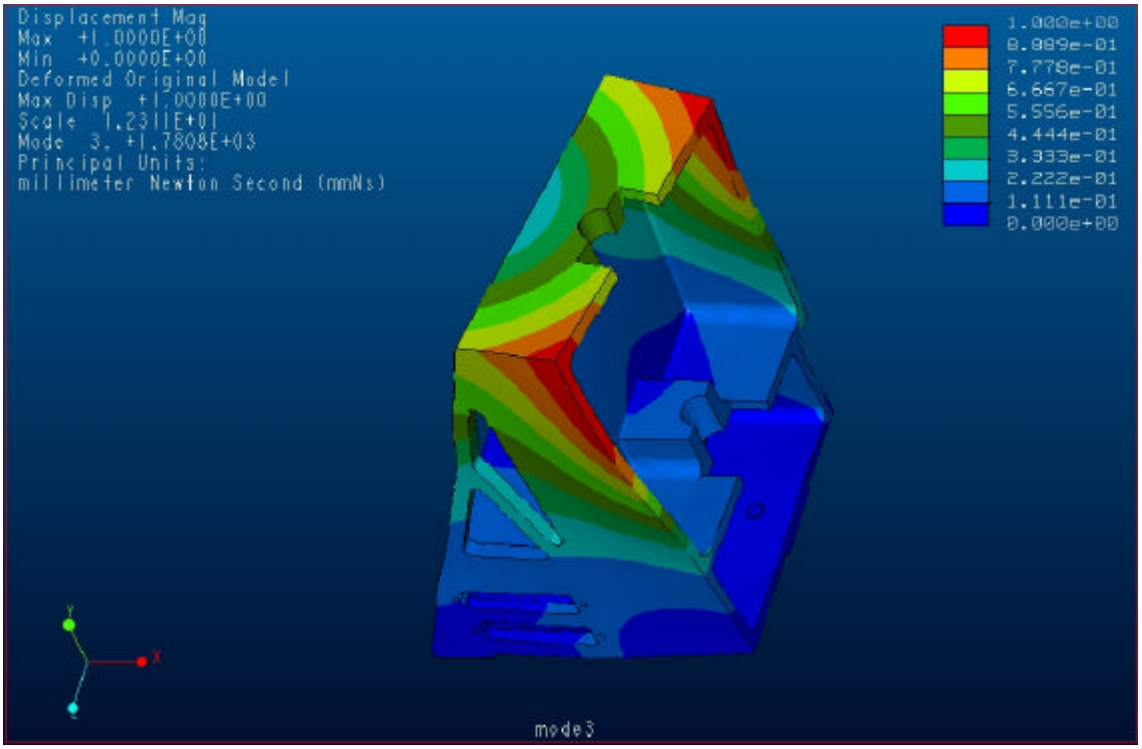

Figure 6 Mode 3 , 1780- Hz, rocking forward of whole structure

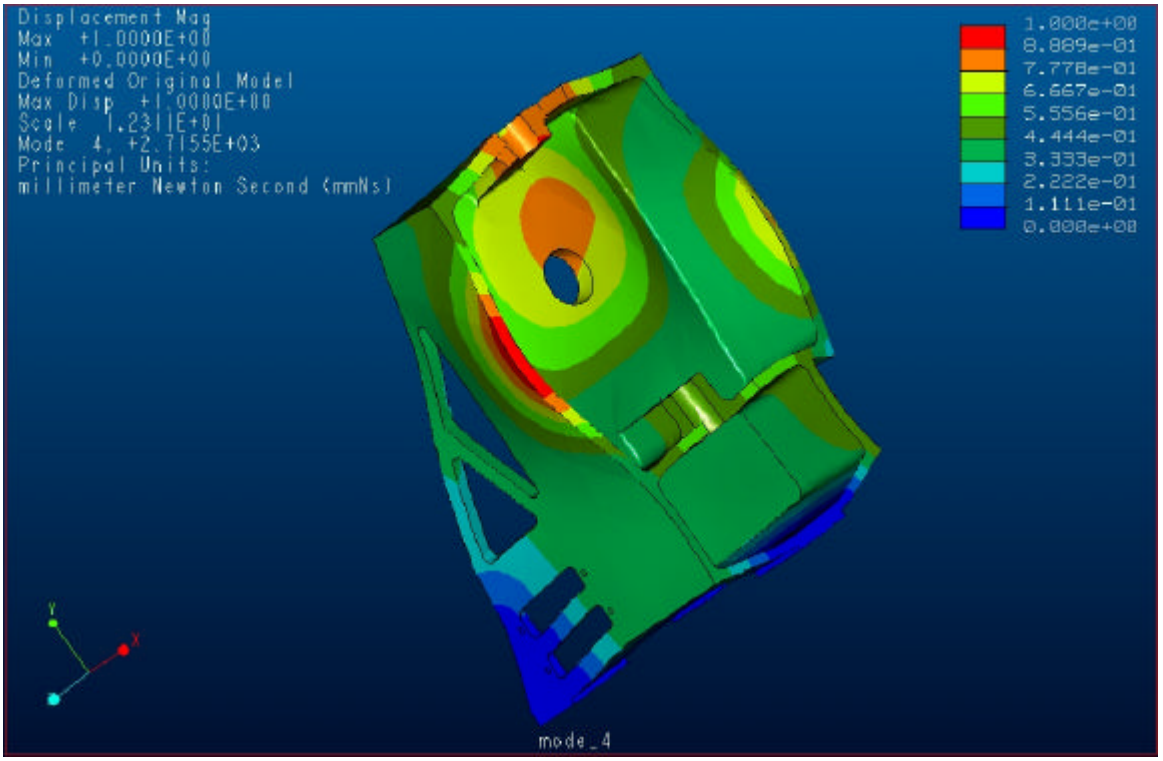

Figure 7 Mode 4, 2716 Hz, local resonance of plates

3.2.2 Model report (extracts)

```
---------------------------------------------------------------
Pro/MECHANICA STRUCTURE Version 22.3(305)
Summary for Design Study "modal"
Tue Jun 05, 2001   08:32:47
---------------------------------------------------------------

No errors were found in the model.

Pro/MECHANICA STRUCTURE Model Summary

  Principal System of Units: millimeter Newton Second (mmNs)

  Length:         mm
  Force:          N
  Time:           sec
  Temperature:    C

  Model Type: Three Dimensional

  Points:      1146
  Edges:       5435
  Faces:       7465

  Springs:       0
  Masses:        0
  Beams:         0
  Shells:        0
  Solids:      3189

  Elements:    3189

---------------------------------------------------------------

Standard Design Study

Description:
  basic modal analysis

Modal Analysis "modal":

  Convergence Method: Single-Pass Adaptive
  Plotting Grid:     4

  Convergence Loop Log:                    (08:33:15)

  >> Pass  1 <<
     Calculating Element Equations         (08:33:15)
       Total Number of Equations:   57792
       Maximum Edge Order:              3


  >> Pass  2 <<
     Calculating Element Equations         (08:36:33)
       Total Number of Equations:   65469
       Maximum Edge Order:              5

     RMS Stress Error Estimates:

     Mode   Stress Error  (% of Max Modal Stress)
     ----  --------------
       1       0.8%
       2       0.7%
       3       2.4%
       4       1.3%
       5       1.1%
```

6	0.8%
7	0.9%
8	1.6%
9	4.3%
10	2.4%
11	2.0%
12	1.0%

Total Mass of Model: 2.943847e-04

Mass Moments of Inertia about WCS Origin:

Ixx: 1.41233e+00
Ixy: -2.35807e-01 Iyy: 3.84633e-01
Ixz: -4.52996e-03 Iyz: 1.01220e-03 Izz: 1.29888e+00

Principal MMOI and Principal Axes Relative to WCS Origin:

Max Prin	Mid Prin	Min Prin
1.46399e+00	1.29874e+00	3.33110e-01

WCS X:	9.76566e-01	2.74581e-02	2.13461e-01
WCS Y:	-2.13377e-01	-5.97632e-03	9.76952e-01
WCS Z:	-2.81010e-02	9.99605e-01	-2.26723e-05

Center of Mass Location Relative to WCS Origin:
(1.02862e+01, 4.89316e+01, -5.38177e-02)

Mass Moments of Inertia about the Center of Mass:

Ixx: 7.07486e-01
Ixy: -8.76379e-02 Iyy: 3.53484e-01
Ixz: -4.69293e-03 Iyz: 2.36968e-04 Izz: 5.62882e-01

Principal MMOI and Principal Axes Relative to COM:

Max Prin	Mid Prin	Min Prin
7.28123e-01	5.62755e-01	3.32974e-01

WCS X:	9.73328e-01	2.64026e-02	2.27892e-01
WCS Y:	-2.27705e-01	-9.92492e-03	9.73680e-01
WCS Z:	-2.79695e-02	9.99602e-01	3.64820e-03

Constraint Set: ConstraintSet1

Number of Modes: 12

Mode	Frequency
1	6.881738e+02
2	8.638142e+02
3	1.780816e+03
4	2.715497e+03
5	3.058290e+03
6	3.283797e+03
7	3.344646e+03
8	3.614443e+03
9	3.957047e+03
10	4.096691e+03
11	4.676689e+03
12	5.185199e+03

3.2.3 Verification

- need checking manually

Appendix 3C: Structural Interface Manual Calculations

1 Scope

This document records a calculation performed on the SPIRE Beam Steering Mirror flex pivots and structure mounting bolts.

2 Calculation

The Input load is as provided in the table below. A static equivalent acceleration load is applied by assuming a Single Degree of Freedom system and using the Miles approximation:

rms accel = (pi . Fn. Wx(Fn)) / 4L)^0.5

where,
Fn = natural frequency
Wx(Fn) = structure input accel from the PSD at the frequency
L = damping ratio = 1/sqrt(Frequency)

BSM random Specification			Ref. instrument co-ordinate system							
			calc by I.Pain from ramp profile supplied by B.Winters, 01.Oct.01							
X 60 sec	X g^2/hz	X g^2/hz		Y 60 sec	Y g^2/hz	Y g^2/hz		Z 60 sec	Z g^2/hz	Z g^2/hz
f	Accept	Qual		f	Accept	Qual		f	Accept	Qual
20		0.008		20		0.028		20		0.012
40		0.032		40		0.112		40		0.048
60		0.072		60		0.252		60		0.108
80		0.128		80		0.448		80		0.192
100		0.2		100		0.7		100		0.3
150		0.2		150		0.7		150		0.3
200		0.2		200		0.7		200		0.3
300		0.2		300		0.1		300		0.133333
400		0.1125		400		0.1		400		0.075
600		0.05		600		0.044444		600		0.033333
800		0.028125		800		0.025		800		0.01875
1000		0.018		1000		0.016		1000		0.012
1500		0.008		1500		0.007111		1500		0.005333
2000		0.0045		2000		0.004		2000		0.003
g-rms				g-rms				g-rms		

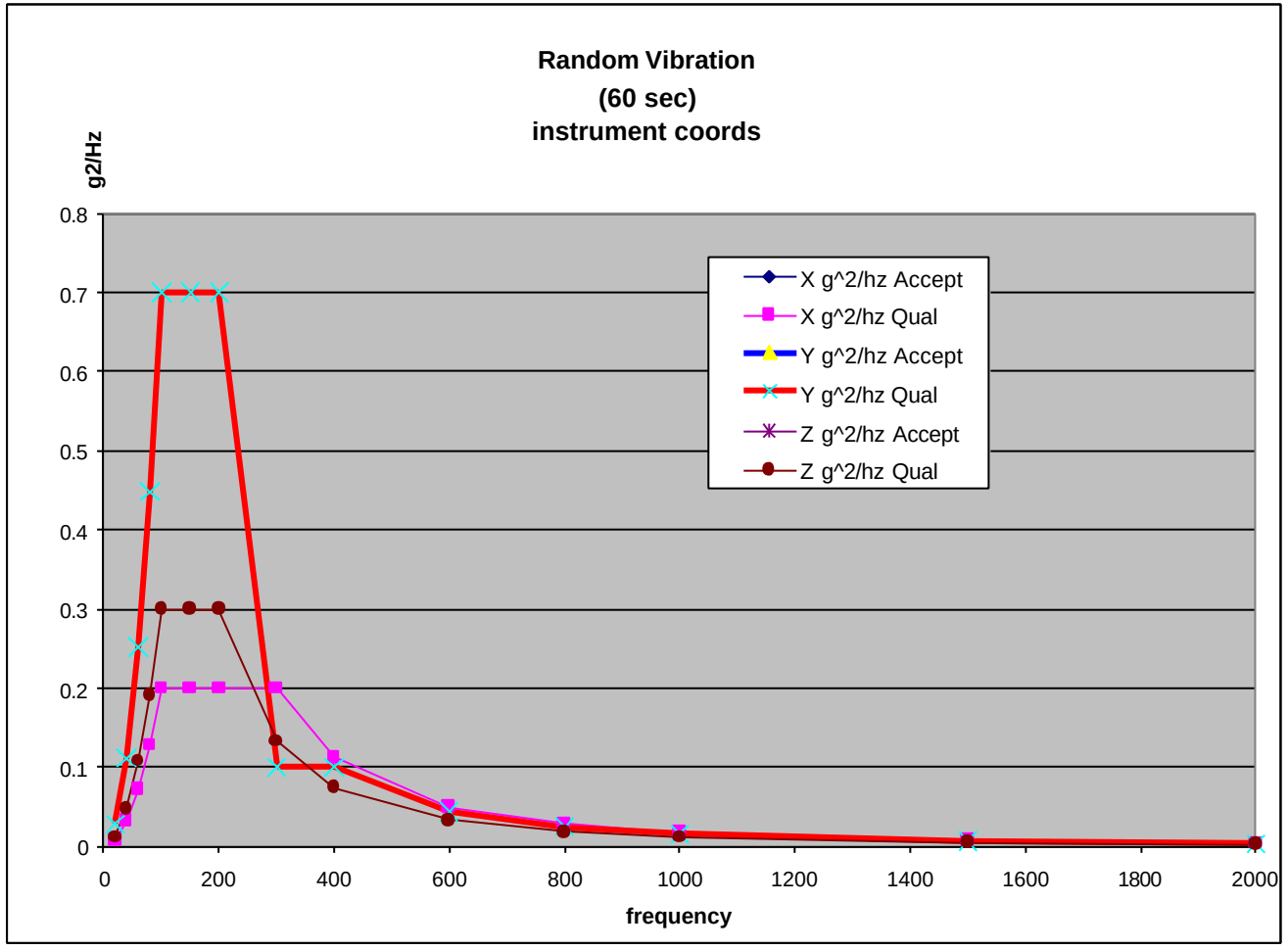
Random Vibration
(60 sec)
instrument coords
g2/Hz
0.8
0.7
0.6
0.5
0.4
0.3
0.2
0.1
0
0
200
400
600
800
1000
1200
1400
1600
1800
2000
frequency
X g^2/hz Accept
X g^2/hz Qual
Y g^2/hz Accept
Y g^2/hz Qual
Z g^2/hz Accept
Z g^2/hz Qual

BSM Response			calc I.Pain 10.OCT.01				version 3.0
fn	freq	interpolate spec	damping = 1/freq^0.5	rms accel (Miles)	multiplier: probable peak response, 120 sec test	50 % peak response	X qual 3sigma peak response
Hz	Hz	g²/Hz	Hz-1	'g' = x9.81m/s²		'g' = x9.81m/s²	'g' = x9.81m/s²
				X qual rms			
350	350	0.156	0.053452	28.3	4.7	134.3	170.6
400	400	0.113	0.05	26.6	4.8	126.7	161.0
450	450	0.097	0.04714	27.0	4.8	129.1	164.0
500	500	0.081	0.044721	26.7	4.8	128.6	163.3
550	550	0.066	0.04264	25.8	4.8	124.6	158.3
600	600	0.050	0.040825	24.0	4.9	116.6	148.0
650	650	0.045	0.039223	24.1	4.9	117.2	148.8
				Y qual rms			Y qual 3sigma peak response
350	350	0.100	0.053452	22.7	4.7	107.5	136.5
400	400	0.100	0.05	25.1	4.8	119.5	151.8
450	450	0.086	0.04714	25.4	4.8	121.8	154.6
500	500	0.072	0.044721	25.2	4.8	121.2	154.0
550	550	0.058	0.04264	24.3	4.8	117.5	149.2
600	600	0.044	0.040825	22.6	4.9	109.9	139.6
650	650	0.040	0.039223	22.7	4.9	110.5	140.3
				Z qual rms			Z qual 3sigma peak response
350	350	0.104	0.053452	23.1	4.7	109.7	139.3
400	400	0.075	0.05	21.7	4.8	103.5	131.4
450	450	0.065	0.04714	22.0	4.8	105.4	133.9
500	500	0.054	0.044721	21.8	4.8	105.0	133.3
550	550	0.044	0.04264	21.1	4.8	101.8	129.2
600	600	0.033	0.040825	19.6	4.9	95.2	120.9

650	650	0.030		0.039223	19.7	4.9		95.7	121.5
				Max (all axes)	28.3	4.9		134.3	170.6

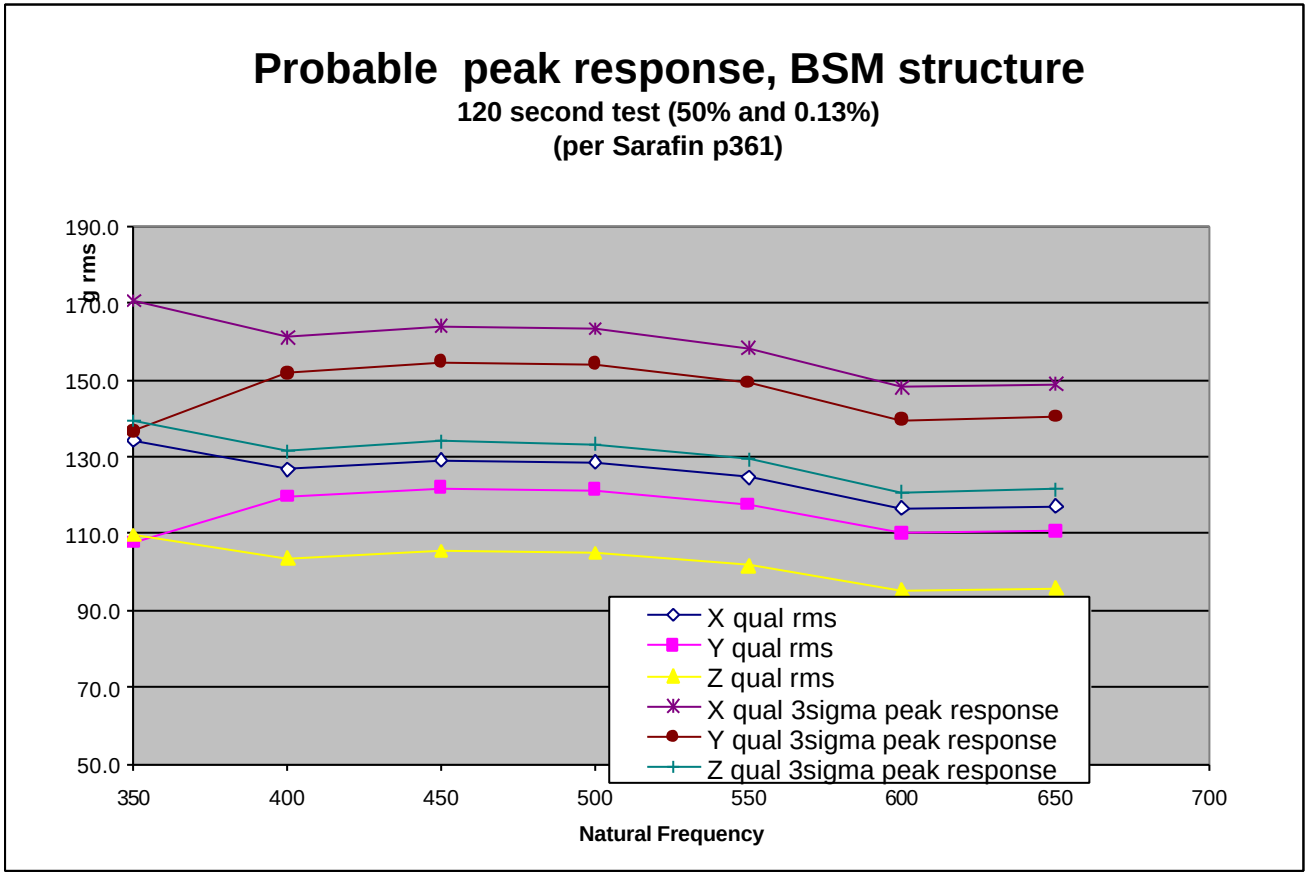

BSM margin - flex pivots & structural bolt					calculated I.Pain 20.Feb.02		version 3.0	
	Component	mass (incl contingency)	load limit of component (N)	required FoS	survival load (in g) for 2 pivots	margin on rms response	margin on 50% peak response	margin on 3-sigma peak response
WARM	C-Flex Chop axis flex pivot	21.0	25.4	1.0	246.6	8.70	1.84	1.45
	C-Flex Jiggle axis flex pivot	96.0	248.3	1.0	527.3	18.60	3.93	3.09
	LUCAS chop axis flex pivot	21.0	25.4	1.0	246.6	8.70	1.84	1.45
	LUCAS jiggle axis flex pivot	96.0	245.0	1.0	520.3	18.35	3.87	3.05
COLD	C-Flex Chop axis flex pivot	21.0	28.1	1.0	273.1	9.63	2.03	1.60
	C-Flex Jiggle axis flex pivot	96.0	275.0	1.0	584.0	20.60	4.35	3.42
	LUCAS chop axis flex pivot	21.0	26.9	1.0	260.9	9.20	1.94	1.53
	LUCAS jiggle axis flex pivot	96.0	259.2	1.0	550.4	19.42	4.10	3.23
WARM	structure bolt : yield (1 M4 only)	1112.0	3451.0	2.0	316.4	11.16	2.35	1.85
COLD	structure bolt yield (1 M4 only)	1112.0	3910.0	2.0	358.4	12.64	2.67	2.10

Buckling mode failure, scales with E					
	E warm	E cold	Ratio		
CuBe	121	134	1.11		
304 SS	190	201	1.06	(no data on 420 SS)	

Load limit on Structure interfaces TBC by MSSL (modified UNC bolt approximated by M4 bolt)

3 Discussion

This analysis does not cover

(a) flex pivots at their resonant frequency (approx >1000hz)
(b) flex pivots at resonant frequencies of rotating masses (approx 15 and 30 Hz), as these are not the driving design case

The load limits are as per the catalogue data for 429 grade stainless steel components.

The baseline and alternate flex pivots have a positive survival margin for qualification.

Document Ends

Appendix 4

This Appendix is not used.

This page intentionally left blank

Document Ends.

Appendix 5

This Appendix is not used.

This page intentionally left blank

Document Ends.

Appendix 6
v1.0
Thermal Calculations

Contents

Figures

Calculation: thermal equilibrium of motor coils, materials G10 vs Aluminium

1.1 Discussion

The motor coils operate at an average power of 1mW per motor, 0.5mW per coil. These are cooled via a conductive path through the motor core, potted joint to aluminium housing, bolted joint to BSM structure and thus to the optical bench and/or thermal strap.

1.2 Variables:

data			Source	
Stephan-Boltzman	5.67E-08			
Motor area	5.18E-04	m^2		
Motor emissivity	8.00E-01	%		
Aluminium thermal integral (AL 6082)	14	W/mK	RAL	6-4.2K
Stycast 1266	1.00E-01	W/mK	Cornell	3-4K
vespel sp-1	0.0125	W/m	RAL	6-4.2K
mild steel (use for motor cores)	6.1111	W/mK		6-4.2K
joints :				
al-al	6.00E+01	W/m^2K	RAL	
al-au-al	7.50E+02	W/m^2K	RAL	
stainless-stainless	1.00E+02	W/m^2K	RAL	
inconel-al	4.00E+02	W/m^2K	approx	
Al-eccobon-inconel	4.00E+02	W/m^2K	approx	

Motor Dissipation (W)	0-1.5	mW
Surface area (coils)	0.0005208	m^2
BSM structure temperature (worst case)	6.0	K

Coil surface area based on dimensions (mm)		
L	B	W
15.5	12	6.2

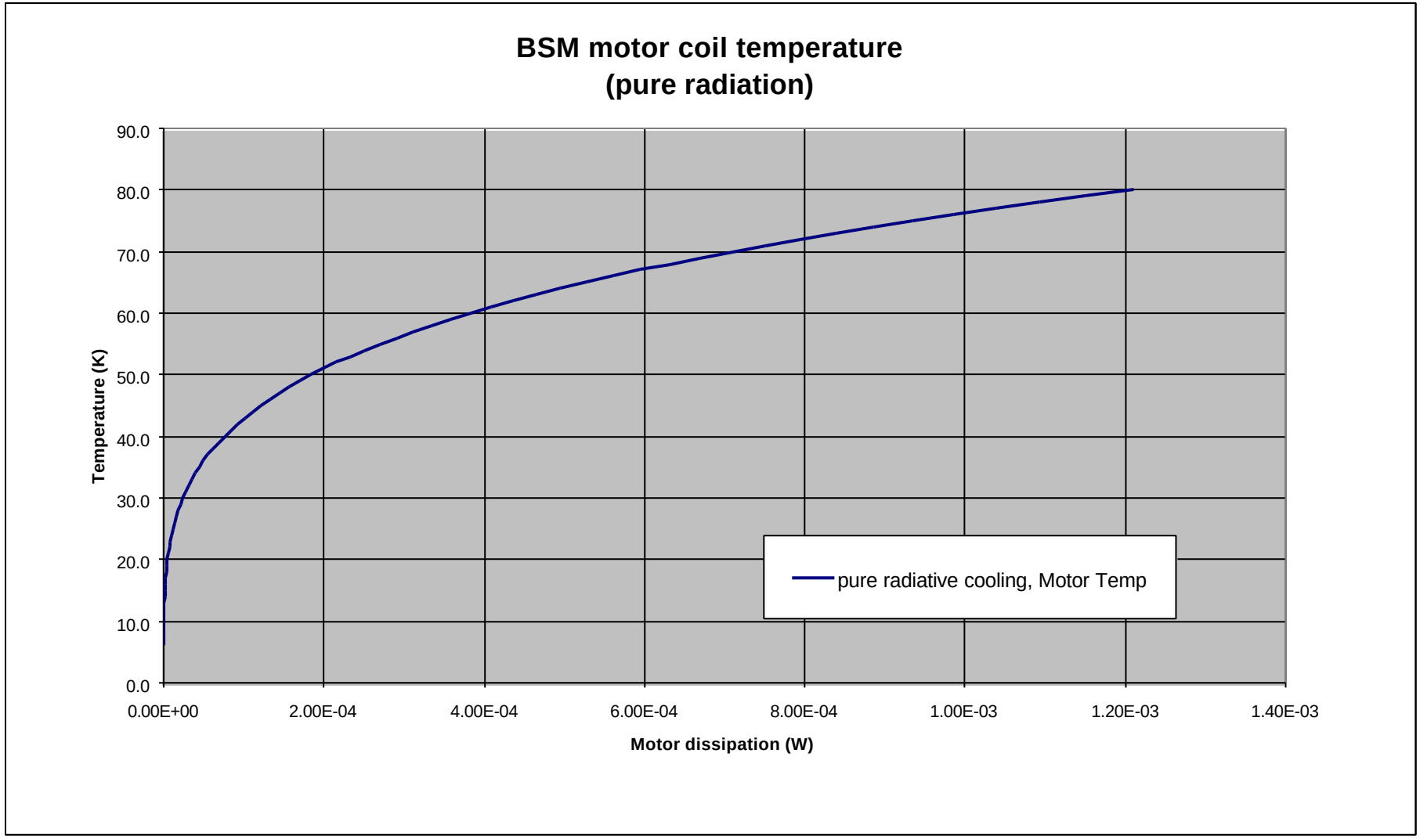

Figure 2: Pure radiative cooliunng

The figure above indicates that at 1mW the motors would reach temperatures of ~76K. In the case with conductive cooling, however, the situation is much improved.

For example, at a 1.0 K temperature differential, driven by a load of ~33 nanoW, the cooling path 'choke point' provides approximately:17mW of cooling path

Conductive cooling via Aluminium		
c(at temp, valid 4-80K)	Wm	134.1697
Area of Aluminium (min restriction)	m^2	3.78E-05
length (to inner coil)	m	0.0097
length (to outer coil)	m	0.0199
Q = A.c/L	inner	0.5228
	outer	0.2549
limit on conduction - joint		0.0173
limit on conduction - potting (0.5mm Stycast)		0.0187
Heat conduction capability (away from inner coil)		0.0169
Heat conduction capability (away from outer coil)		0.0162
margin on heat flow away from inner coil (W)		0.0168
margin on heat flow away from outer coil (W)		0.0168

To study this further, a balanced heat flow situation is considered, looking at the temperature rise required to 'drive' 0.5mW of power through the heat path.

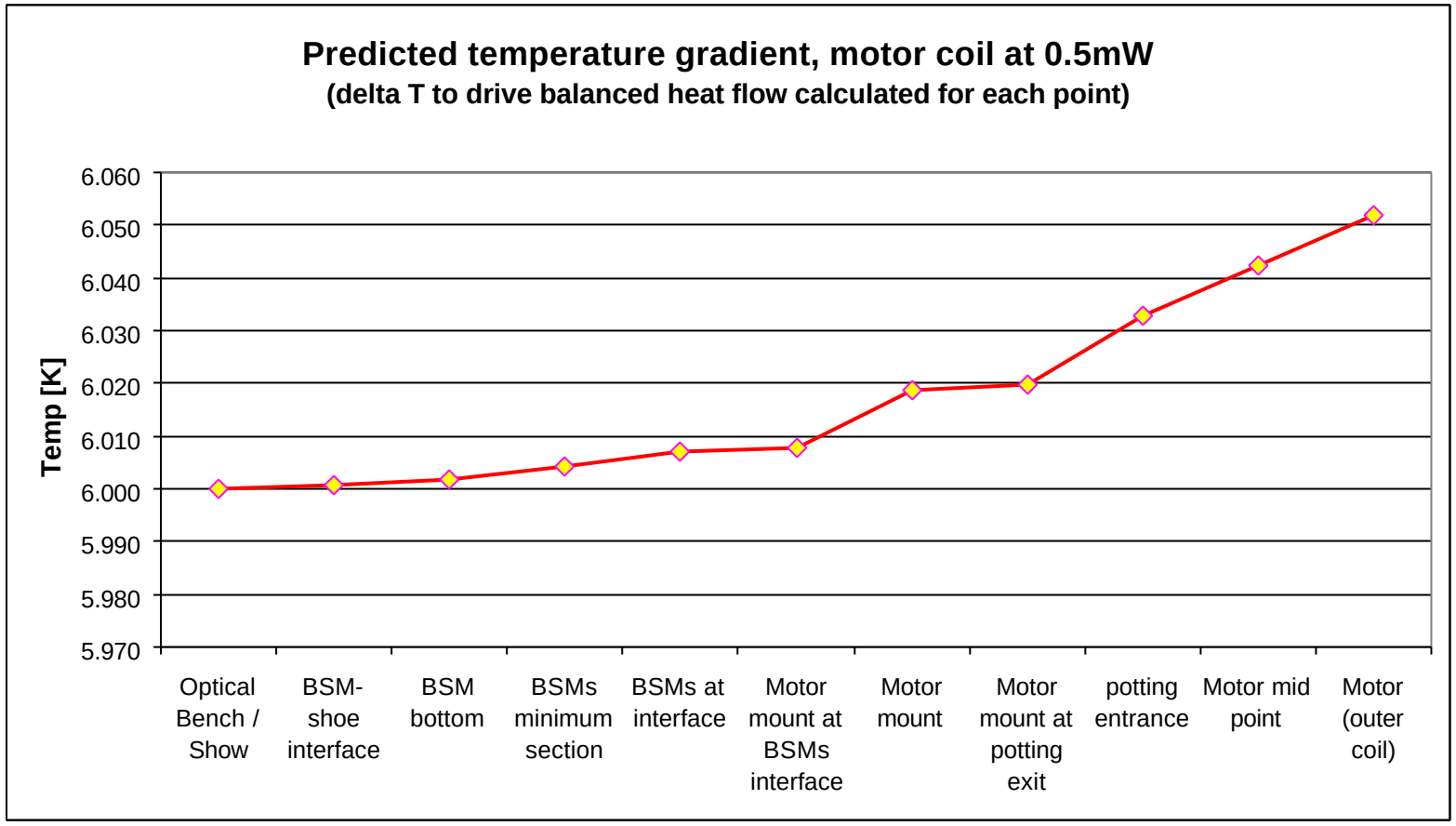

Figure 3: Predicted temperatures, motor mount components

2 Mirror temperature estimate

2.1 Block Diagram

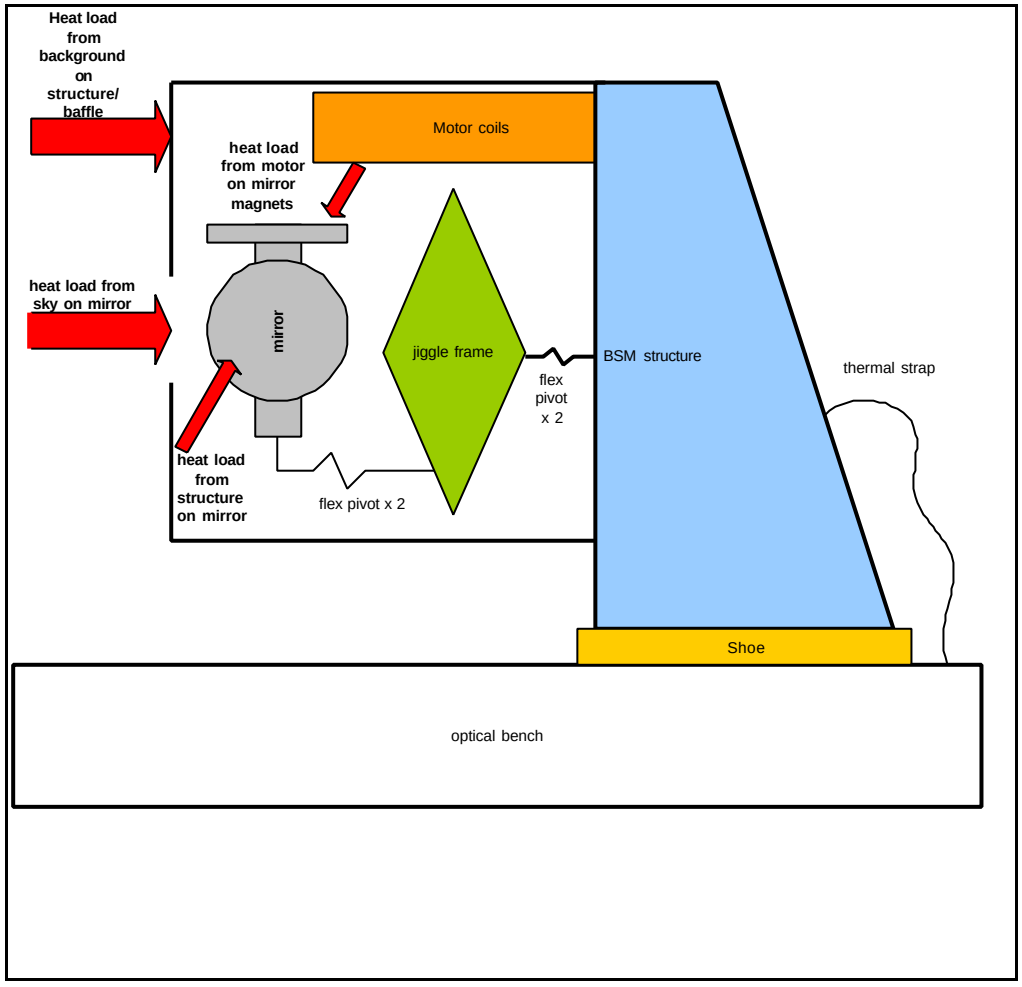

Figure 4: thermal block diagram

2.2 Calculation

Ac	8.30E-04	m^2	Chop axis area sees sky
Am	3.00E-04	m^2	Chop axis area sees motor
Ap	4.48E-07	m^2	csa pivots
Cp	0.6	W/ m^2	conduction pivots (stainless steel)
Lp	6.53E-03	m	length pivots (approx)
Tj	5	K	bsm structure & jiggle frame temp
Ts	4-150	K	Temperature of sky
Tm	4-180	K	temperature of motors

Steady state:

Q sky + Q motor = Q flex pivot (ignoring re-radiation by mirror)

$Ac.s.(Ts^4 - Tc^4) + Am\ s.(Tm^4 - Tc^4) = Ap.cp/Lp\ (Tc - Tj)$

$(Ac-Am)Tc^4 \quad +(Ap.Cp/Lp.\ s).Tc = (Ap.cp/Lp.\ s).Tj + Ac.Ts^4 \quad +Am.Tm^4$

Solve for Tc, results below

2.3 Results

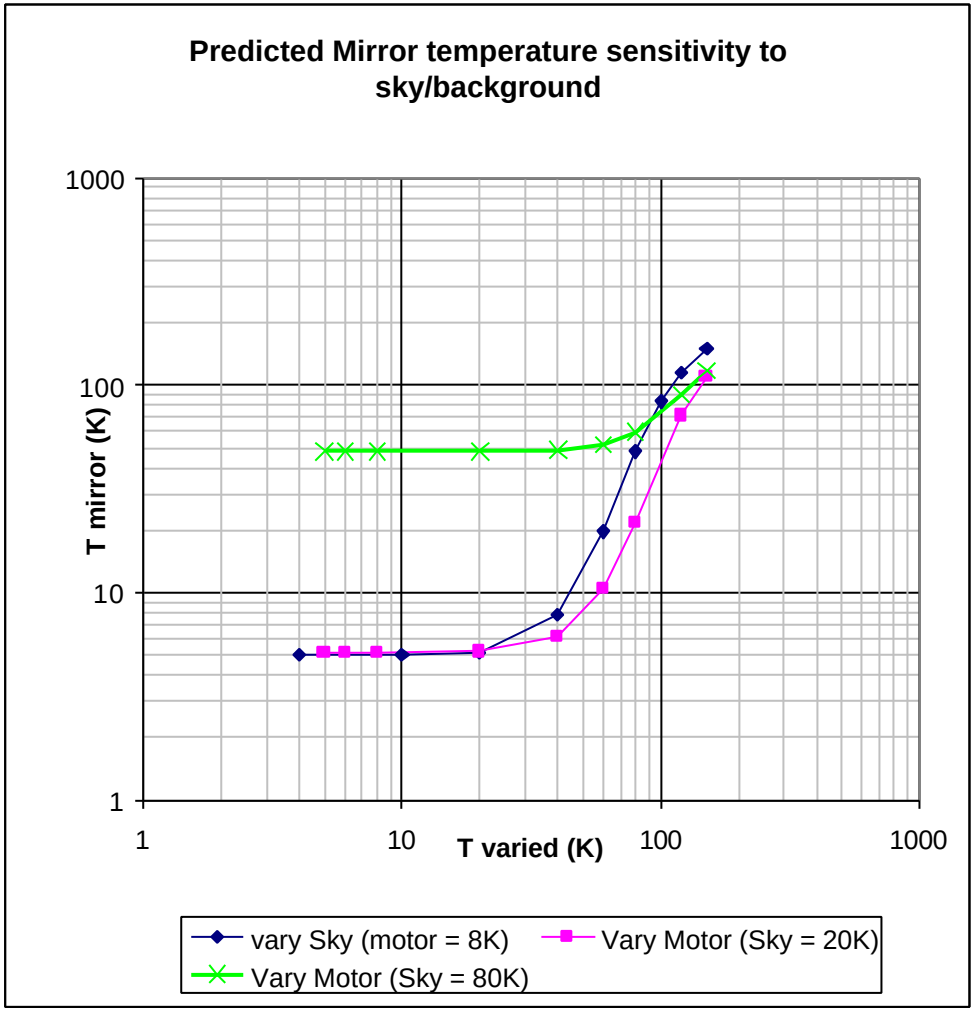

Figure 5 mirror temperature sensitivity

2.4 Check on limiting heat path

Note the above assumes the Stainless Steel flex pivots are the limit on the heat path. This can be confirmed by crude calculation, below.

Allowing a 0.1 deg K differential across each section or interface, the chop axis pivot clearly has the lowest conducted heat.

Component	Conduction (4-6k)	conductance (W/m^2K)	Contact Area	min CSA	Length	max Conducted heat (W)	Delta-T	Notes
Optical Bench							0.1	
Bench-Shoe interface		7.50E+02	4.10E-04			3.08E-02	0.1	Al-Au-Al
Shoe minimum section	33.600			4.00E-04	0.008	1.68E+00	0.1	Al 6082
shoe-BSMs interface		7.50E+02	4.00E-04			3.00E-02	0.1	Al-Au-Al
BSMs minimum section	33.600			3.37E-04	0.093	1.22E-01	0.1	Al 6082
BSMs-flex pivot capture sleeve		6.00E+01	1.30E-04			7.80E-04	0.1	al-al. surface area of top pivot half factored by .75 to allow for joint conduction
Flex pivot capture sleeve x2	33.600			2.14E-02	0.006	2.40E+02	0.1	Al 6082
Flex pivot capture sleeve- flex pivot x2		4.00E+02	1.37E-04			5.48E-03	0.1	Al-eccobon-inconel
Jiggle flex pivot minimum section x2	0.600			3.00E-06	0.008	4.50E-04	0.1	Inconel (or stainless)
Jiggle flex pivot - jiggle frame		4.00E+02	1.00E-02			4.00E-01	0.1	inconel-al
Jiggle frame minimum section	33.600			2.00E-05	0.040	1.68E-02	0.1	Al 6082
Jiggle frame - capture sleeve x2		6.00E+01	1.00E-02			6.00E-02	0.1	al-al
capture sleeve - chop flex pivot x2		4.00E+02	1.00E-02			4.00E-01	0.1	Al-eccobon-inconel
chop flex pivot min section x2	0.600			2.00E-06	0.008	3.00E-04	0.1	Inconel (or stainless)
chop flex pivot - chop stage		4.00E+02	1.00E-02			4.00E-01	0.1	inconel-al
Chop stage (mirror) min section	33.600			2.00E-05	0.025	2.69E-02	0.1	Al 6061

Data:

Aluminium thermal integral (AL 6082)	33.6 6-4.2K		W/m	RAL doc gives ~14 W/mK	ATC has 85 for Al 6063
inconel (use stainless steel)	0.6 6-4.2K		W/m	RAL & ATC agree	
vespel sp-1	0.0125 6-4.2K		W/m	RAL	
joints :					
al-al		6.00E+01	W/m^2K		
al-au-al		7.50E+02	W/m^2K		
stainless-stainless		1.00E+02	W/m^2K		
inconel-al		4.00E+02	W/m^2K	guess	
Al-eccobon-inconel		4.00E+02	W/m^2K	guess	

3 Cernox 1030 Thermometer data sheet

See

http://www.lakeshore.com/temperature/cernox.pdf

This page intentionally left blank

Document Ends.

Appendix 7:
Controls Analysis
v1.0

Table of Contents

Table of Figures

7 Controls Analysis

7.1 BSM Control System Analysis

7.1.1 SCOPE

This analysis describes the control system for the SPIRE Beam Steering Mirror (BSM).
The BSM is a two-axis device, using flex-joint supports to give a negligible friction control of the axes, allowing high accuracy positioning.
The description concentrates on the Chop axis, as the Jiggle axis has exactly the same control scheme, with parameters changed to suit the larger inertia and flex-joint spring rate. However some Jiggle modelling results are included.

7.1.2 LINEAR ANALYSIS

As the lowest BSM structural resonance has been estimated at around 800 Hz by FE modelling, The BSM axes can be modelled for the purposes of control as a simple spring-mass-damper system, using the flex-joint spring rate.

The mechanism can be represented by the second-order system

$$G(s) = \frac{w_n^{\,2}}{s^2 + 2 * d * w_n * s + w_n^{\,2}}$$

where the system natural frequency

$$w_n = \sqrt{\frac{Ks}{J}}$$

with Ks = flex joint spring rate, 0.047 Nm/rad Chop and 0.37 Nm/rad Jiggle
J = axis inertia. 1.7e-6 Kgm^2 Chop and 45.0e-6 Kgm^2 Jiggle
d = flex joint damping 2.3e-5 Nm/rad/sec

The Chop step specification requires a sinusoidal step profile to be achieved in less than 20mS. With a design target of 15 mS, a nominal system risetime of about 5mS is required to closely follow the externally generated profile.

A second order linear system has a 2% settling time of 4 time constants, or $\frac{4}{d * w_n}$. With d = 0.707, this becomes $\approx \frac{5.7}{w_n}$. This requires a bandwidth of approximately 200 Hz to meet the design target.

A linear frequency-domain model was constructed to evaluate a standard nested velocity and position loop control system.
All linear elements in the mechanism, motor power amplifier and position sensor were included in the model. An acceleration loop was included to limit the system acceleration, as the slew rate of the electronic power amplifier may produce instability for large step demands.

The following control parameters were used. Note that the position loop integrator is of the form (1 +s*t) / s .

Parameter	Description
position sensor gain	100
position loop gain	21.9
position loop integrator time constant	0.013
rate loop feedback gain	2.66
Acceleration loop feedback gain	0.5e-3

Figure 1 Chop Axis Closed-Loop Bode Diagram

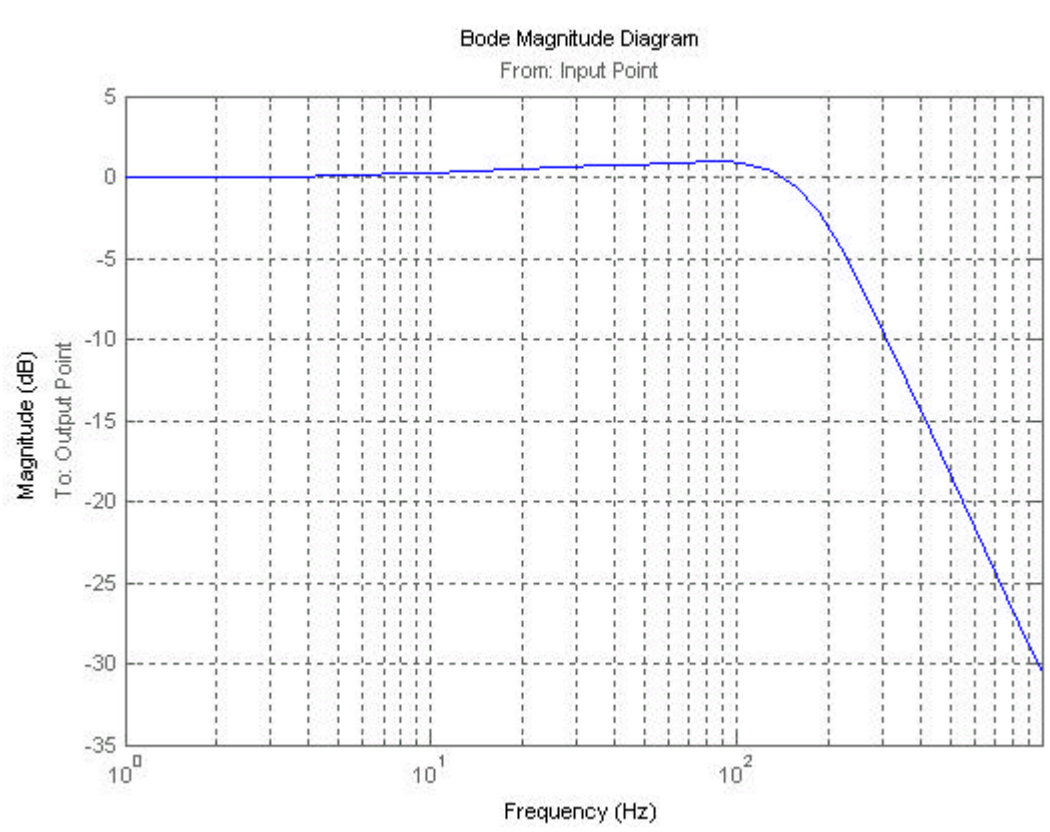

It can be seen from the above closed-loop Bode plot that the –3dB bandwidth is approximately 200 Hz.

The loop stability can be evaluated using the Nichols chart, which plots open-loop response with overlaid closed-loop contours.

Figure 2 Chop Axis Nichols Chart

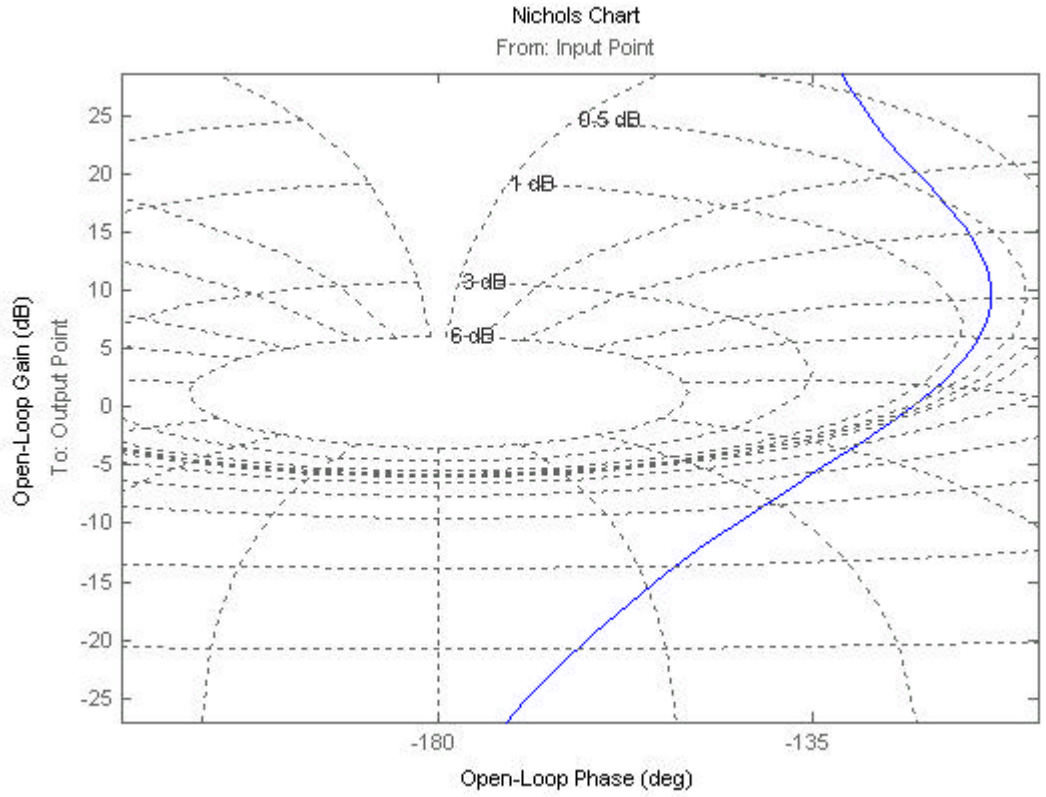

The gain margin is 33dB and the phase margin is approximately 57 degrees.

7.1.3 NON-LINEAR SIMULATION

Though the foregoing analysis gives a good guide to general performance, there are a number of significant non-linearities present in the system, particularly the voltage limits of the power amplifier. More significantly, the control system will be implemented entirely in software, apart from the power amplifier and the position sensor preamplification. Standard linear analysis cannot handle the sampling effects and quantisation in a simple manner.
There is also the assumption in the above modelling that rate and acceleration signals were available for feedback, however the system uses only a magnotorestive position sensor. Therefore the required signals need to be estimated from the existing information. A standard method of achieving this is using a state observer, which employs a basic model of the system, and uses feedback from the available system signals to correct any errors in these estimates due to, for example, incorrect estimates of system parameters such as inertia and spring rate. This method also copes with variations in parameters such as the spring rate. However, the calculations can only be done accurately by a processor and associated software.

For these reasons, a detailed time domain non-linear simulation of the BSM axes control system has been created using matlab-Simulink, an industry standard tool.
This model is described in detail in the SPIRE BSM Design Description document, however, some results are presented here for convenience.

The following figure shows the demanded sinusoidal position step demand (blue) for the Chop axis, and the system response (green).

Figure 3 Chop Axis Step Response (non-linear simulation)

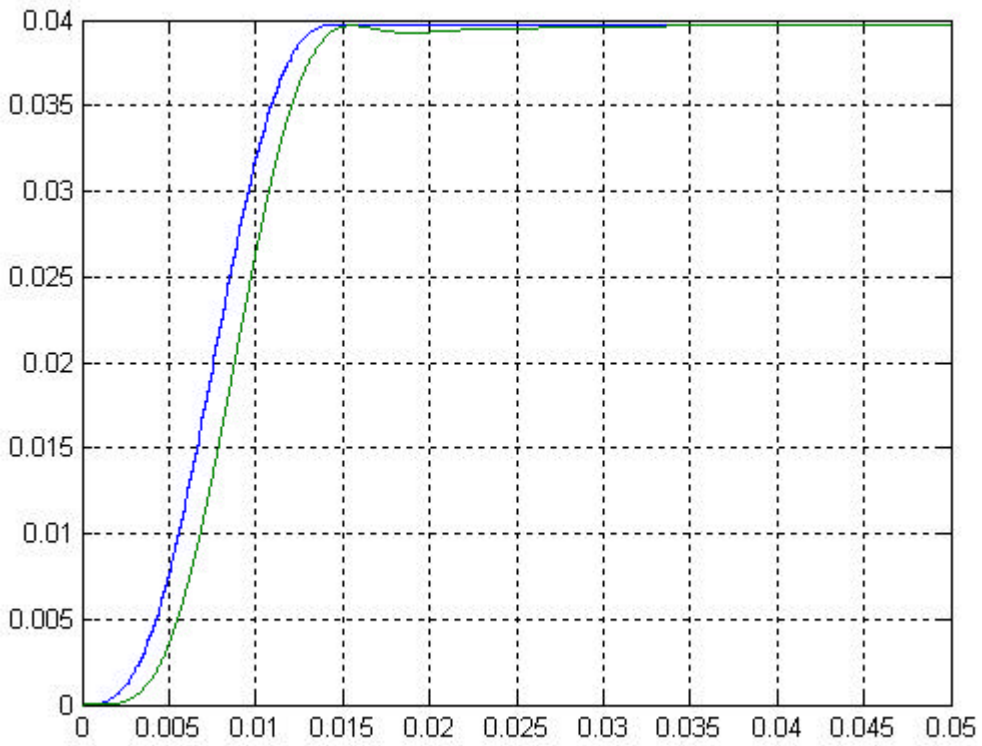

Note that the simulated performance meets the original design target step response of 15 mS.

Finally, as power dissipation is an important parameter to be minised for the BSM, as it is in a cryogenic environment, the non-linear simulation enables the calaculation of dynamic power dissipation. It is interesting to note from the following figure that the peak motor power required to slew the axis is approximately the same as that required to hold the axis at a fixed angle.
Indeed over time, the dominant power dissipation requirement for the BSM mechanism is that required to hold the axes against the flex joint spring forces – this is the trade-off for almost zero friction during axis rotation.

Figure 4 *Chop Axis Motor Power Dissipation (at 4 deg.K)*

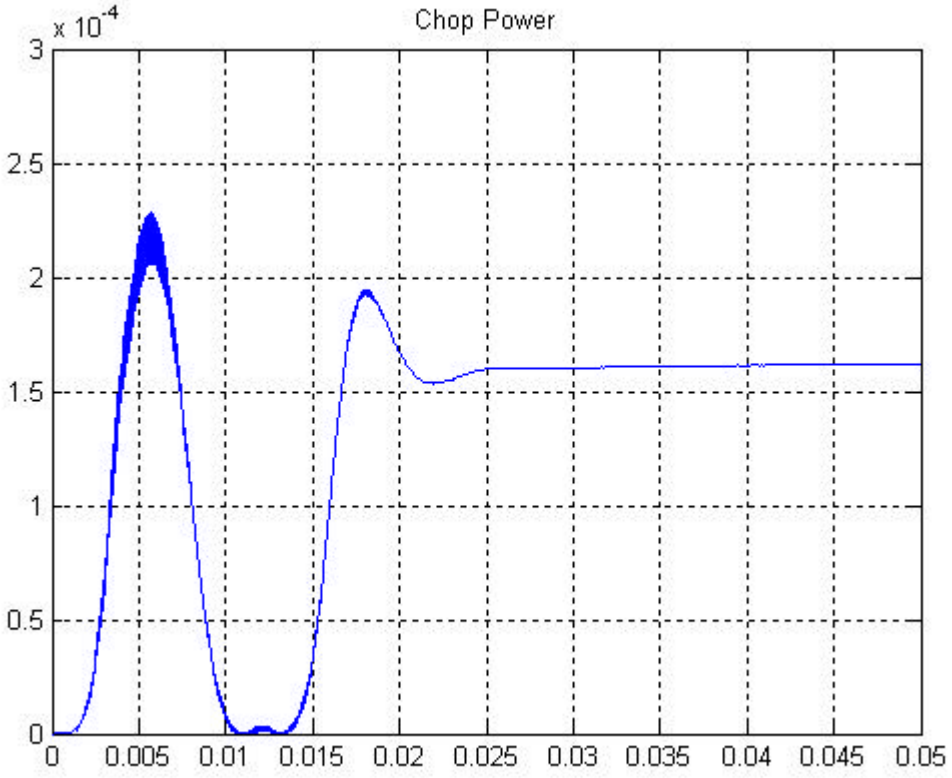

Document Ends

Appendix 8
Prototype cool-down report

Table of Contents

Table of Figures

As part of an infrared detecting instrument the BSM must be cooled down to 5K to prevent it from emitting radiation that would interfere with the detectors. This document summarises the results of the first cool-downs of the single axis prototype and of the two axis prototype.

8.1 Single Axis Cooldown

8.1.1 Procedure

The cool down was performed in two stages. After evacuating the cryogenic chamber, liquid nitrogen was used to cool the prototype down to 77K. Once the mirror had cooled to this temperature liquid Helium was added to complete the cool-down to 4.6K (base-plate) / 5.2K (mirror).

8.1.2 Results

A Servigor 102 Temperature monitor was used to record the process, the output of which can be viewed in figures 1,2 and 3 (pages 2,3,4). It was found as expected that the mirror was cooling significantly slower than the base-plate of the mechanism. The reasons for this are:

- the flex pivots are poor heat conductors and so the mirror was taking far longer to cool then the rest of the prototype.
- the mirror was being heated by the radiation shield which is only cooled to 77K (and in practice has a temperature gradient across it with a mean temperature close to 85K).

This radiation load issue was resolved by placing a radiation shield attached to the 4K base-plate over the entire prototype, thus preventing it from being heated by other parts of the cryostat.

Total cool-down time was 9 hours.

8.1.3 Conclusions

From these tests (calculated from 20K/hr at 300K – 4K) it was concluded that the single axis prototype was cooled down well within the required time (14 hours).

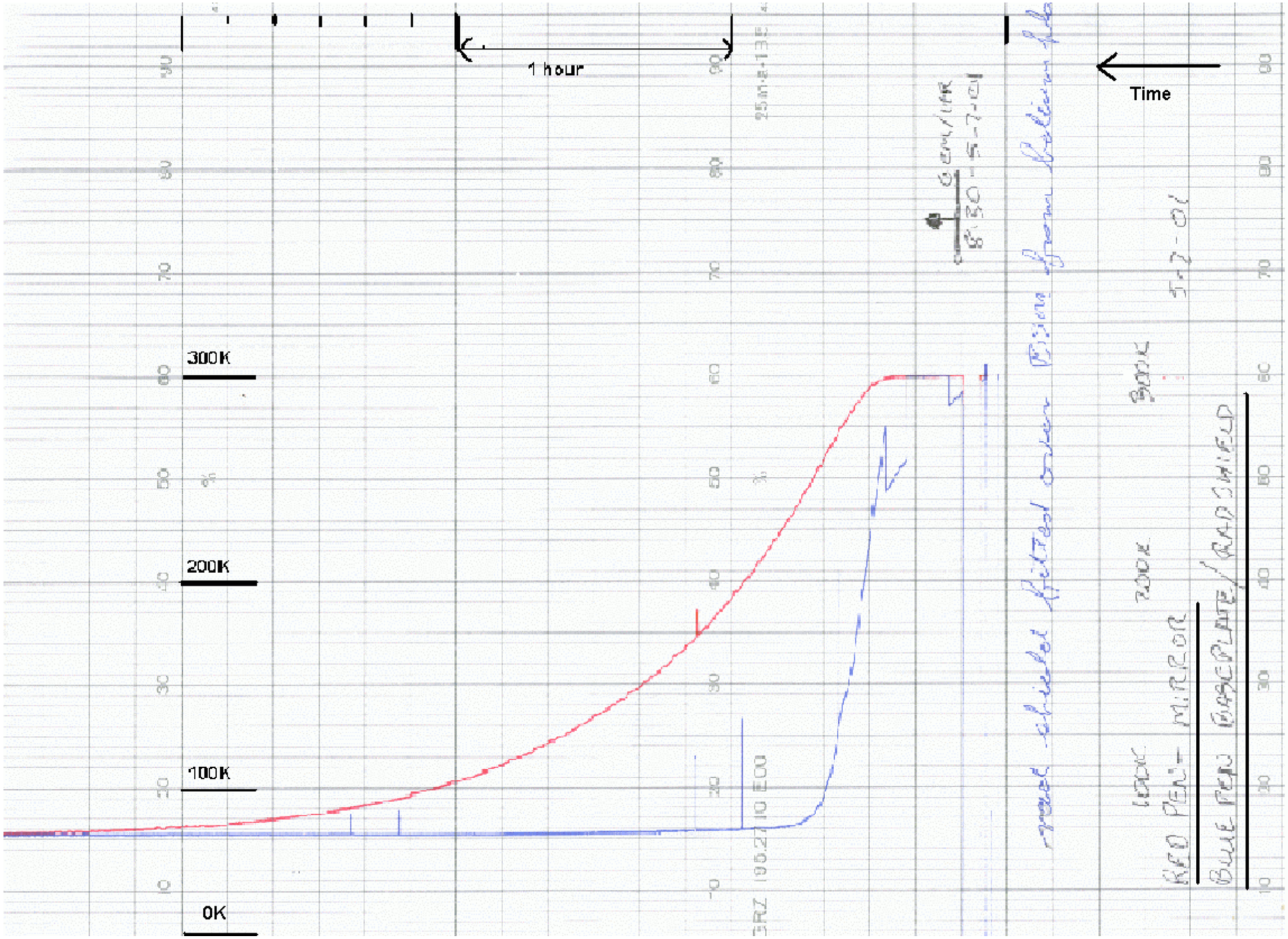

Figure 1 - Temperature monitor output, part 1

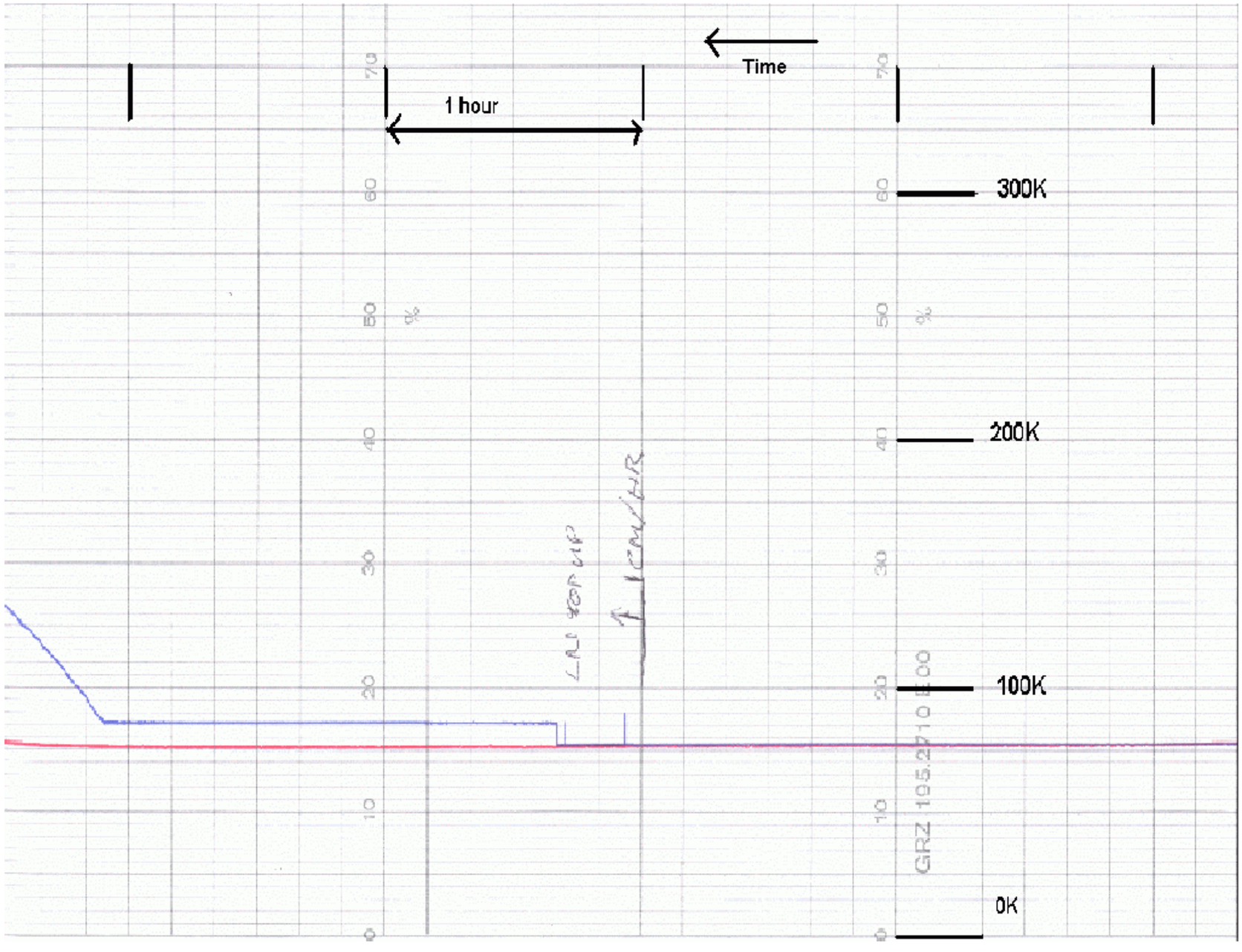

Figure 2 - Temperature monitor output, part 2

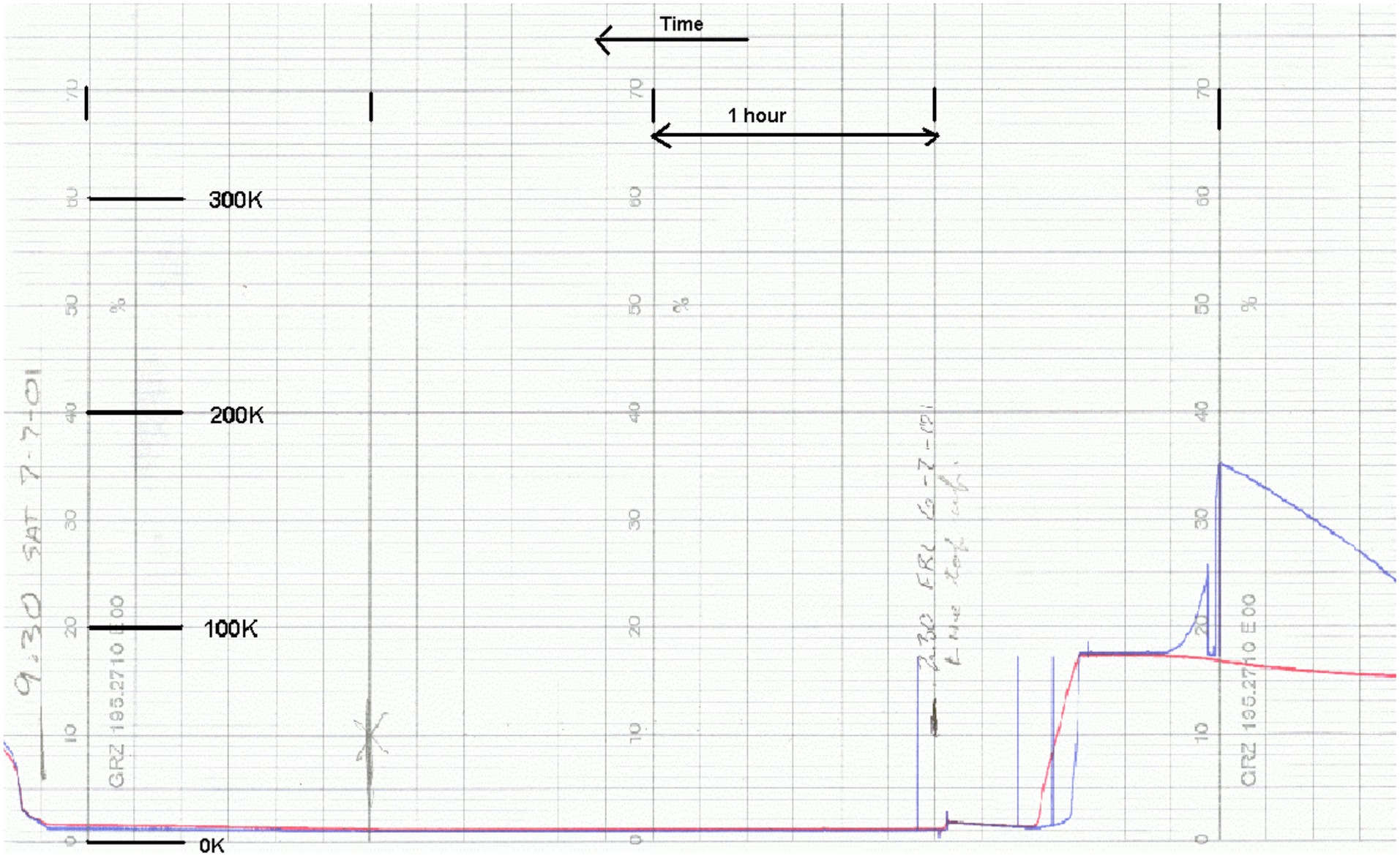

Figure 3 - Temperature monitor output, part 3

8.2 Two Axis Cooldown

A cooldown of the 2 axis prototype in Aug.01 indicated that the BSM would cool to operating temperature within < 8 hours.

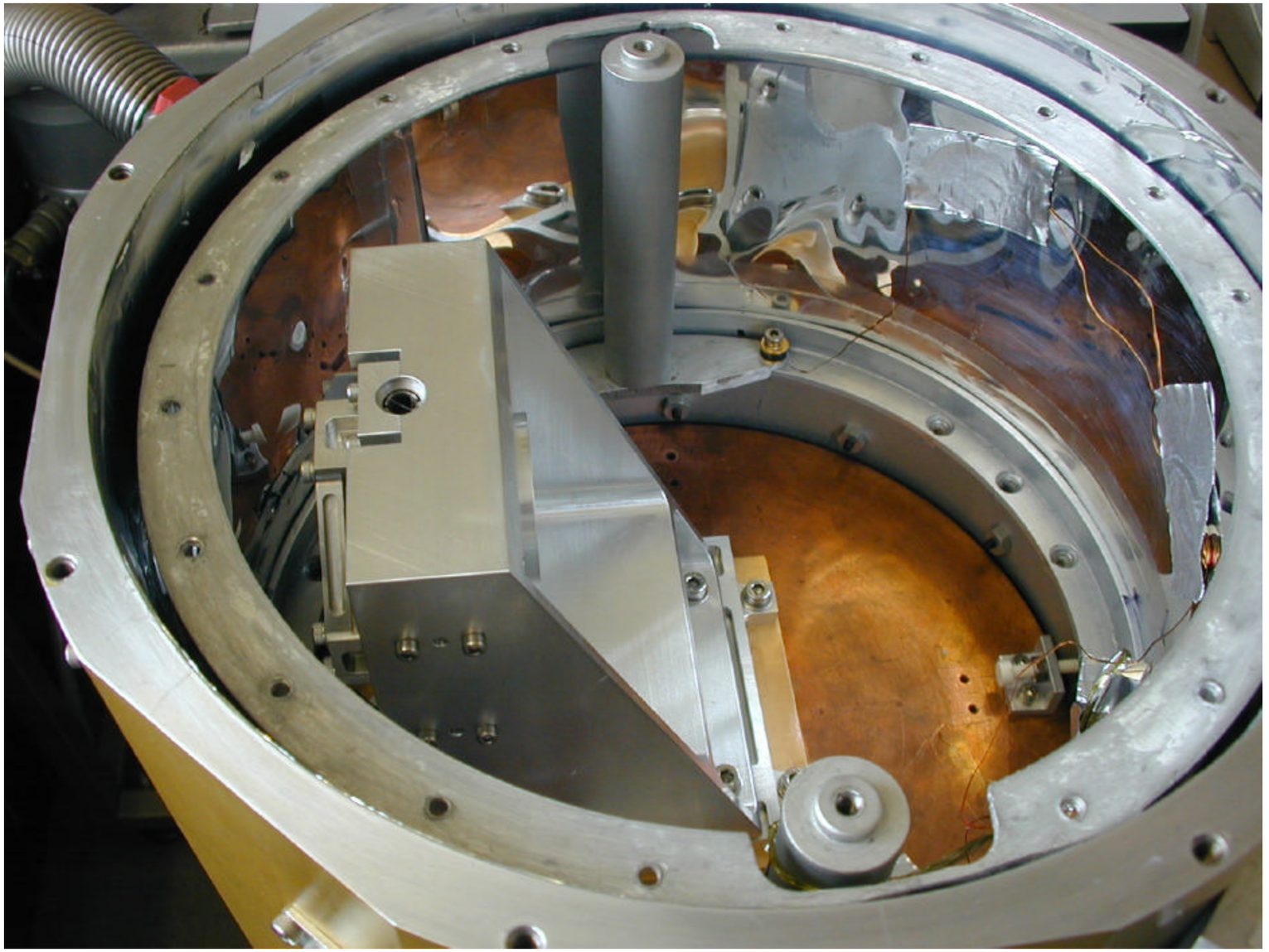

Figure 4 Two Axis Cooldown

In order to do this a radiation shield was placed over the BSM (where the baffle would normally go, but completely blocking the view of the room temperature 'sky. Without this baffle the mirror does not cool below 20K.

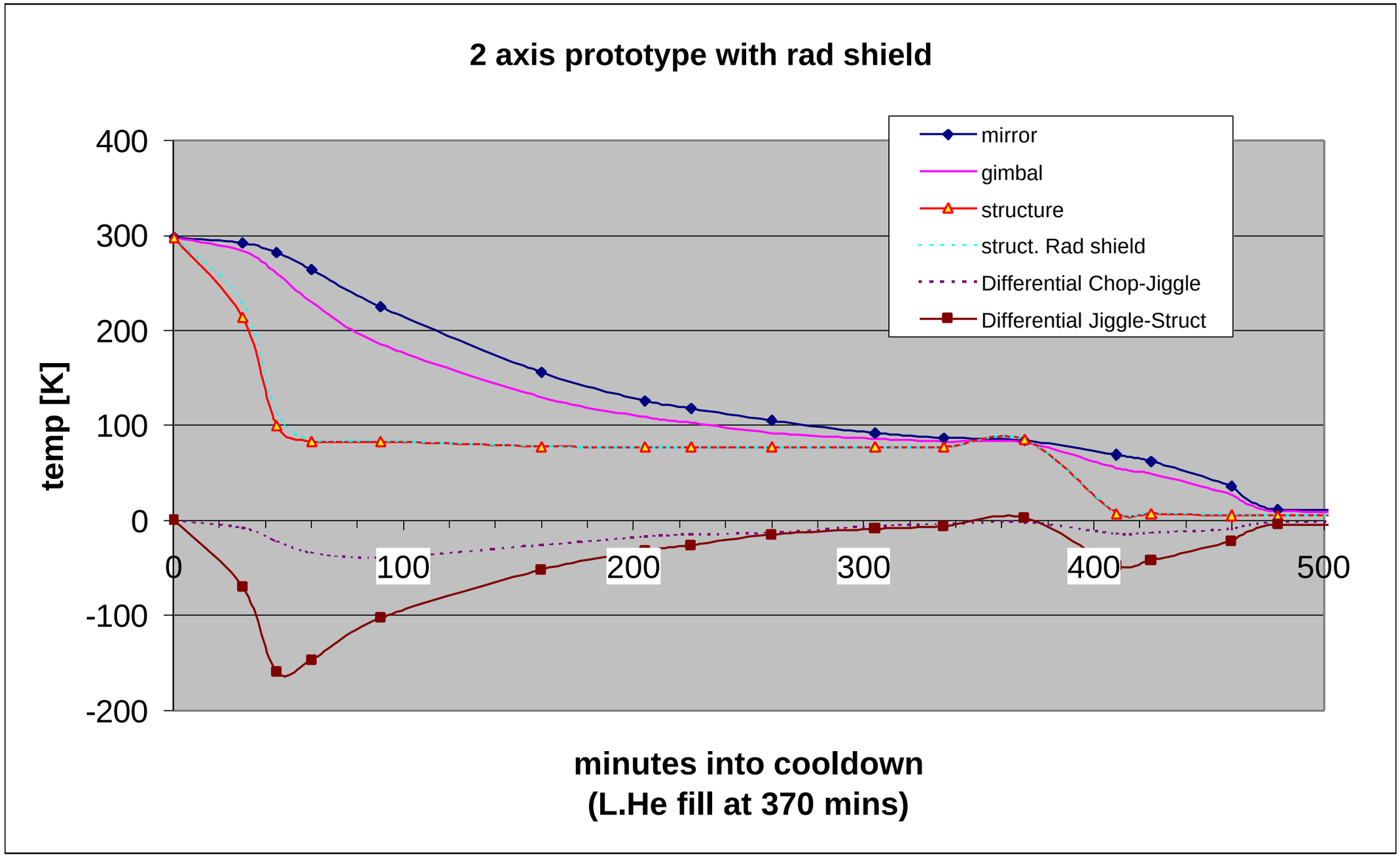

Figure 5 Two axis Protptype With Rad Shield

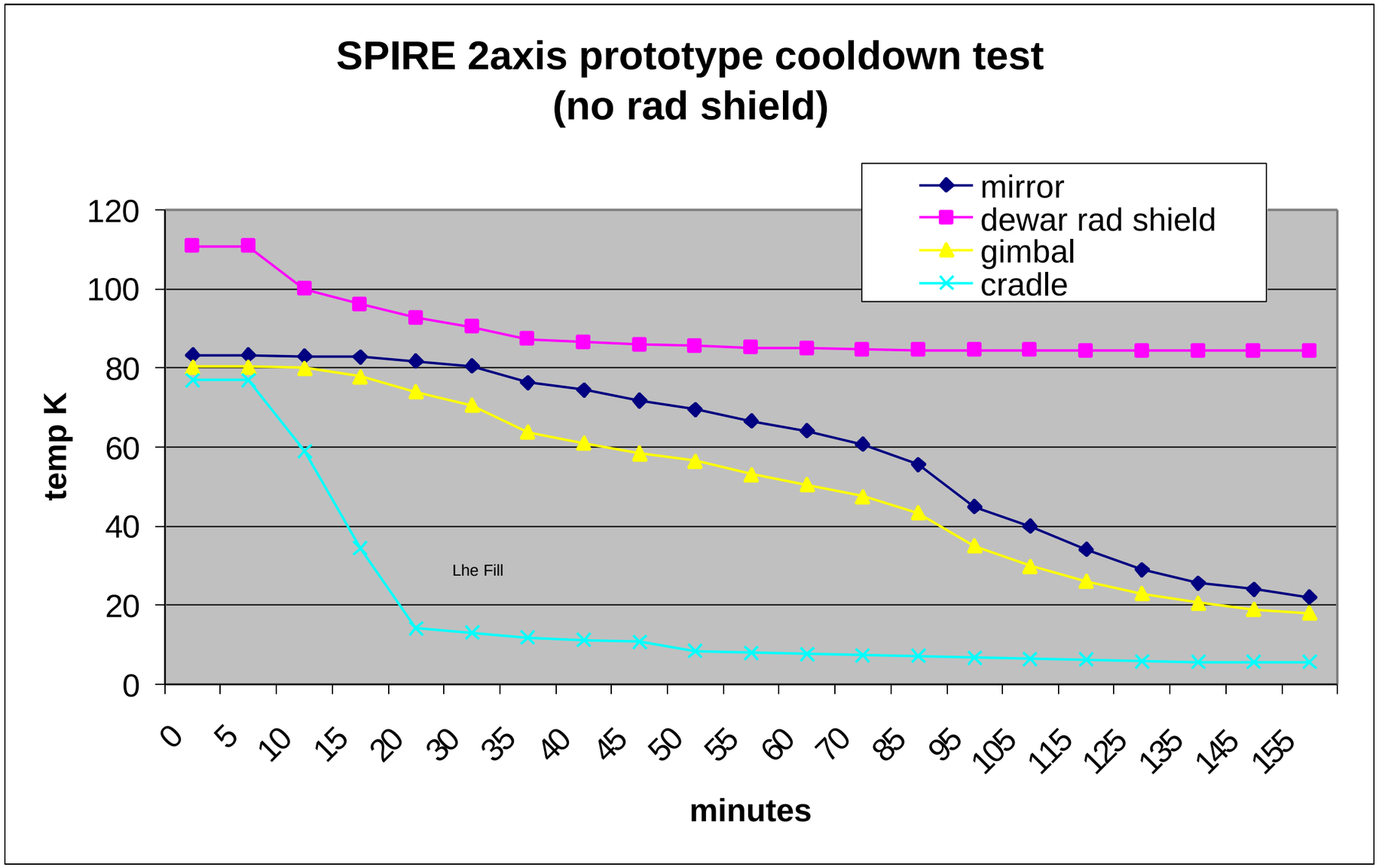

Figure 6 2 Axis Prototype Without Rad Shield

This page intentionally left blank

Document Ends

Appendix 9: v1.0
Single Axis Prototype Test Report

Table of Contents

Table of Figures

As described in the development plan, single and two axis prototypes are being constructed and tested prior to the DM, in order to validate the design of the BSM and identify as early as possible any critical areas, or issues where further development work is needed. For example meeting the requirements for the positional stability and power consumption with the design presented here requires specific performance from the position sensors and the motor torque. The validity of many of these design assumptions can be tested to first order with warm tests of the simple single axis prototype, followed by cold tests and without the need for space rated components. The results of these tests and their conclusions are described in the following sections. The two-axis prototype, which is currently under construction, will be tested in a more rigorous fashion.

9 Single Axis Prototype Warm Tests

The single axis prototype BSM was machined to the design drawing so that it had approximately the correct mass. Since the prototype did not have a polished test spot on the surface, a glass mirror was mounted on it for the motor torque measurements. The motor was one of the PACs prototypes assembled in the BSM two coils/one-magnet configuration. A Dspace program constructed in the Simulink programming environment - which emulated the final controlling software (and hardware) - was used to control the motor and monitor the feedback. A PC based ADC provided the interface between the Dspace software and BSM hardware. A photograph of the single axis prototype is shown in figure 1.

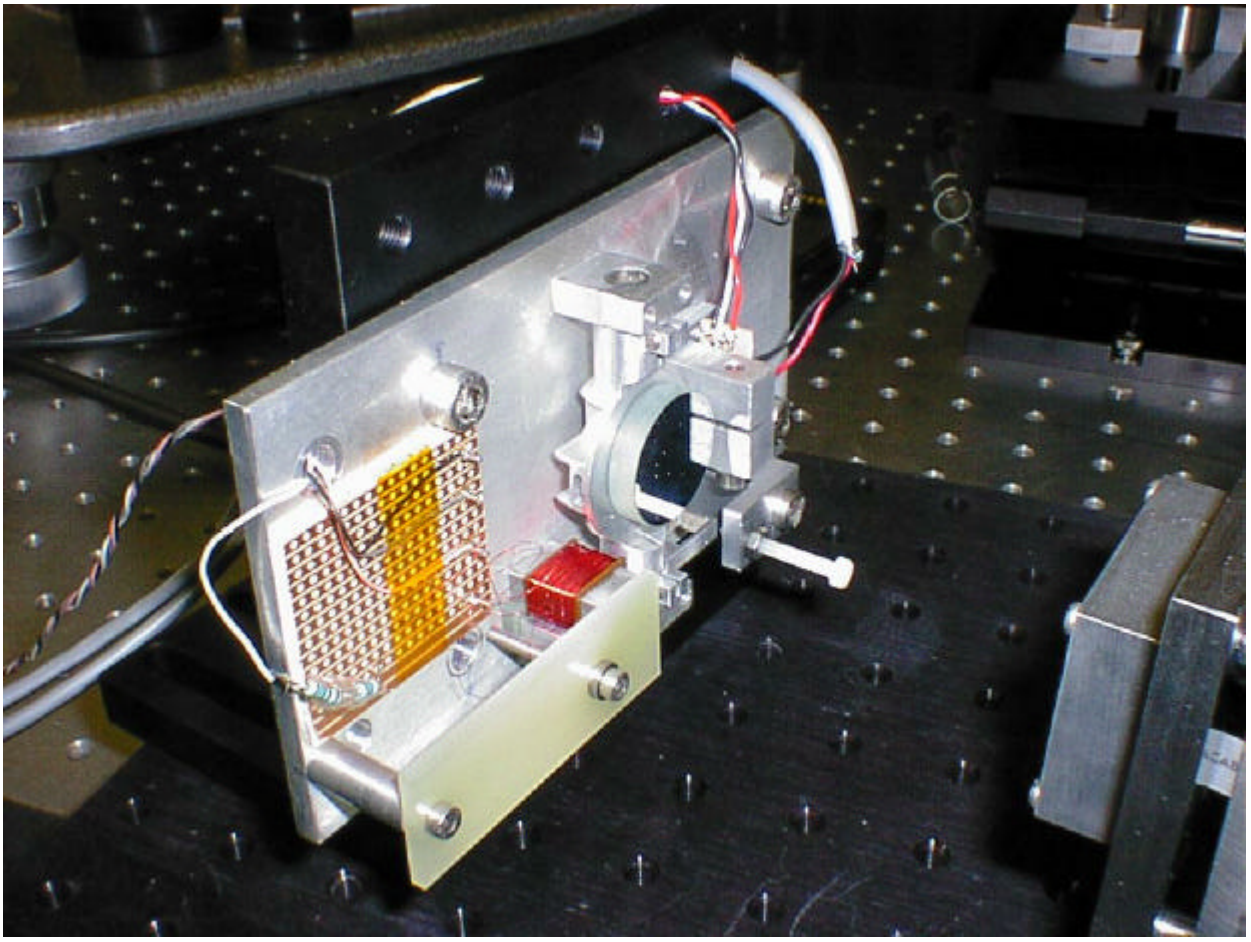

Figure 1 Single Axis Prototype

9.1 BSM Control System: Position Sensor Output Noise

9.1.1 INTRODUCTION

The specification requires a maximum position error of 0.34%rms (including motor drift). Allowing 25% of this error to be electrical noise in the position sensor electronics means that the noise limit is 0.085 % of the output of the preamplifier when the mirror is at an end-stop, measured at approximately 11.2V magnitude (see page 13). This gives a maximum noise output of 9.5 mV. Since the BSM design is based on use of the ISOPHOT chopper position sensors, this ought to be the case - however the details of the performance of the position sensors were poorly documented and the SPIRE requirements differ in that they are far more demanding. We therefore carried out the following test of the position sensor output noise.

In order to investigate sightline noise in the single-axis BSM prototype, the output from the position sensor and its preamplifier was captured using a Tektronix TDS 224 digital oscilloscope, but without closing the BSM control loop. Therefore the noise measured was due to the sensor and its associated electronics (current source and preamplifier) only. The measured noise was then analysed in the frequency domain using the FFT function on a Hewlett Packard 3562A Dynamic Signal Analyser. If the noise had a flat spectrum, it would be sensible to anti-alias filter it to remove any high frequency element that would be folded down into the control loop bandwidth by the subsequent 10 kHz sampling process.

9.1.2 RESULTS

Figure 2 shows the output from the preamplifier, with the motor depowered. The amplitude of the noise is approximately 10mV.

Figure 3 shows the frequency spectrum of the sensor and preamplifier over a 100KHz bandwidth. Implementing a high frequency filter into the electronics can easily eliminate the large peaks at and after 50kHz. Figures 4 and 5 show the spectra for low frequency bandwidth. Figure 5 demonstrates that by even crudely shielding the preamplifier - in this case a very thin metal shield was used - will reduce extraneous noise significantly.

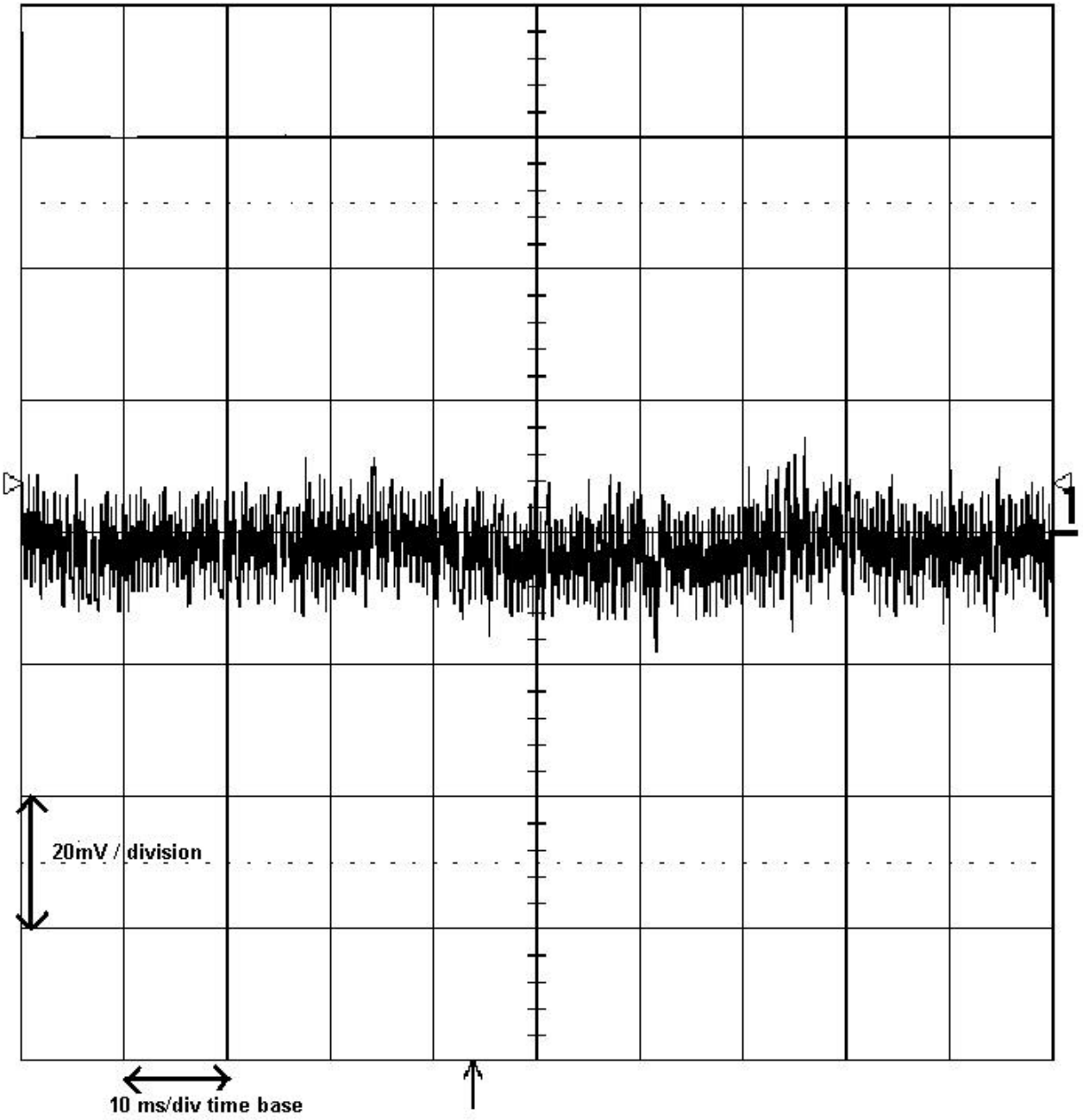

Figure 2 Noise in the Sensor and Preamplifier Electronics

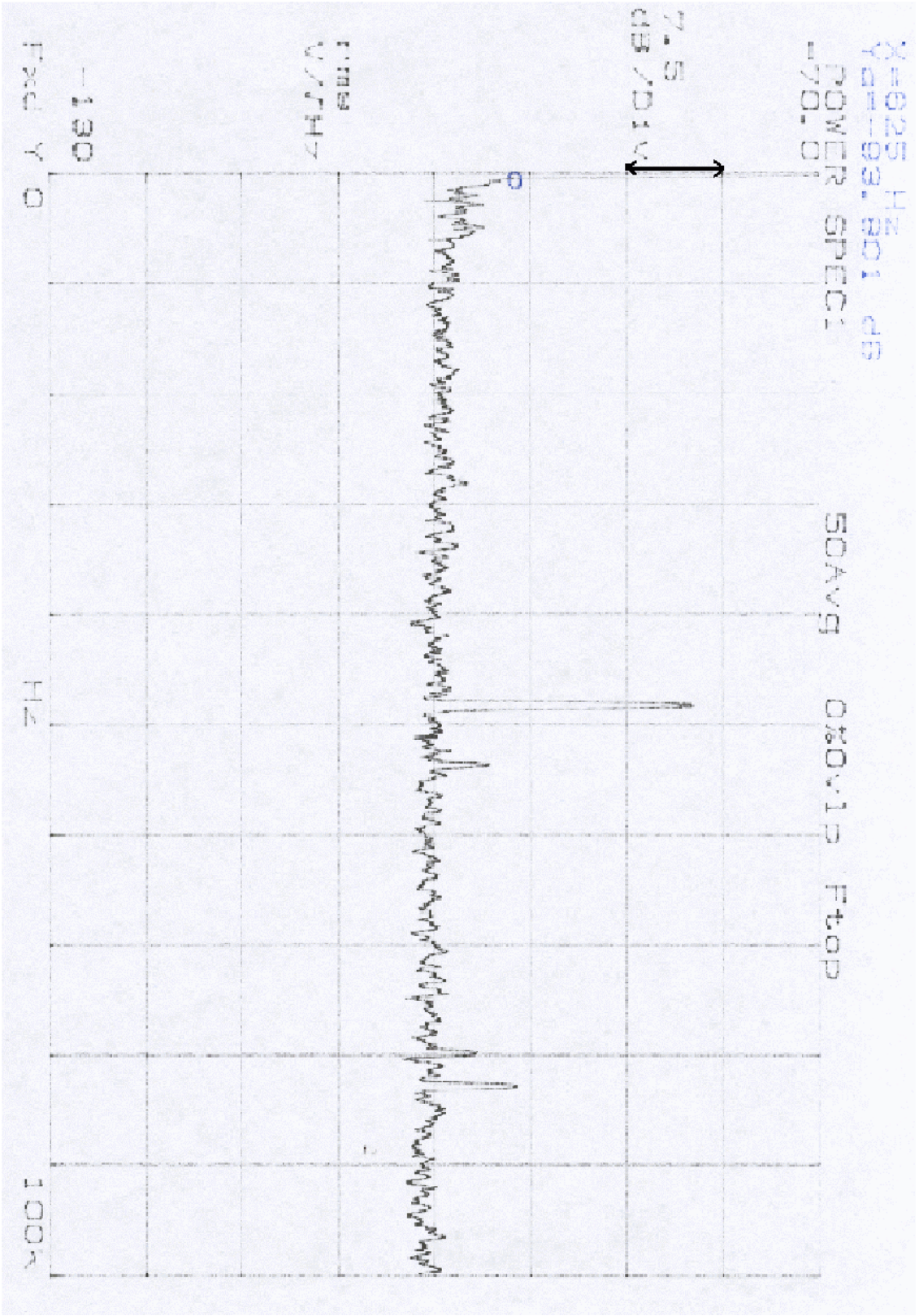

Figure 3 100kHz Spectrum Bandwidth

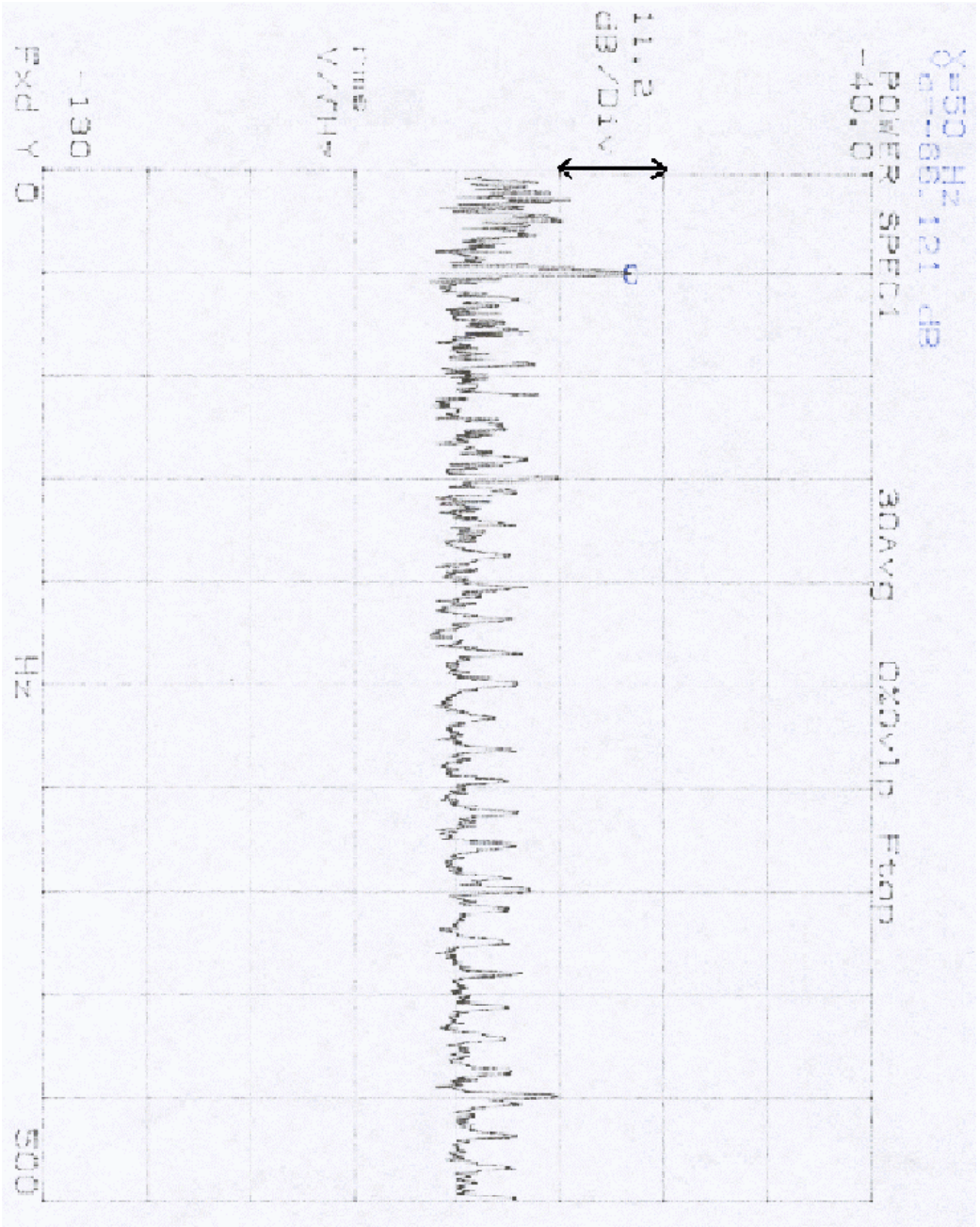

Figure 4 Ungrounded low frequency spectrum (500Hz bandwidth

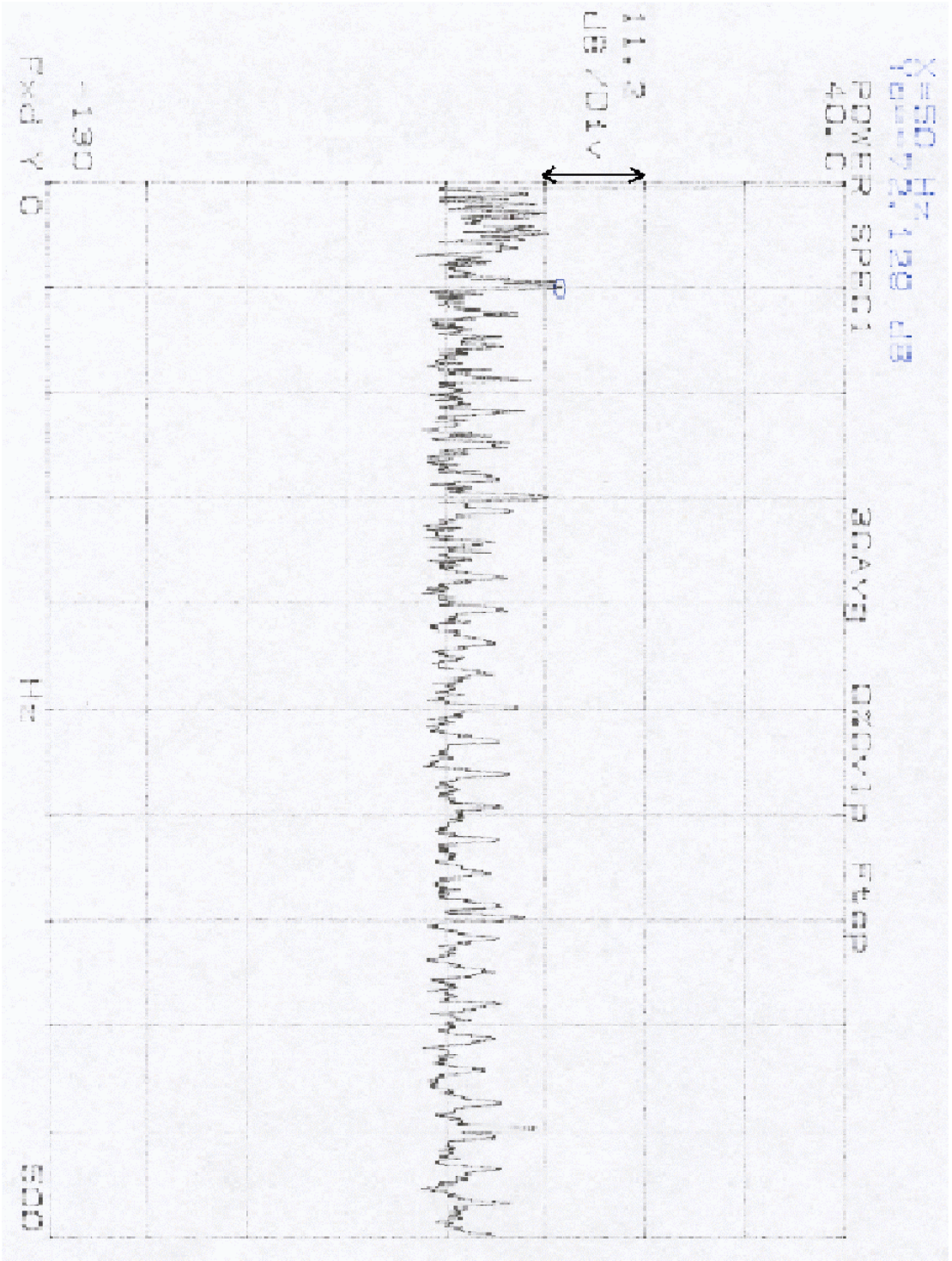

Figure 5 Grounded Low Frequency Spectrum (500Hz)

9.1.3 CONCLUSION

These tests demonstrate that the noise output of the sensor and preamplifier can be easily brought within the required parameters by implementing a high frequency filter into the sensor electronics and by ensuring that they are properly electromagnetically shielded from external interference.

9.2 BSM Electronics: Motor Torque Constant

9.2.1 INTRODUCTION

The motors used for the BSM are constructed from parts used in the MPIA-designed PACS system. Though the MPIA motors were designed in a thorough manner, UKATC has neither the expertise nor necessary magnetic modelling software to follow a similar process to produce a space-qualified motor. It was in any case desirable to build on the extensive MPIA experience in this area and have some commonality of design between PACS and SPIRE.

Based on simple calculations, it was concluded that two coils and one magnet (from the PACS three-coil two-magnet design) would give the required torques for our BSM system. Therefore the motor 'design' task is limited to simply verifying this conclusion, by testing.

In order to establish the motor torque constant, the single-axis prototype was tested with various applied voltages, and the subsequent angular movement measured using the 'C.D.L.' Tilt Measurement Apparatus (TMA). Figure 6 demonstrates the set-up and configuration of the TMA.

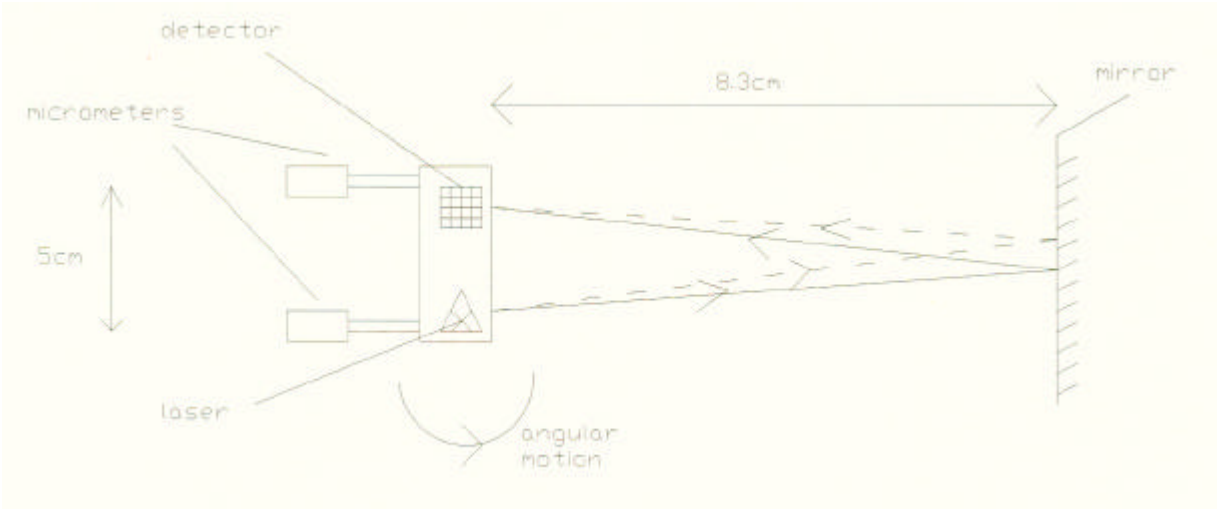

Figure 6 Tilt Measurement Apparatus Configuration

As the axis was restrained by the flex pivot mountings, which have a known spring constant, the angular movement could be converted to an equivalent force and the motor torque constant derived.

9.2.2 RESULTS

Firstly, the TMA was calibrated using a simple laser reflection against a fixed scale, as shown in figure 6.

The following results were obtained:

Mirror distance to TMA = 8.30E-02 m

Beam Movement	TMA o/p	angle	Scale Factor rad/pixel
1.00E-04	262	2.00E-03	7.63E-06
2.00E-04	525	4.00E-03	7.62E-06
3.00E-04	787	6.00E-03	7.62E-06
4.00E-04	1045	8.00E-03	7.66E-06
5.00E-04	1316	1.00E-02	7.60E-06

Average Scale factor = 7.63E-06 Rad/pixel

The following test data was obtained by applying a range of voltages to the motor, and using the following measurements and catalogue data:

Resistance of coils + series resistor	=	1720	ohm
Flex pivot scale factor (2 off)	=	6.40E-02	N-m/Rad
Mirror distance to TMA	=	8.30E-02	m
Micrometer-to-pivot distance	=	5.00E-02	m
Magnet distance from centre of rotation	=	1.70E-02	m

Volts	Current	TMA o/p	angle	Torque	Kt Nm/A	Kf N/A
5	0.002906977	655	5.00E-03	3.20E-04	0.109972917	6.47E+00
4	0.002325581	522	3.98E-03	2.55E-04	0.109553173	6.44E+00
3	0.001744186	390	2.97E-03	1.90E-04	0.109133429	6.42E+00
2	0.001162791	259	1.98E-03	1.26E-04	0.108713685	6.39E+00
1	0.000581395	130	9.91E-04	6.34E-05	0.109133429	6.42E+00
-1	-0.000581395	-132	-1.01E-03	-6.44E-05	0.110812405	6.52E+00
-2	-0.001162791	-265	-2.02E-03	-1.29E-04	0.111232149	6.54E+00
-3	-0.001744186	-398	-3.04E-03	-1.94E-04	0.111372064	6.55E+00
-4	-0.002325581	-532	-4.06E-03	-2.60E-04	0.111651893	6.57E+00
-5	-0.002906977	-662	-5.05E-03	-3.23E-04	0.1111482	6.54E+00

		Kt Nm/A		Kf N/A	
AVERAGE VALUES	=	0.110272334	+/- 0.011	6.486607909	+/- 0.649

(Error originates from 10% error in flex-pivot scale factor, which is the dominating error in test data. The above data is below presented as a graph.)

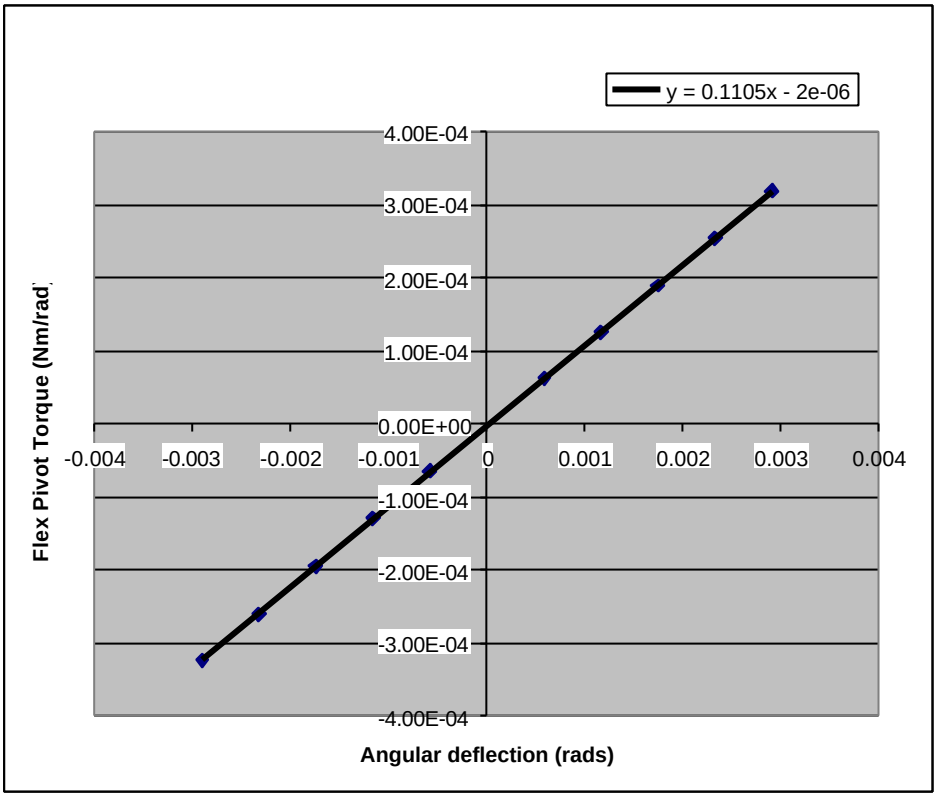

Figure 7 Torque Analysis Graph

9.2.3 CONCLUSION

The tests indicate that an average motor torque constant of 0.11 Nm/A can be obtained for the BSM Chop axis motor. As can be seen from figure 7, the flex-pivot torque varies linearly with the angular deflection of the mirror.
By extrapolation, Figure 7 predicts that at the maximum required angular deflection (+/- 0.042 rad) the motor torque will produce an acceleration sufficient to meet the Angle Step Time requirements. The motor torque will also be enough to meet the required settling times.

9.3 SPIRE: Current Source Test

9.3.1 INTRODUCTION

Current source stability directly impacts the long-term stability of the BSM mirror. In order to verify the current source stability with time the ISOPHOT current source design (which is used on the SPIRE BSM) was built with 1% resistors and a 0.1% 333 ohm load and was tested by measuring the load voltage over time using an H-P 3478A multimeter.
Voltage supplies were maintained at +/- 15.1V.

9.3.2. RESULTS

Time – min.	Load Voltage	% variation from start
0	0.34180	0
0.5	0.34418	0.696314
1	0.34472	0.854301
1.5	0.34499	0.933294
2	0.34513	0.974254
2.5	0.34522	1.000585
3	0.34528	1.018139
3.5	0.34532	1.029842
4	0.34535	1.038619
4.5	0.34537	1.04447
5	0.34538	1.047396
5.5	0.34539	1.050322
6	0.34541	1.056173
6.5	0.34542	1.059099
7	0.34543	1.062025
7.5	0.34544	1.06495
8	0.34544	1.06495
8.5	0.34546	1.070802
9	0.34547	1.073727
10	0.34548	1.076653
11	0.34549	1.079579
12	0.34550	1.082504
13	0.34550	1.082504
14	0.34550	1.082504
15	0.34550	1.082504
16	0.34550	1.082504
17	0.34546	1.070802
18	0.34545	1.067876
19	0.34548	1.076653
20	0.34549	1.079579

The results are also plotted in the following graph:

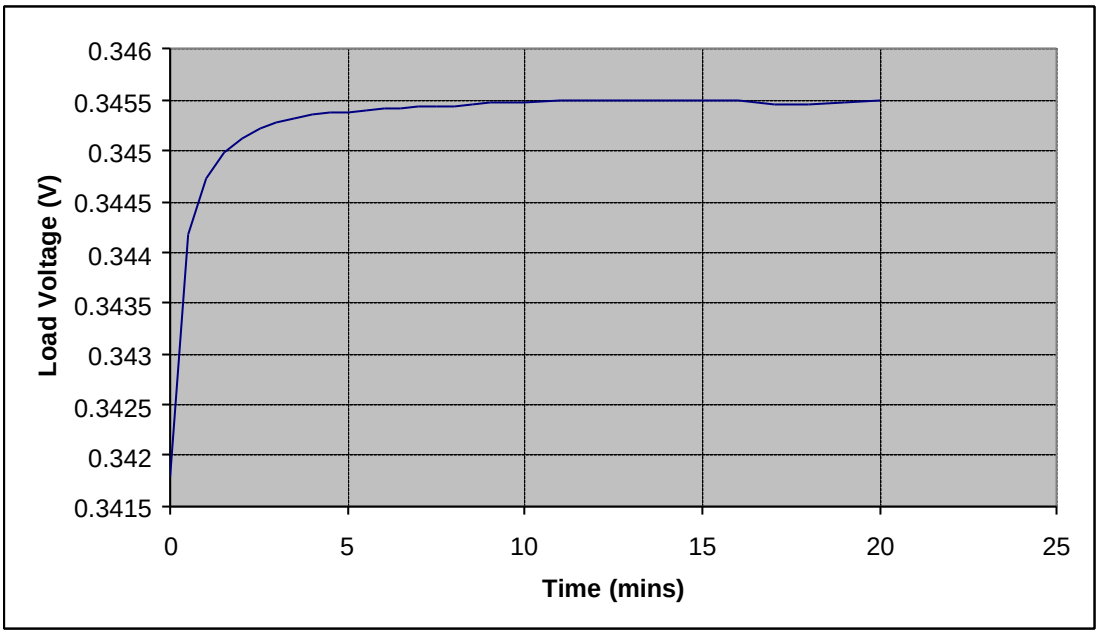

Figure 8 Current Load Source Voltage vs Time

9.3.3 CONCLUSION

It is clear (assuming that there is negligible variation in the 0.1% precision resistor) that the source current - after an initial warm-up period - settles to a value that is constant to about 30 PPM. The current source stability will therefore be a negligible component of the position stability requirement, which corresponds to about 0.16% over 4 hours.

9.4 Preliminary Cross-talk test

9.4.1 INTRODUCTION

An instruction to move the BSM to a given position will consist of two independent orthogonal steps. Given the proximity of motor coils and position sensors it is important that there is no significant cross talk between the motor coils of one axis and the position sensor of the other. If the sensor from one axis was able to detect magnetic field fluctuations caused by motion in the other axis the controlling hardware/software would try to compensate for what it would see as a position error thus reducing position accuracy.

In order to verify that cross talk would be unlikely in the two-axis prototype the sensor output with the motor on was compared to that with the motor off. If there was no distinct change in the results then it would seem unlikely that cross talk would occur.

The experiment was as follows;

1) Position sensor was held in its correct position and it was verified that there was an output when the motor was powered.

2) Removed the sensor and held it in the position of the Jiggle axis sensor. Here no signal was picked up at the output of the sensor amplifier, whilst the chop motor was running. The output from the sensor was the same as when power is removed from the motor, i.e. noise in the sensor circuit only (see figure 2).

3) Moved the sensor close to the motor and still no output was obtained hence there should be no cross talk between the position sensors of the two axes.

4) Replaced the position sensor and found that the sensor had to be very close to the mirror before an output was obtained

9.4.2 CONCLUSION

The results of this experiment strongly suggest that there should be no cross talk between the two axes, therefor positional accuracy will not be jeopardised. This will be confirmed with more precise tests on the two-axis prototype.

9.5 Single Axis proto-type Cold tests

9.5.1 INTRODUCTION

In order to test the performance of the BSM at the operating temperature of 4K the single axis prototype described above was fixed inside the cryostat and was cooled in two stages, firstly to 77K using liquid Nitrogen and then to 4K using liquid Helium. As the mirror cooled significantly slower then the base-plate it was concluded that the flex pivots are poor heat conductors - in order for the mirror to cool at a reasonable rate an aluminium shield had to be place over it.

The primary motives for cooling the single axis prototype were;

a) to check whether the power dissipation in the motor coils were within the required parameters (approximately 2mW)
b) measure the resistance of the motor coils at operating temperature
c) to look for changes in the BSM's performance when cooled for potential faults

Power Dissipation Tests

Using a Phillips PM5135 Function Generator, an AC voltage wave - sinusoidal, frequency 2Hz - of varying amplitude was used as the input to the motor. An ammeter was placed in series with the input signal so that the rms current could be measured, and thus the total power dissipated in the drive circuit could be calculated. The output from the sensor was viewed on a Tektronix TDS 224 oscilloscope.

To find the resistance of the coils at 5K and at room temperature the coils were probed with a FLUKE multimeter. It was found that the resistance dropped from 330Ω at room temperature to 60Ω at 5.2K.

9.5.2 POWER DISSIPATION RESULTS

Test results at 5.2K

Voltage (V)	Current (A)	Total Power (W)	Sensor offset (V)	sensor fdbk (pk-pk) (V)
0.5	2.75E-03	9.72E-04	-4.6	6.4
1	5.80E-03	4.10E-03	-3.6	12.6
1.5	8.90E-03	9.44E-03	0	16.4
2	1.14E-02	1.61E-02	0	18.8
2.5	1.41E-02	2.49E-02	0	22.4
3	1.73E-02	3.67E-02	0	22.4
3.5	1.97E-02	4.88E-02	0	23.2
4	2.14E-02	6.05E-02	0	23.2
4.5	2.46E-02	7.83E-02	0	23.2
5	2.75E-02	9.72E-02	0	23.2

Test results at 295K

Voltage (V)	Current (A)	Total Power (W)	Sensor offset (V)	sensor fdbk (pk-pk) (V)
0.5	5.70E-04	2.02E-04	-7.60E-01	7.60E-01
1	1.55E-03	1.10E-03	-7.60E-01	1.4
1.5	2.00E-03	2.12E-03	-7.60E-01	2.9
2	2.63E-03	3.72E-03	-7.60E-01	3.8
2.5	3.35E-03	5.92E-03	-7.60E-01	5
3	3.92E-03	8.32E-03	-7.60E-01	6
3.5	4.70E-03	1.16E-02	-7.60E-01	7.2
4	5.21E-03	1.47E-02	-7.60E-01	8.2
4.5	5.80E-03	1.85E-02	-7.60E-01	9
5	6.60E-03	2.33E-02	-7.60E-01	9.8

These results were then plotted on a graph:

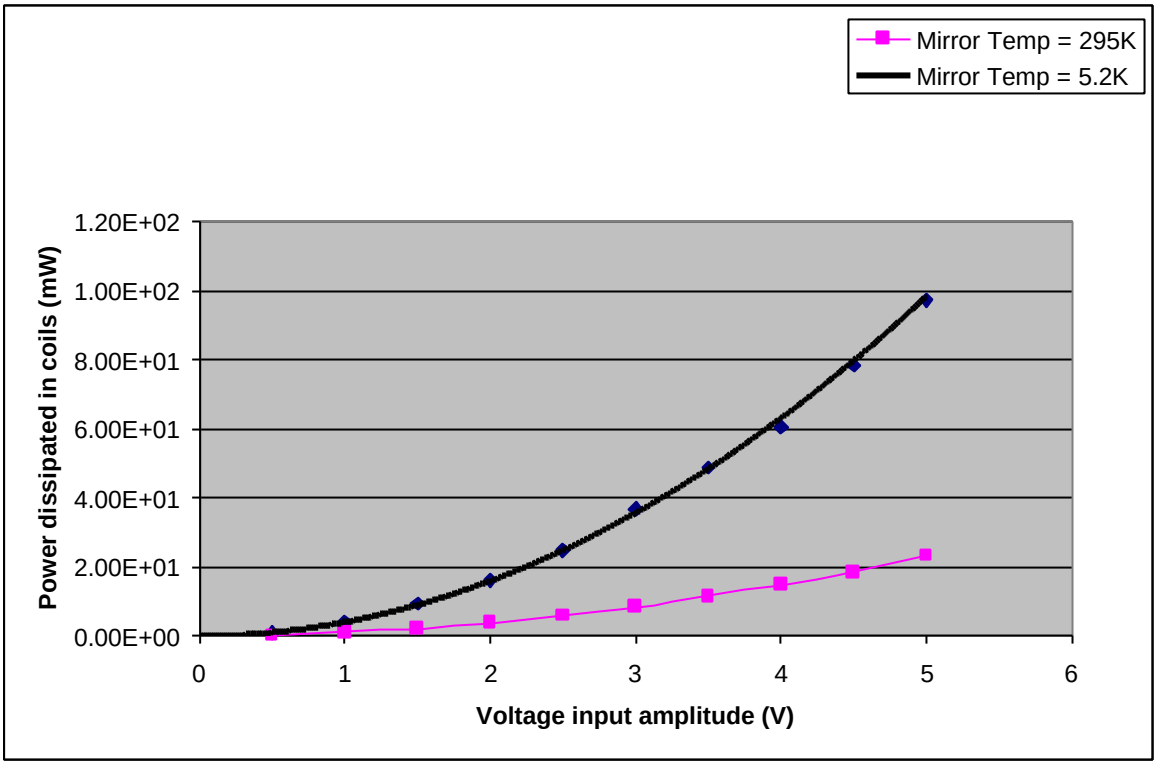

Figure 9 Power Dissipation (AC input)

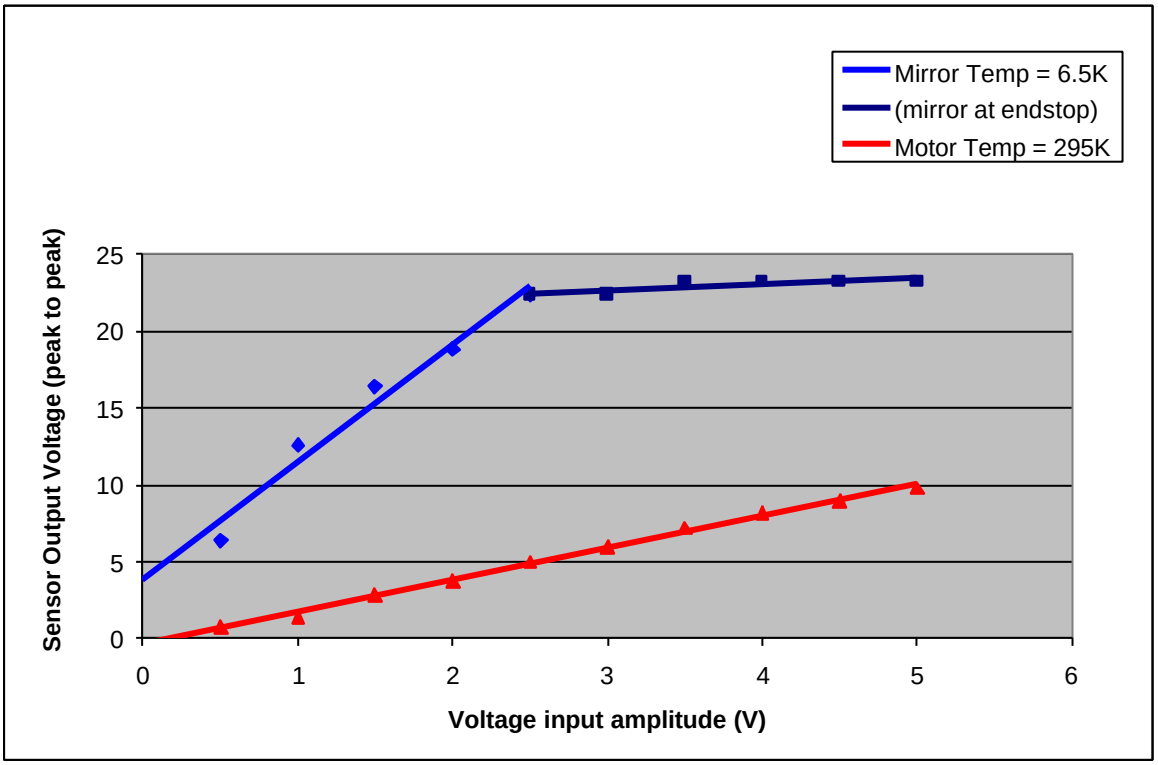

Figure 10 Sensor Output vs Motor Input

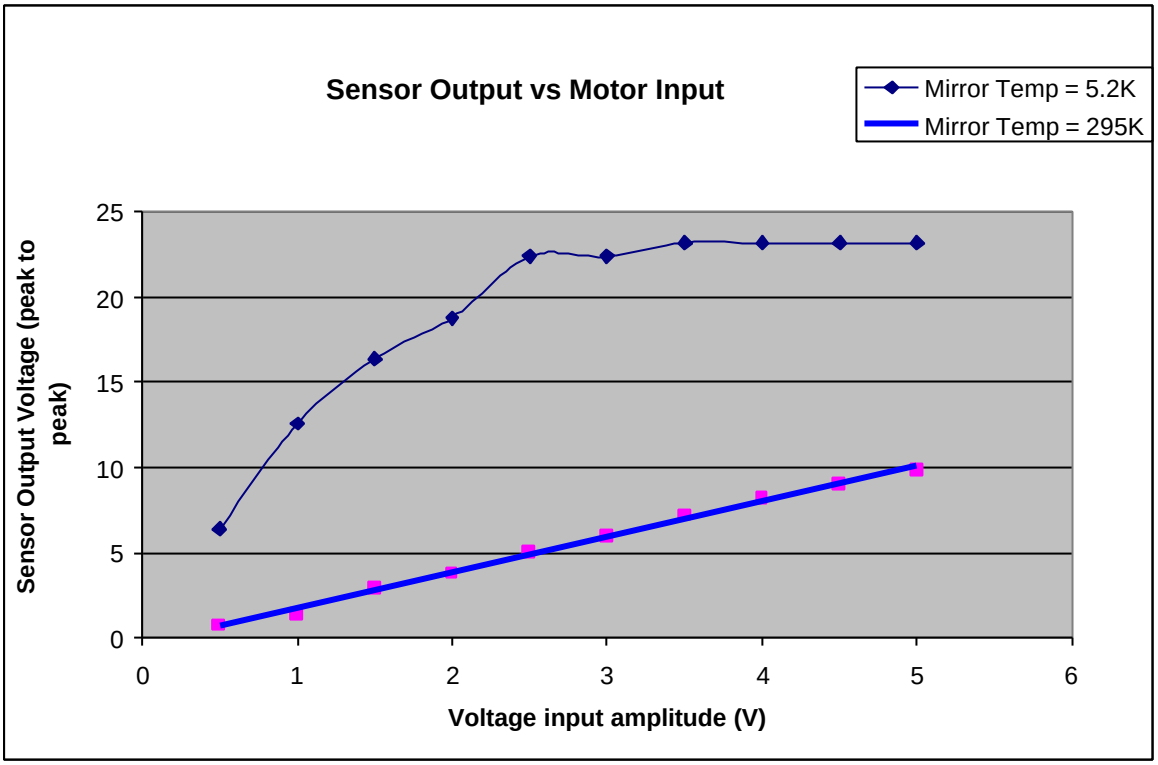

Figure 11 Sensor Output vs Motor Input

9.5.2 POWER DISSIPATION CONCLUSION

Far more power is dissipated when the motor is cold. This is because as the temperature decreases the resistance of the coils will decrease, so if the input voltage is kept constant as the temperature drops the current (and therefore the power dissipated) through the coils will increase. Figure 10 shows the sensor output levels at about 2.5V suggesting the motor has reached its endstop. It also indicates that a current of around 22mA will be sufficient to drive the motor to an end-stop.
There are two reasons why the measured power dissipation in these tests was far greater then the 2.5mW requirement. The first is that the single-axis prototype motor coils were constructed out of copper, which is not superconductive at 5K. It is hoped that aluminium, which has a far lower resistance when cold, will be used in future test (and the flight) models. A coil resistance of 5 Ω (combined with a reduced input voltage) would be sufficient to bring the dissipation down to the specification requirement. An input voltage of 0.11V would generate the 25mA current required to move the motor to an endstop. A second reason is that in these tests a 2Hz continuous sine wave was used as the motor input signal whereas a DC input would have been a better representation (in practice the mirror would not be continuously moving). It is possible that this may have also significantly effected the results.
More cold tests are required (and are planned) to verify these conclusions.

9.6 Two- Axis proto-type

The two-axis prototype is, at the time of writing, nearing completion. More varied and rigorous tests are planned for the two-axis model, including a repeat of all the tests described here on the Jiggle axis. Figure 11 shows the Two-Axis Prototype at its current status.

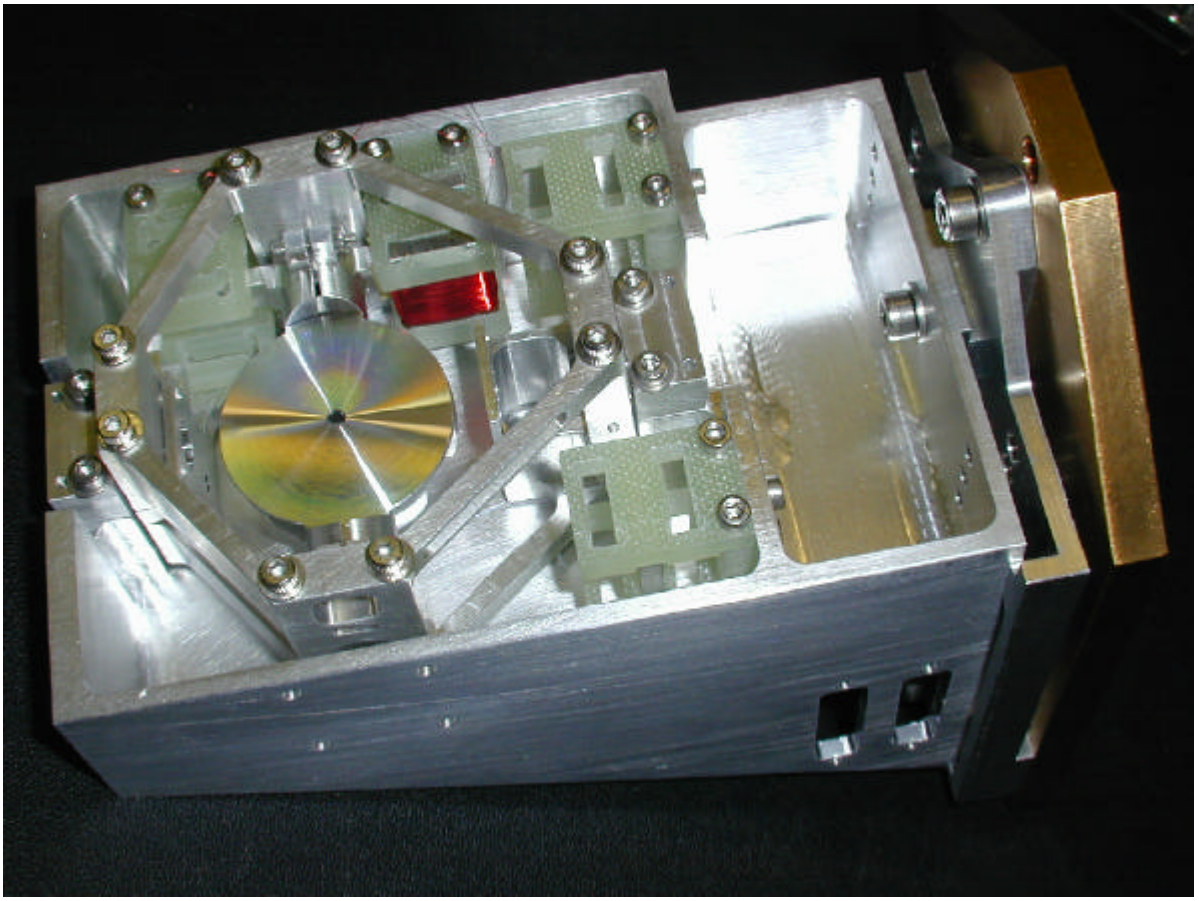

Figure 12 Two-axis Prototype

This page intentionally left blank

Document Ends

Appendix 10

This Appendix is not used.

This page intentionally left blank

Document Ends.

Appendix 11
v1.0

Compliance & Outstanding issues

2.1 Contents

2.2 General

At the release date of this document (21 Feb.02) the following issues are known, or have been resolved since the preceding release (20.Jul at DDR).

The design was placed under configuration control on 31.Jul.01 and all changes thereafter raised as discussed in the Product Assurance plan (Engineering Change Requests and CTD'S)

2.3 *Compliance matrix*

The current design status is compared to the requirements (RD 5). A simple yes/TBC/TBD approach is taken at this stage to indicate whether the design is currently shown to meet the requirements. Where data from single-axis tests is relevant it has been noted. Two axis prototype and development model tests have complete the bulk of the table over the months following DDR. Changes are highlighted.

Requirement	Met by baseline design	Design description reference	Supporting test data	Notes
Angular Travel - Chop Axis	Yes	Drawing SPIRE-BSM-020-001		By design - no fouls at max travel
Angular Travel - Jiggle Axis	Yes	Drawing SPIRE-BSM-020-001		By design - no fouls at max travel
Minimum Step Size	Yes	10.6.9		By design - limit will in digitization & noise
Chop Frequency	Yes	10.5.1, 7.2.2.3	Partial	Power dissipation modeled at specified frequency. 1-AP and 2-AP chops OK at 2 Hz sine and square wave.
Jiggle Frequency	Yes	10.5.1, 7.2.2.3	TBW	Power dissipation modeled at specified frequency.
Holding position	Yes	10.5.3	see appendix 9	Additional 2 axis data available
Stability	Yes	10.5.3	see appendix 9	Additional 2 axis data available
Position Measurement	Yes	10.5.3 (partial)	see appendix 9	Additional 2 axis data available
Settling Time	Yes	10.5.2	see appendix 9	Additional 2 axis data available
Chop repeatability	Yes	Not covered.	2 axis	Confirmed warm, anti-reflection coating on dewar window needed to confirm cold.

Requirement	Met by baseline design	Design description reference	Supporting test data	Notes
Mechanical Dimensions	Yes	Mech ICD	DM inspection reports	
Operating Temperature	Yes	8.1.2	Single and two axis : see appendix 8	Cooldown data supports modelling. Mechanism functions cold
Thermal Isolation	Yes	8.1.2, 8.1.3	Single and two axis : see appendix 8	Cooldown data supports modelling. Mechanism functions cold
Cold Power Dissipation	Yes	10.5.1	See Appendix 9 Data ???	Tests were on Cu coils. Al Coils TBC but based on PACS performance should be OK
Warm Electronics Power Dissipation	Yes	N/A	N/A	Deleted from BSM spec
Mirror Surface Dimensions	Yes	SPIRE-BSM-020-004-001	Yes	2 axis prototype mirror is correct size
Mirror Surface Finish	Yes	9.2	Report on 2AP flycut	
Mirror Surface Reflectivity	Yes	9.2	Report on 2AP flycut	
Mirror Surface Emissivity	N/A	N/A		
Baffle	Yes	9.3		All fouls on beam profile now cleared.
Position of Rotation Axes	Yes	Drawing SPIRE-BSM-020-001		Assembly jig designs required
Orthogonality of Rotation Axes	Yes	Drawing SPIRE-BSM-020-001		Assembly jig designs required
Fail Safe (No Drive Signal) Position	Yes	13.2, Drawing SPIRE-BSM-020-001		Assembly jig designs required
Fail Safe (Mechanical Failure) Position	Yes	7.2.4.2-4		
Mass	Yes	8.5		Report on DM to follow

Requirement	Met by baseline design	Design description reference	Supporting test data	Notes
Cool-down time	Yes	8.1.2, 8.1.3	Single & two axis : see appendix 8	Cooldown data supports modelling. Mechanism functions cold
Reliability	Yes	11		Non-quantitative spec
Failure Modes	Yes	11		
Operational Safety	Yes	N/A		ATC safety risk assessment performed
Lifetime	Yes	7.2.4.1 (flex pivots)		Motors & sensor life TBC, but as PACS, ISOPhot.
Operating modes	Yes	10.8.2, 10.8.3		
Jiggle Mode	Yes	10.8.2, 10.8.3		
Chopping Mode	Yes	10.8.2, 10.8.3		
Scan mapping	Yes	10.8.2, 10.8.3		
Stare or 'holding' mode	Yes	10.8.2, 10.8.3		
Combinations of Modes	Yes	10.8.2, 10.8.3		
Data Outputs	TBC	10.6.1 (overview only)		Spec agreed with LAM
Data Inputs	TBC	10.6.1 (overview only)		Spec agreed with LAM
Exported vibration	Yes	7.3.7		
Stray Magnetic fields	TBC	8.1.4	Add data here	No externally imposed spec
Electro-Magnetic Compatibility	TBC	8.1.4, 10.6.7		No externally imposed spec
ICD's	Yes	12		
Design requirements	Yes	AD3, 13.1		PA Plan - configuration control etc
Electronics Card Format	Yes	Not covered		
Mirror Flatness (optical alignment)	Yes	9.2	Report on 2AP flycut	

Requirement	Met by baseline design	Design description reference	Supporting test data	Notes
Mirror Reflectivity (optical alignment)	Yes	9.2	Report on 2AP flycut	
Cleanliness	Yes	AD3, 13.1		SPIRE Contamination plan
Material selection	Yes	7.4.4, AD3		
Storage	Yes	13.5		
Shock	N/A	N/A		No shock spec.
Quasi Static Loads	Yes	7.1, 7.2.4.1, 7.3.2		
Sine Vibration	Yes	7.1, 7.2.4.1, 7.3.2		
Random Vibration	Yes	7.1, 7.2.4.1, 7.3.2		
Vacuum Level	Yes	Not covered	partial	Lab book notes, material choice
Vacuum Outgassing	Yes	Not covered		Covered by material selection
Temperature	Yes	8.1.2, 8.1.3	Single axis : see appendix 8	Cooldown data supports modelling. Mechanism functions cold
Magnetic Fields	TBC	TBC		No externally imposed spec
Survival Temperature	TBC	Not covered		Magnets limited to 80 deg C
Radiation environment	TBC	Not covered		Infineon sensor requires rating. LAM to rate BSMe

2.4 *Known Issues*

ID	Issue	Plan to resolve
1.	Motor corners clip the 20% oversize optical beam	Chamfer corners and shields - work in hand as at 20.Jul.01 Done. Motors chamfered
2.	Chop sensor assembly edge clip the 20% oversize optical beam	Chamfer corners, move sensor back slightly done
3.	Chop sensor is G10 and emissivity/cooling needs to be modelled	Consider material change. Not considered yet
4.	Baffle design is TBC	Liaise with RAL, Confirm before IBDR completed
5.	Random vibration regime remains a challenge	Liaise with MSSL. DM vibration test Analysis placed with consultancy. DM test scheduled. MSSL have optimized bench to reduce BSM loads
6.	Jiggle flex pivots inconel survivability data needs updating in discussions with TRW	Resolve with TRW. Superceded. TRW inconel pivots not selected.
7.	Harness cut-outs and securing to the BSM structure interface need to be determined	Mock up harness on 2 axis prototype and make design changes Not considered yet
8.	Harness layout to be optimized to allow overlay of prime on redundant.	
9.	MPIA motor space envelope is TBC after Zeiss optimization	Liaise with MPIA/Zeiss Update received - design mods in hand
10.	Parts list needs update after LAM finalize MCU parts list	Liaise with LAM. Update at SMEC/MCU DDR. Resolved. Baseline damping included
11.	Warm electronics do not have baseline motor coil damping	

ID	Issue	Plan to resolve
12.	Minimum step size & position measurement need more depth in design description	work in hand as at 20.Jul.01 update ???
13.	Model damping due to redundant motors, and evaluate need for cross-switching	Liaise with LAM, MPIA ongoing
14.	Plan & cost qualification of Infineon position sensors	Update by IBDR Not considered yet
15.	Flex pivot costing requires programmatic solution	Solve by IBDR Solved. Baseline COTS SS-420. Option CuBe
16.	Model harness & RF Filters for cross-talk & EMC	Not considered yet
17.	Show how connections are made to motors, particularly if aluminium wires are specified by Zeiss	Liaise with MPIA/Zeiss Resolved.
18.	EMC not specified - stray magnetic fields etc	Measure BSM magnetic fields and communicate to systems team. Measured - need tech note
19.	Data I/O has TBC's	Liaise with LAM. Update at SMEC/MCU DDR. Resolved ??
20.	Warm power dissipation is TBD	Liaise with LAM. Update at MCU DDR Resolved/deleted from BSM spec
21.	Bake out temperature is TBC	Perform bake out tests on 2 axis prototype Not considered yet
22.	Hysterisis, backlash etc need to be considered	Analyze before IBDR Studied - tech note required
23.	Chatter & impact on end-stops	Consider compliant end stops, possibly as part of motor design Not considered yet
24.	Cryo-Harness mechanical layout is not included in ATC drawing pack	Incorporate backshells & cable harness in ICD to structure – ensure avoidance of optical beams Incorporated by MSSL.
25.	No detailed design for flexible wiring to chop axis position sensors	Outline design before IBDR Tayco - need tech note
26.	Drawing pack is incomplete	Complete by IBDR. Completed (except harness)

ID	Issue	Plan to resolve
Items 27 onwards added after DDR		
27.	Revised Zeiss motors are larger than the 2 axis prototype packages. This requires movement of the packages and some adjoining elements by 1.5-3mm	Being incorporated into a revised development model at the time of writing. The effects on resonance, mass, inertia are all trivial (and overlaid by the much improved power dissipation characteristics of the Al coils.)
28.	Harness position - change requested from MMSL to re-orient connectors by 90deg to facilitate routing	Done. Incorporated in DM structure (BSM-020-001-001 Rev 3)

2.5 *Changes Required to Design Description Document Pack*

Page number /Section heading	**Description of change to be made**	**Notes**	**Change complete**
All	Fix typographical errors		8 January, 2002
Appendix 10	Declared lists to be removed and cited as applicable documents (make sure are now listed in AD table)		24 January 2002
Annexes	ICDs to be removed, consolidated, and cited as AD		22 January 2002
Appendix 6	Add TAP's cooldown calculations (as appendix 6a and 6b, IP's thermal calcs become appendix 6c)		
Page 21, line 2	Type -600 & -800 pivots transposed		8 January, 2002
Page 42, 9.2 line 1	RD1 should read RD7		8 January 2002
Elec section	a written talk through of the circuits (what the circuit does, what major components are called out, eg the DAC & ADC - do they meet the noise, response time etc requirement)	covered	21.Feb.02
Elec section	the minimum step size is not covered.	covered	21.Feb.02
Elec section	position measurement	Tests made and documented, not written as tech notes	
Elec section	how do we ensure configuration control on dSpace models	Latest configuration stored in Q-Pulse as a SOF category (software)	Completed
Elec Section	Model damping due to redundant motors, and evaluate need for cross-switching	Tech note SPI-BSM-NOT-0004	23.AUG.01
Elec section	Plan & cost qualification of Infineon position sensors		
Elec section	Model harness & RF Filters for crosstalk & EMC		
Elec section	Show how connections are made to motors, particularly if aluminium wires are specified by Zeiss	Zeiss connection changed. Added figure to Design Description	20.FEB.02
7.2.1	Note to be written by IP re confirming that SS disc spring is adequate (Will be RD14)	SPI-BSM-NOT-0009	21.Feb.02
7.2.1	Report from FEA Study to be written (will be RD15)	Work in progress	
7.2.1	Need description of air gaps; size and impact	Tests performed. Air gaps will be as close as possible in DM	
7.2.4.2	IP to arrange mechanical tests on flex pivots and their protection	In progress . SPI-BSM-NOT-	

Page number /Section heading	**Description of change to be made**	**Notes**	**Change complete**
		0009	
7.3.6	IP to fix table where wrongly uses 1.25 multiplier.	Done.	21.Feb.02
8.1.4	IP to write new section "Flex Pivot Thermal Stresses"	Done.	21.Feb.02
10.5.3	BS to update or resolve comments on angle measurement stability	TBC	TBC
10.6.9	BS to add discussion on signal to noise	Not done	Not done
11	need to resolve fail safe tolerance – 0.18 or 0.35	Done. +/-0.18 applied universally	21.Feb.02
13.2	need to determine marking methods	Work in progress	
spire-bsm-021-001 (sheet 2 of 2)	resolve 0.35mm gap	Not done	
9.1.1	Need cold position sensor noise data		
Appendix 9 9.1.2	clarify if there is a higher frequency filter	Filter in WE (see 10.6.3, Fig 35)	19.Jun.01
Appendix 9.2.1	figure 6: to be redone with white background and better arrows	Not done (low priority)	
Section 10, App4	pull Mechanical FMECA out to separate doc, and reformat to match ESA format	Document number SPIRE-ATC-PRJ-001118	9 Jan 2002
Section 10, App 5	Create Electronics FMECA	Not done	
7.2.4.4	push for launch latch descope by restricting angle?	Raised at 23.Aug.01 meeting. Not adopted, but angle range changes to +/-1.5 and -/+2.4 which helps	23.Aug.01 Not adopted
8.1.4 (new)	ask Berend for thermal stress details	superceded	20.Feb.02
9.3 (baffle)	note open item – resp RAL to resolve	ATC supply	21.Feb.02
10.6.5	need better details on thermometry interface and write up of screening	Harness ICD (John Delderfield)	yes
10.8.4	major issue – coil shorting	LAM baseline design includes. But keep under review	TBC
PA Plan	Raise CTD to update FMECA in line with RIDS		06/12/2001
11.3	update principal recommendations resulting from the FMECA	FMECA broken out as unique document.	Completed

2.6 *BSM DDR Meeting close-out - status update*

Source	Description of change to be made	Notes	Change complete
DDR MINUTES ACTION Summary	1) Action: ATC to add diagnosis/trace mode telemetry rate to the spec. (and let Didier Ferand know)	In BSM spec.	Done
	2) ACTION : RC/IP to contact Smiths about pivots. Ray will speaking to contact at DTI.	Option has potential but too costly. Closed	Done.
	3) Action: RAL (BMS) to provide a traceable document with the optical scaling factor.	referenced in BSM spec	Done.
	4) Action ATC (IP) : BSM Specification document should be brought up to date to meet current optical model.	2.53deg chop is main change	Done.
	5) Action: BMS to check spec. on FoV requirements (a few weeks from now). Will do this as formal change request to the IRD	in BSM spec	Done
	6) Action: IP to investigate relocating the launch lock	Can now be relocated to +ve or -ve chop pos.n exact placement TBD.	In progress.
	7) ACTION : RAL (BMS) to check specification on FoV of 126 arc secs if + some number other than what we have.	now 130 arcsec. in BSM spec	Done
	8) ACTION : ATC(IP) to check launch latch against motor assemblies.	can be positioned to suit.	Done
	9) Action ATC (BS) High priority: to determine damping before MCU DDR.	SPI-BSM-NOT-0004	Done.
	10) Action ATC (IP) to quantify how well balanced can get BSM.	No tech note, but in principle can be balanced to better than 0.5gm.cm.	Done.
	11) ACTION ATC (BS) Calculate maximum input disturbance at 15Hz at max frequency with power on.	SPI-BSM-NOT-0005	Done.
	12)) Action: MJG/BMS to revise microvibration susceptibility number (at next Alcatel meeting)		
	13) Action: ATC (BS) to specify the max input disturbance that can be withstood at the resonant freq. (when powered up)	SPI-BSM-NOT-0005	27.Aug.01
	14) Action: Cardiff to look at putting the end of the light pipe behind the mirror to eliminate any possibility of fouling on the BSM.	No drawing change yet, but confirmed at PCAL DDR	TBC
DDR MINUTES Agreement Summary	1) Agreed to put stainless steel pivots in STM or nothing.		N/A

Source	Description of change to be made	Notes	Change complete
DDR MINUTES Agreement Summary	2) Agreed to go with stainless steel pivots if Smith's option a no-go; though this is a high risk option.	CuBe a better alternative - being investigated	N/A
	3) Need to do cold/warm tests on stainless steel or Smith's pivots. Have six months to do this. If neither preferred option a go then need to go (reluctantly) with inconel pivots.	Up-Screen rig design in hand. SPI-BSM-NOT-0005	Done
	4) IP will order small batch of stainless steel pivots	6 off each type ordered, received	Dec.01
	5) Start up-screen programme for SS (77 K) and investigate Smiths Industries (i.e., adopt Option 5 as working baseline). ATC to design up-screening test equipment	Up-Screen rig design in hand. SPI-BSM-NOT-0005	Done
	6) [CRC's] routine systems responsibilities can be done by RAL.		Done
	7) CRC to act as systems roving "Devil's Advocate".		Done
	8) that a restricted systems telecom (~ 30 mins) every other week to discuss systems engineering would be beneficial.		Done
	9) Savings in ATC systems would remain inside ATC allocation		Done
RID HR-SP-ATC-RID-08 : SPIRE Interface Control Drawing/Manufacture Drawings/Circuit Diagrams	1) John Delderfield, Ian Pain, Peter Hargrave and Berend Winter need to sign off the I/F Control Drawing	No sign off page on revised ICD	
	2) Include the distance of the optical reference from the SOB on the interface control drawings (Berend to check with the structure ICD as well)	Sheet 4 of SPIRFE-BSM-021-001	Done
	3) Connector location needs to be identified on the Drawings along with the Connector identification number (J1/J2)	Positions identified. J1/J2 TBC after MMSL routing	Done
	4) All drawings need to go under configuration control including Unique Identification Number, Revision Number, Change Control and Signatures	Done. Signature is electronic via Intralink. CTD's manually signed.	Done
RID HR-SP-ATC-RID-09 SPIRE Beam Steering Mechanism Design Description	5) A justification of the cryo-mechanical design of the magnet holder needs to be made to show that any differential contraction between the alloy and the magnetic material will not adversely affect the BSM reliability.	Not Done	
DDR REPORT (DOUG GRIFFIN)	Motor winding material	selection made … Aluminium.	closed
DDR REPORT (DOUG GRIFFIN)	flex pivot selection.	Baseline choice SS-420 grade lucas off the shelf Alternate C-flex CuBe Upscreening rig in manuf, vib test scheduled.	closed

Source	Description of change to be made	Notes	Change complete
	Launch load survival – Motor coil shorting:	Baseline choice - shorting adopted.	closed
	Inclusion of conformal stray light baffle:	not base-lined. RAL happy with current baffle, assuming 1K temperature met.	Closed
	Confirmation is required on the telemetry rate for the BSM.	Closed. Email Didier Ferrand Tuesday, October 09, 2001 10:01	Closed
	Confirmation (by Tony Richards) that a 32.5mm diam mirror is OK	email?	Closed, TBC
	Include a maximum OD on PCAL (diffraction) 4.2.8 Offset due to modulation.(current requirement is no less than diam 2.8). DKG to check up this with BMS		
	Technical memorandum to be produced on the technical options for the flex pivots / Co-procurement / Sinusoidal chopping	Close out meeting 23rd Aug.01	Done
	Latch inclusion (to be investigated with the use of a model)		Done
	DKG to ask instrument team whether sinusoidal chopping would be OK	.it's not.	Done
	What is the impact on the design if the maximum chop throw was less than or equal to 1.5degrees	considered. Not adopted.	Done
	Zeiss can provide either Aluminium or Copper windings on the motors. We have little control over this. We are in margin with Copper and two flex pivot types. If we go to one flex, we are out with aluminium and very out with copper	Resolved. Motors will be Al. Pivots will be two types	Done
	We need to get the harness impedance at cold and warm conditions	Done. Email ref ???	TBC
	ATC to investigate magnet differential expansion	not done	

This page intentionally left blank

Document Ends.